

Myosin-X and Myosin-XIX in Intracellular Transport

Melinda Maria DiVito

A dissertation submitted to the faculty of the University of North Carolina at Chapel Hill
in partial fulfillment of the requirements for the degree of Doctor of Philosophy in the
Department of Cell and Molecular Physiology.

Chapel Hill
2009

Approved by:

Richard Cheney, PhD, Advisor

Keith Burrridge, PhD

Carol Otey, PhD

Leslie Parise, PhD

Eleni Tzima, PhD

ABSTRACT

Melinda Maria DiVito
Myosin-X and Myosin-XIX in Intracellular Transport
(Under the direction of Dr. Richard E. Cheney)

Myosin motor proteins travel along actin filaments and power the movements responsible for force generation, vesicle and organelle trafficking, and formation of protrusive cellular structures. This dissertation discusses myosin-X and the novel myosin-XIX. Myosin-X is a MyTH4-FERM myosin that localizes to the tips of the slender, actin-based cellular protrusions known as filopodia. Moreover, it undergoes intra-filopodial motility and is a master regulator of filopodia formation. Previously, we demonstrated that through its FERM domain, myosin-X binds to β -integrins. Here we describe experiments designed to elucidate the functional consequence of the myosin-X- β -integrin interaction. We report that: 1) knock-down of myosin-X inhibits cell spreading and adhesion, 2) the FERM domain of myosin-X, unlike that of talin, does not activate integrins, and 3) myosin-X co-transport with integrins in filopodia. These results support a model in which myosin-X is a component of the filopodia tip complex and participates in the intrafilopodial transport of other tip proteins. Myosin-XIX is the founding member of a novel class of myosins and is the last uncharacterized human myosin. Here we report that myosin-XIX is expressed in many cell types and shows striking localization to mitochondria. Additionally, over-expression of a GFP-tagged myosin-XIX results in a dramatic gain of function phenotype in which mitochondria

become hyper-motile. To reveal the endogenous function of myosin-XIX, we designed and tested a series of siRNAs against myosin-XIX. With this tool, we can further characterize the function of myosin-XIX, the first vertebrate myosin shown to localize to the mitochondria. These studies advance our understanding of the role of myosin-X in filopodia and provide the first report of the mitochondria-associated myosin-XIX.

ACKNOWLEDGEMENTS

I have loved science since I was a child. But the cultivation of that affection was not without the influence of some remarkable teachers. I thank Mrs. Malek, Mrs. Lambert, and Mrs. Schmitt for their exceptional dedication to, enthusiasm for, and skill in teaching science. Their instruction provided the basis for my success in college and beyond.

“So you want to go to graduate school!” Although he may not recall, this was the first statement my undergraduate research advisor said to me on my first day in lab. At the time, I was unsure of which academic path I wanted to take. With the training and guidance of Dr. Ken van Golen, I happily and confidently transitioned into graduate school. I thank Ken for being extraordinarily enthusiastic and encouraging. His mentoring was invaluable to my development as a young scientist.

A student’s experience in graduate school is most certainly accompanied by an extensive list of those to whom she is indebted. First, I would like to thank my graduate advisor, Richard Cheney. His insatiable scientific appetite and sincere love for science are infectious – one cannot help but absorb these qualities while working with him. Richard’s careful and thoughtful approach to designing, performing, and reporting experiments has provided an excellent example upon which to model my skills as a scientist. I have thoroughly enjoyed working with Richard and all of the Cheney lab

members: Omar Quintero, Aparna Bohil, Damon Jacobs, Brian Robertson, Aurea Sousa, Taofei Yin, Michael Kerber, Brian Dunn, Alex Raines, and Katy Liu. I am grateful for these fantastic past and present lab mates. Together, the “Cheneyites” made the lab both a fun and constructive place to do science. I owe special thank to Omar Quintero, my “scientific big brother”, for training me as a first-year graduate student, including me on the Myo19 project, and being a great friend.

Other labs, scientists, and students across campus have been an important part of my experience in graduate school. In particular, I would like to thank our neighbors in our “sister” lab, the Otey lab. Carol and her lab members are wonderful coworkers who have generously shared their reagents, advice, and celebratory treats with the Cheney lab. In addition I am grateful for the excellent faculty, staff, and students of the Cell and Molecular Physiology Department, the terrific cohort of IBMS students with whom I entered graduate school, and the numerous people across campus that have helped me with an assortment of research related endeavors.

I would also like to thank my friends and family. I have met and befriended many fantastic people throughout graduate school who have made the good times great and the bad times certainly more bearable. I would like to thank my wonderful family, especially my parents, Elio and Denise DiVito, and my siblings, Jessica and Tony, for their continued love and support throughout this time in my life. Finally, I am forever grateful for my husband Mark Jezyk. Meeting him in graduate school was a splendid surprise and his unconditional friendship, love, encouragement, and advice have been an incredibly important contribution to my completion of graduate school.

PREFACE

Throughout my time in graduate school, I worked on several projects exploring the cell biological functions of myosin-X. During my final two years, I became involved in a project examining the novel myosin-XIX. In this dissertation, I discuss the results of one of those myosin-X projects and the myosin-XIX project. In Chapter 1, I provide a brief introduction to the myosin family of motor proteins, which will prepare the reader for subsequent discussion of several different myosins. In Chapter 2, I examine the myosin-X literature and discuss what is known about myosin-X's structure, biochemical properties, and participation in filopodia formation and function. This review was recently published in the book *Myosins: A Superfamily of Molecular Motors*. Next, in Chapter 3, I review the field of filopodia biology, paying particular attention to the filopodial tip complex and intra-filopodial transport. This chapter will serve as the basis for a review article on filopodia that Richard and I will submit to *The Journal of Cell Science*. In Chapter 4, I report the results of one of my projects exploring the functional consequence of the interaction between myosin-X and β -integrins. The research presented in this chapter will be combined with additional data in our lab to compose a research article describing the myosin-X and its interaction with components of the filopodial tip complex. Chapter 5 contains the results of a project started by a former postdoctoral researcher, Omar Quintero, describing the novel

mitochondria-associated myosin-XIX. In this chapter I present a combination of data, some of which has very recently been accepted for publication in the journal *Current Biology*. My major contributions to this ongoing project included: 1) live-cell imaging of mitochondria under various conditions and quantification of their movements, 2) optimization of two new antibodies directed against mouse myosin-XIX and characterization of a mouse cell system to study myosin-XIX, and 3) development of and siRNA strategy directed against mouse myosin-XIX to test for a loss of function phenotype. The mouse system, siRNA strategy, and forthcoming loss of function results will be the topic of a future paper on myosin-XIX. Lastly, I conclude my dissertation in Chapter 6 with a discussion of the future research directions regarding myosin-X and myosin-XIX.

In addition to the content of this dissertation, I have some notable accomplishments to mention here. First, in 2006, I applied for and was awarded an American Heart Association pre-doctoral fellowship. The aims proposed in my fellowship application addressed the role of myosin-X in the membrane protrusions produced by cells during the processes of phagocytosis and trans-endothelial migration. I encountered several substantial obstacles while trying to address these aims and was not able to carry them to completion. However, as a result of working on a new area of research, I was able to develop fruitful relationships with other labs performing similar research. I was able to lend my expertise in live cell imaging to a collaborative project with the Cam Patterson lab at UNC, which resulted in a publication in *The Journal of Cell Biology* describing the interaction between myosin-X and BMP signaling in endothelial cells. Lastly, I presented some of the myosin-X and β -integrin research described in Chapter 4 at the 2007 annual meeting for the American Society of Cell Biology.

TABLE OF CONTENTS

LIST OF TABLES.....	xi
LIST OF FIGURES.....	xii
LIST OF ABBREVIATIONS.....	xiv
Chapter	
I. INTRODUCTION TO THE MYOSIN FAMILY OF MOLECULAR MOTORS.....	1
General domain structure and features of myosins.....	1
Functional diversity of human myosins.....	4
II. MYOSIN-X: A MOLECULAR MOTOR AT THE CELL'S FINGERTIPS.....	12
Introduction.....	12
Structure of Myosin-X.....	13
Biochemical Properties of Myosin-X.....	18
Cell Biological Functions of Myosin-X.....	20
Outstanding Questions.....	29
III. POINTING FINGERS: HOW THE CELL CREATES, MAINTAINS, AND EMPLOYS FILOPODIA.....	37
Filopodia Functions.....	37
Filopodia Architecture and Dynamics.....	39
Classification of Filopodia and Related Actin Structures.....	40

	Key Molecules in Filopodia Formation.....	42
	The Filopodia Tip Complex: At the Forefront of Filopodia Formation and Function?.....	47
	Intra-Filopodial Transport.....	49
	Emerging Topics and Outstanding Questions in Filopodial Biology.....	53
IV.	DETERMINING THE FUNCTIONAL CONSEQUENCE OF THE MYOSIN-X – BETA INTEGRIN INTERACTION.....	59
	Introduction.....	59
	Knock-Down of Myosin-X Impairs Cell Adhesion and Spreading.....	60
	The FERM Domain of Myosin-X Does Not Activate Integrins.....	62
	Myosin-X Co-Transports with Integrins in Filopodia.....	66
	Discussion.....	69
	Experimental Procedures.....	72
	Movie Legends.....	83
V.	MYOSIN-XIX: A NOVEL MYOSIN THAT LOCALIZES TO MITOCHONDRIA.....	84
	Introduction.....	84
	Myo19 Encodes a Novel Metazoan Myosin.....	87
	Myo19 is Expressed in Multiple Tissues and Cell Lines.....	88
	Myo19 Localizes to Mitochondria.....	89
	Expressing GFP-Myo19 Alters Mitochondrial Dynamics.....	90
	GFP-Myo19 Induced Mitochondrial Motility is Likely Due to Myo19 Motor Activity.....	91

siRNA Oligos Directed Against Myo19 Effectively Kock-Down Myo19 Protein.....	92
Myo19 is a Novel Mitochondrial-Associated Myosin That is Likely to Function in Actin-Based Mitochondrial Dynamics.....	94
Experimental Procedures.....	98
Movie Legends.....	116
VI. CONCLUSIONS AND FUTURE DIRECTIONS.....	118
Myosin-X.....	118
Myosin-XIX.....	121
REFERENCES.....	125

LIST OF TABLES

I. INTRODUCTION TO THE MYOSIN FAMILY OF MOLECULAR MOTORS

Table 1.1	Human myosin functional diversity.....	11
-----------	----------------------------------------	----

III. POINTING FINGERS: HOW THE CELL CREATES, MAINTAINS, AND EMPLOYS FILOPODIA

Table 3.1	Proteins that localize to the tips of filopodia.....	58
-----------	------------------------------------------------------	----

LIST OF FIGURES

I.	INTRODUCTION TO THE MYOSIN FAMILY OF MOLECULAR MOTORS	
1.1.	General domain structure of myosin motor proteins.....	8
1.2.	Human myosins contain a diverse array of protein domains.....	9
1.3.	The mechanical myosin cycle.....	10
II.	MYOSIN-X: A MOLECULAR MOTOR AT THE CELL'S FINGERTIPS	
2.1	Myo10 is a MyTH-FERM myosin.....	31
2.2	Myo10 localizes to the tips of filopodia.....	32
2.3	Myo10 domains required for localization to filopodial tip and induction of dorsal filopodia.....	33
2.4	GFP-Myo10 undergoes intrafilopodial motility.....	34
2.5	Myo10 is a potent inducer of filopodia.....	35
2.6	Schematic representing intrafilopodial motility of Myo10.....	36
III.	POINTING FINGERS: HOW THE CELL CREATES, MAINTAINS, AND EMPLOYS FILOPODIA	
3.1	Architecture and molecular components of filopodia.....	56
3.2	Classification of filopodia, microvilli, and stereocilia.....	57
IV.	DETERMINING THE FUNCTIONAL CONSEQUENCE OF THE MYOSIN-X – BETA INTEGRIN INTERACTION	
4.1	Endogenous myosin-X and integrins colocalize in filopodia.....	77

4.2	Knock-down of myosin-X impairs cell adhesion and spreading.....	78
4.3	The FERM domain of myosin-X does not activate $\alpha_{11b}\beta_3$	79
4.4	Myosin-X does not contain the loop structure necessary to activate integrins.....	80
4.5	Myosin-X co-transport with integrins in filopodia.....	81
4.6	Myosin-X cotransports with integrins on actin bundles in CAD cells.....	82
V.	MYOSIN-XIX: A NOVEL MYOSIN THAT LOCALIZES TO MITOCHONDRIA	
5.1	Myo19 is myosin motor protein with a novel tail domain.....	104
5.2	Myo19 is expressed in multiple tissues and cell lines.....	106
5.3	Myo19 localizes to mitochondria.....	108
5.4	Myo19 co-sediments with mitochondria.....	109
5.5	GFP-Myo19 localizes to mitochondria through its tail domain.....	110
5.6	Expressing GFP-Myo19 increases mitochondrial motility.....	111
5.7	Expression of Myo19 increases mitochondrial dynamics.....	113
5.8	GFP-Myo19 induced movements in A549 cells are actin-depedent.....	114
5.9	siRNA sequences directed against mouse Myo19 knock-down endogenous protein.....	115

LIST OF ABBREVIATIONS

ADP	Adenosine diphosphate
ALK6	Bone morphogenic protein-6 receptor
ARP2/3	Actin related proteins 2 and 3
ATP	Adenosine diphosphate
B16	Mouse melanoma cell line
BAEC	Bovine aortic endothelial cells
BMP	Bone morphogenic protein
Ca	Calicum
CAD	Cath.a-differentiated cell line
CHO	Chinese hamster ovary cell line
CI	Cell index
CLP	Calmodulin-like protein
COS-7	African green monkey kidney cell line
CPAE	Cow pulmonary aortic endothelial
DI	Displacement index
DCC	Deleted in colorectal cancer
ECM	Extracellular matrix
EGF	Epidermal growth factor
EGFR	Epidermal growth factor receptor
Ena	Enabled
EM	Electron microscopy

EVH1	Ena-VASP homology 1
ESTs	Expressed sequence tags
FAK	Focal adhesions kinase
FERM	4.1, ezrin, radixin, moesin
Flk-1	Fetal liver kinase 1 (aka VEGFR)
FN	Fibronectin
GAP	GTPase accelerating protein
GFP	Green fluorescent protein
GTP	Guanosine triphosphate
HMM	Heavy meromyosin
I-BAR	Inverse Bin-Amphipysin-Rvs167
IRSp53	Insulin receptor substrate of 53kDa
kB	Kilobases
kDa	Kilodaltons
MAX-1	Motor axon guidance-1
mDia	Mammalian diaphanous
MnCl ₂	Manganese chlororide
IMD	IRSp53 and Missing-in-metastasis Domain
Mena	Mammalian enabled
MyTH4	Myosin tail homology 4
NS	Non-specific
PCR	Polymerase chain reaction
PDZ	PSD95, DlgA, ZO-1

PEST	Proline, glutamate, seine, and threonine
Pi	Inorganic phosphate
PH	Pleckstrin homolgy
pLL	pLentiLox
PTB	Phosphotryosine binding
PtdIns(3,4,5)P ₃	Phosphatidylinositol-3,4,5-trisphosphate
PtdIns(3,5)P ₂	Phosphatidylinositol-3,5-bisphosphate
PtdIns(4,5)P ₂	Phosphatidylinositol-4,5-bisphosphate
Rif	Rho in filopodia
RNA	Ribonucleic acid
RT-CES	Real-time cell electronic sensing
SAH	Single alpha helix
SDS-PAGE	Sodium dodecyl sulfate polyacrylamide gel electrophoresis
SH3	Src homology 3
shRNA	Short hairpin ribonucleic acid
siRNA	Short interfering ribonucleic acid
TEM	Trans-endothelial migration
TIRF	Total internal reflection
VASP	Vasodilator-stimulated phosphoprotein
VEGF	Vascular endothelial growth factor
VEGFR	Vascular endothelial growth factor recptor
WASP	Wiskott-Aldrich syndrome protein

CHAPTER 1

INTRODUCTION TO THE MYOSIN FAMILY OF MOLECULAR MOTORS

The myosin family of actin-based molecular motors is a large protein family found in eukaryotes. Sequence comparisons from the genomes of more than 300 eukaryotic organisms have identified over 30 classes of myosins (Odrionitz and Kollmar, 2007). These classes are denoted using roman numerals and define groups of myosins that are structurally and functionally related. Humans have at least 39 myosin genes that encode for myosins from 12 classes (Coluccio, 2008). Myosins participate in a wide range of cellular activities including force generation, vesicle and organelle trafficking, and formation of protrusive cellular structures. Here I provide a brief introduction to the basic molecular and cellular biology of myosins and set the stage for the detailed discussions of myosin-X and myosin-XIX in later chapters.

GENERAL DOMAIN STRUCTURE AND FEATURES OF MYOSINS

Myosin motor proteins bind actin filaments in an ATP-regulated manner and hydrolyze ATP to power movements along actin filaments. They form multimeric protein complexes containing one or more myosin heavy chains, which each associate with one or more light chains. Myosin heavy chains can generally be divided into three functional parts: the head or motor, the neck, and the tail (Figure 1.1). The amino-

terminal motor domain coordinates ATP hydrolysis with actin binding and translocation. This is the most highly conserved part of the protein and is what defines a myosin. Much of the sequence comparison that has led to the current method of myosin classification has been performed using the motor sequences. Following the motor, the neck usually contains one or more IQ motifs, which each contain approximately 24 amino acids with a core sequence of IQXXXRGXXXR (Cheney and Mooseker, 1992). The IQ motifs serve as binding sites for light chains, with most myosins binding the light chain, calmodulin, or other calmodulin-related proteins. Lastly, the carboxy-terminal tails of myosins vary greatly and confer each myosin with a unique function. Several types of specialized protein domains have been identified in the tails of myosins including SH3, PDZ-binding, MyTH4, FERM, GAP, and PH domains. Additionally, many myosin tails contain a coiled-coil-forming alpha-helical domain that mediates dimerization. Figure 1.2 provides a representative domain diagram for each of the 12 classes of myosins expressed by humans, highlighting the diversity in myosin tails.

All myosins appear to share a common ATPase mechanism that couples ATP hydrolysis to actin binding (reviewed in Coluccio, 2008; De La Cruz and Ostap, 2004). A basic diagram of the myosin mechanical cycle is depicted in Figure 1.3 and consists of four stages. In stage 1, in the absence of nucleotide, the myosin motor binds tightly to the actin filament in a “rigor-like” state. In stage 2, the binding of ATP to the ATPase site causes detachment of the motor from the actin filament. This antagonistic behavior of actin binding versus nucleotide binding is a characteristic property of myosins. Next, the myosin hydrolyses ATP and forms a stable ADP+Pi complex. As depicted in stage 3,

during this reaction, the myosin becomes primed to bind actin again and undergoes its “recovery stroke”. The ADP+Pi-myosin complex reattaches to actin in stage 4 and is ready to undergo its power stroke. Actin acts as a nucleotide-exchange factor for myosin; upon actin binding, the phosphate is released first, followed by the ADP. It is during this time that the myosin undergoes its power stroke, and returns back to the strong binding actomyosin complex in stage 1.

With each power stroke that the myosin motor domain makes, the conformational change induced by Pi and ADP release must be transmitted from the motor domain to the force-generating lever arm of the myosin. The neck region of the myosin, stiffened by binding to its light chains, functions as the lever arm. During the power stroke, the neck swings through an approximately 60° angle to drive forward along the actin filament (Coluccio, 2008; De La Cruz and Ostap, 2004). Interestingly, the necks of myosins can vary in length and in number of IQ motifs. These variations appear to contribute to the step size of the myosin as it undergoes its power stroke – longer necked myosins take larger steps along an actin filament. Additionally, because the rigidity of the neck/lever arm is maintained by the binding of light chains, changes in light chain binding can serve as a mechanism for regulating motor function. This is important in the context of intracellular calcium levels, as calmodulin and other light chains bind to calcium.

There are two final myosin properties to consider when discussing basic myosin function, processivity and duty ratio (reviewed in Coluccio, 2008; De La Cruz and Ostap, 2004). A processive myosin makes multiple interactions with the actin filament during one ATPase cycle to allow for translocations over long distances. Conversely, a non-

processive myosin detaches from the actin track after a single ATPase cycle.

Processivity can be enhanced by tethering two or more motors together either through direct interaction, as is the case for the dimeric myosin-V, or by binding multiple motors to one cargo. A related concept is that of the duty ratio, which is the time that a myosin spends attached to actin compared to the overall time for the ATPase cycle.

Processivity is often associated with myosins that have high duty ratios.

FUNCTIONAL DIVERSITY OF HUMAN MYOSINS

Humans express myosins from the following 12 classes: I, II, III, V, VI, VII, IX, X, XV, XVI, XVIII, and XIX. The proteins in these classes can facilitate a wide range of processes, as summarized in Table 1.1. Some examples of the diverse roles of myosins in cell biology are described below.

Generation of contractile force/tension. Several myosins function to generate contractile force or tension, with the most extensively studied example of this being class II myosins. Historically, the behavior of myosin-II in muscle has been the prototypical example of myosin function, where bipolar filaments of myosin-II interdigitate between actin filaments to form the contractile units of the muscle known as sarcomeres. Class II myosins also generate contractile force or tension in other types of actin arrays such as stress fibers, the lamellipodial actin array, the contractile ring formed during cytokinesis, and the circumferential ring associated with adherens junctions. Class I myosins have been associated with force/tension generation as well. An important example of class I myosin function is in intestinal microvilli, where Myo1a

mediates tension between the actin bundle at the core of the microvilli and the sheath of plasma membrane that surrounds it (Tyska and Mooseker, 2002; Tyska et al., 2005).

Cell adhesion, protrusion, and motility. Myosins from several classes play diverse roles in cell-substrate adhesion, the formation of protrusive actin structures, and cell migration. As mentioned previously, class II myosins can generate tension and contraction in actin networks. These myosin-mediated forces are necessary during cell migration when a cell must extend its lamella forward, create traction against its substrate, and retract its trailing end. Class II myosins appear to play important roles in each of the stages of cell migration (Vicente-Manzanares et al., 2009). Additionally, the Rho-GAP-containing myosin-IXb is thought to participate in rapid remodeling of the cytoskeleton during cell migration, where it strongly localizes to the leading edge of dynamic actin (van den Boom et al., 2007; Post et al., 1998).

The formation of actin-rich protrusive structures is important to cell migration and other cellular functions. Several myosins have been implicated in the formation and maintenance of such structures including class III, VII, X, and XV myosins. Myosin-III, -VII, and -XV can all be found in the long, thin stereocilia of the inner ear. Myosin-VII can be found in the short, thin microvilli of the intestine and kidney. Finally, myosin-X can be found in filopodia produced by various cell types. The role of myosins in the formation of actin-rich protrusions will be more extensively discussed in Chapter 3.

Endocytosis and exocytosis. Many myosins have been reported to participate in various stages of endocytosis and exocytosis. For example, myosin-VI is reported to function in clathrin-mediated endocytosis where it uses its minus-end directed motor activity to pull inward on forming vesicles and then traffics the newly formed vesicles to

the endosome (Sweeney and Houdusse, 2007). In contrast, class V myosins are known to participate in exocytosis, where they transport various types of secretory vesicles to the cell surface (Coluccio, 2008). Additionally, several myosins are reported to participate in the specialized uptake process of phagocytosis. In one specialized example, myosin-VIIa is required for the phagocytic function of retinal pigment epithelial cells, in which regular ingestion of the outer segment membrane is required for retina function (Gibbs et al., 2003).

Organelle movement and localization. The most extensively characterized examples of myosin-mediated movements of organelles come from studies in yeast where class V myosins power the transport of organelles from mother to daughter cells during cell division. In mammals, class V myosins have been reported to participate in the movement and tethering of the endoplasmic reticulum and in melanocytes, the trafficking of melanosomes (Coluccio, 2008). Interestingly, the novel class XIX myosin is implicated in the actin-based movement and positioning of mitochondria, as discussed in Chapter 5.

Cytoskeleton cross-talk. Remarkably, two myosins have been implicated in “cross-talk” between the actin, microtubule, and intermediate filament cytoskeletons. Myosin-Va has been reported to transport complexes containing intermediate filament subunits in neurons (Rao et al., 2002). Both myosin-Va (Cao et al., 2004) and myosin-X (Weber et al., 2004) can bind directly to microtubules. Moreover, myosin-Va can bind to the microtubule-associated proteins kinesin and EB1 and has been observed to step off of an actin filament and diffuse for a distance along a microtubule (Coluccio, 2008). These interactions might be important for mediating actin-microtubule interactions

during cell migration (Wehrle-Haller and Imhof, 2003) or for the transfer of cargoes from the microtubule cytoskeleton to the actin cytoskeleton.

Myosin function in the nucleus. Several myosins have been shown to localize to the nucleus, where they are thought to participate in transcription and other nuclear activities. A splice variant of myosin-Ic localizes to the nucleus where it has been shown to interact with RNA polymerase I and II to aid in transcription (Hofmann et al., 2006). In several cancer cell lines, myosin-VI is reported to localize to the nucleus and interact with RNA polymerase II. Additionally, inhibition of myosin-VI reduced mRNA levels (Vreugde et al., 2006). Lastly, exogenously expressed myosin-XVIb localizes to the nucleus during interphase in COS-7 cells, although the possible function of this myosin in the nucleus is still unknown (Cameron et al., 2007).

Myosins play a diverse role in cell biology by facilitating numerous processes across the landscape of the cell. Several human myosins, such as myosin-I, -II, and -V, have been studied extensively and many of their functions in the cell are well described. Other, novel human myosins, such as myosin-XVI, -XVIII, and -XIX are only recently being examined for their contribution to cell function. Research on all myosins will continue to surprise and intrigue, with new properties and functions revealed for the recently identified myosins as well as for those that have been studied for decades. In the following chapters of this dissertation, I address two myosins: myosin-X (Myo10) and the novel myosin-XIX (Myo19). I examine what we already know about myosin-X and its role in filopodia formation, discuss my research on these two proteins, and speculate on possible future directions for research regarding these two myosins.

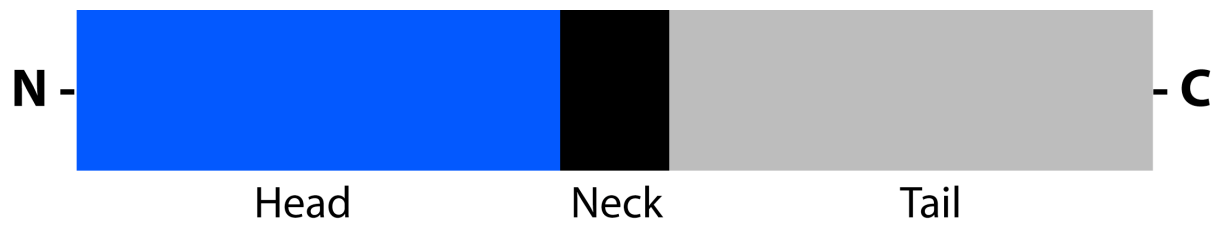


Figure 1.1. General domain structure of myosin motor proteins. Nearly all myosins can be divided into three main parts: a head (blue), a neck (black), and a tail (grey). The head, or motor, is responsible for binding actin and hydrolyzing ATP. The neck contains IQ motifs, which bind light chains. The tail is a variable region that can contain different domains to confer a myosin with a specific function.

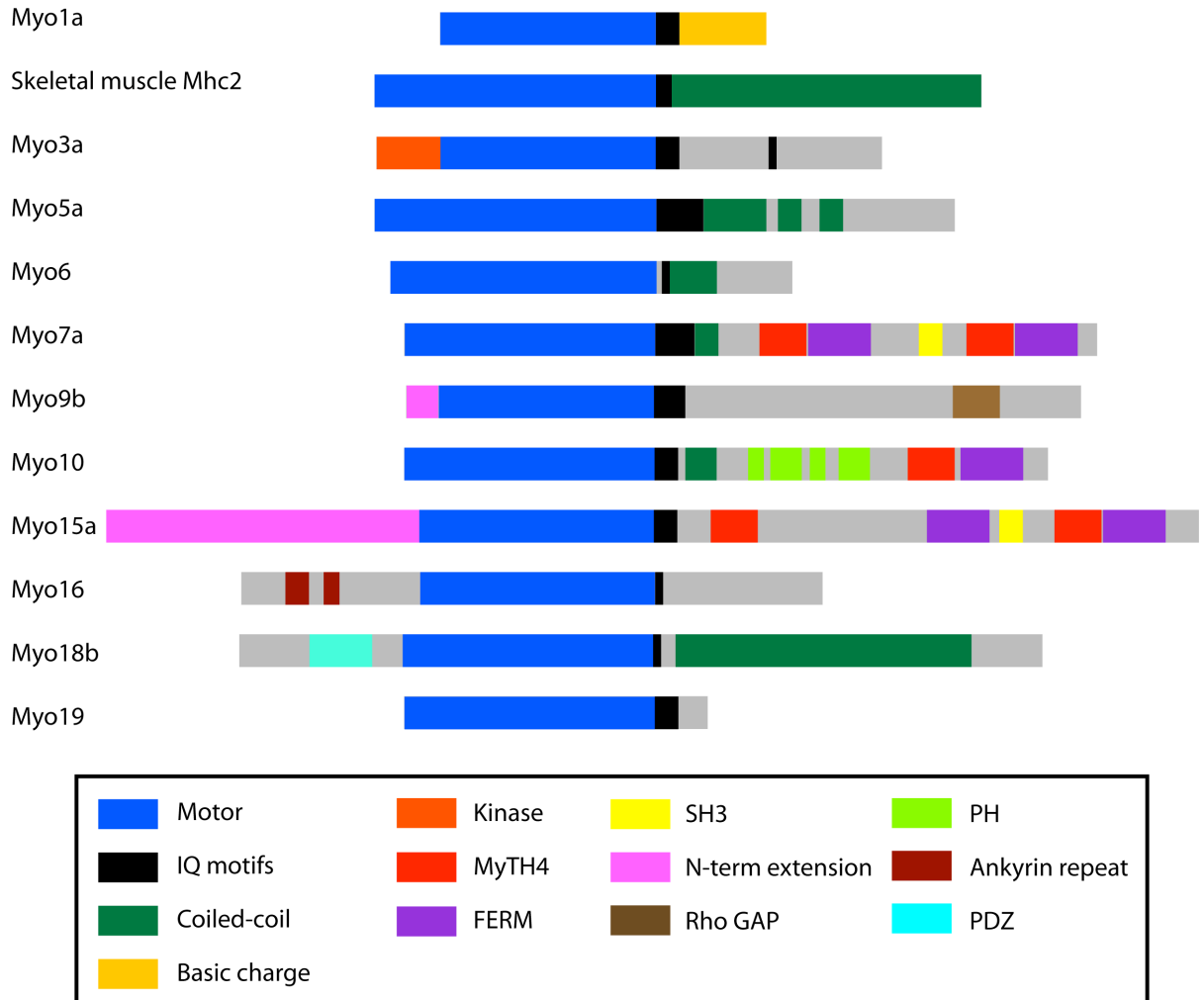


Figure 1.2. Human myosins contain a diverse array of protein domains. The domain architecture of representatives from each of the 12 classes of myosins expressed in humans is displayed using color-coded bars. MyTH4 (myosin tail homology 4), FERM (4.1, ezrin, radixin, moesin), SH3 (Src homology 3), PH (pleckstrin homology), PDZ (PSD95-DlgA-ZO1).

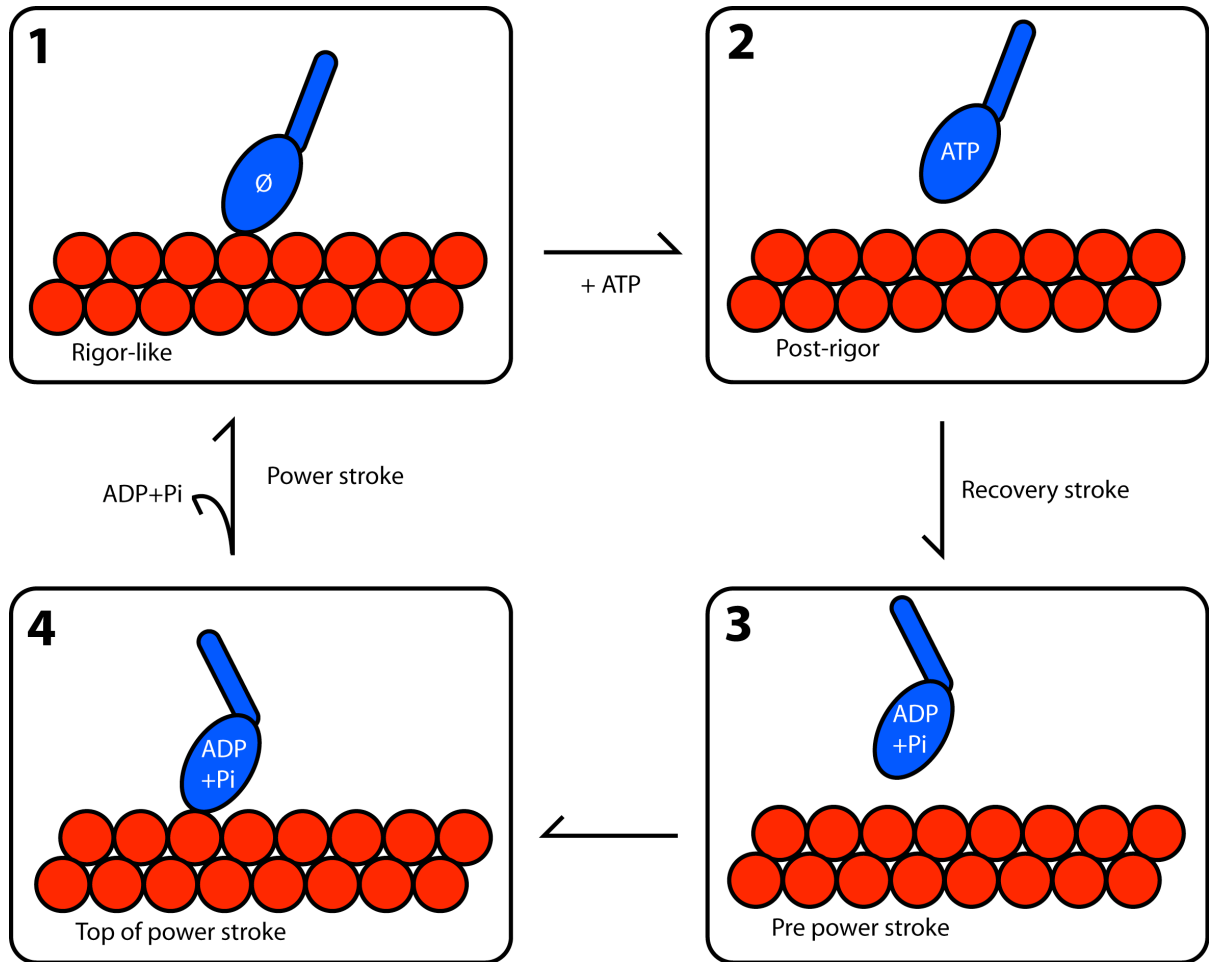


Figure 1.3. The mechanical myosin cycle. The myosin ATPase cycle is divided into four stages. Stage 1: in the absence of ATP (denoted by \emptyset), the motor binds tightly to the actin filament in a “rigor-like” state. Stage 2: once bound to ATP, the motor dissociates from the actin filament. The transition from stage 2 to 3 involves hydrolysis of ATP into ADP+Pi and the motor recovery stroke. Stage 3: the motor is bound to ADP+Pi and the pre-power stroke, or cocked, position. Stage 4: the pre-power stroke motor binds to the actin filament, releases ADP+Pi, and undergoes its power stroke. The cycle is complete and the motor returns to stage 1.

Table 1.1. Human myosin functional diversity

Function	Myosin class
Tension generation	I, II, VII
Cell adhesion, protrusion, and motility	I, II, III, V, VII, IX, X, XV
Endocytosis	
Clathrin-mediated	I, II, VI
Macropinocytosis	I, VI
Phagocytosis	I, II, VI, VII, X
Exocytosis	I, II, V, VI
Organelle movement and localization	V, VII, XIX
Cytoskeleton cross-talk	V, X
Nuclear function or transcription	I, VI, XVI

CHAPTER 2

MYOSIN-X: A MOLECULAR MOTOR AT THE CELL'S FINGERTIPS

INTRODUCTION

Myosins participate in a range of diverse processes within the cell including cell migration, membrane trafficking, and formation of cellular protrusions. These processes not only involve the movement and power generated by molecular motors, but also require the coordination of various cellular components. The tails of myosins allow these motors to interact with a range of intracellular components and confer them with the ability to perform many unique cellular functions. Several unconventional myosins (classes VII, X, XII, and XV) have been recognized to share a conserved structural feature in their tail domains – the presence of a myosin tail homology 4 (MyTH4) domain followed by a band 4.1, Ezrin, Radixin, Moesin (FERM) domain (Figure 2.1). Together, the myosins containing these domains within their tails comprise the MyTH4-FERM superclass of myosins (Berg et al., 2001). Myosin X (Myo10) is a member of the MyTH4-FERM superclass of myosins that is unique in that it contains pleckstrin homology (PH) domains. Although Myo10 is not present in *Drosophila* or *C. elegans*, it is present in sea squirt and sea urchin as well as vertebrates, indicating that Myo10 is deuterostome-specific. MyTH4-FERM myosins have been implicated in mediating membrane-cytoskeleton interactions and recent evidence

suggests that Myo10 is involved in filopodia formation, adhesion, phagocytosis, and actin-microtubule interactions. Through its unique collection of PH, MyTH4, and FERM domains, Myo10 appears to play several important roles within the cell. In this chapter I will discuss the structural, biochemical, and cell biological properties of Myo10.

STRUCTURE OF MYOSIN-X

Myo10 was initially identified in a PCR screen to detect novel myosins expressed in the inner ear (Solc et al., 1994). Examination of the motor domain of Myo10 revealed that it was not closely related to other known myosins; therefore, Myo10 became the founding member of a novel class of myosins called the class X myosins. The full-length heavy chain of Myo10 is an ~240 kDa protein that can be divided into a head, neck, and tail (Figure 2.1) (Berg et al., 2000; Yonezawa et al., 2000). Like other myosins, the head of Myo10 functions as a motor: it can bind to actin and hydrolyze ATP to produce movement and force (Homma et al., 2001). The head domain of Myo10 shares 35% sequence identity with the head domain of human skeletal muscle myosin II and is most similar (45%) to the head domain of Myo7a (Berg et al., 2000). The neck of Myo10 contains three IQ motifs, each of which is expected to bind to either calmodulin or calmodulin-like light chains (Berg et al., 2000). Although the identity of endogenous light chains of Myo10 is not yet clear, baculovirus expressed Myo10 can use calmodulin as its light chain *in vitro* (Homma et al., 2001; Homma and Ikebe, 2005; Kovacs et al., 2005). Additionally, Myo10 can bind to calmodulin-like protein (CLP), an epithelial-specific protein that is expressed during epithelial cell differentiation and down-regulated in several cancers (Chen et al., 2001; Rogers and Strehler, 2001).

Interestingly, expression of CLP increases Myo10 protein levels substantially, apparently by decreasing turnover of the protein (Bennett et al., 2007).

Based on sequence analysis, the first 130 amino acids of the Myo10 tail were initially predicted to form a coiled-coil, which led to the suggestion that Myo10 might form dimers (Berg et al., 2000). More recent analyses, however, have suggested that the first 36 amino acids of this region are likely to form a stable alpha-helix rather than a coiled-coil (Knight et al., 2005). Using several biochemical and biophysical techniques, Knight et al. showed that a peptide containing these 36 residues forms a highly stable single alpha-helix (SAH) in solution and thus hypothesized that this SAH functions to lengthen the lever arm. Interestingly, when a baculovirus-expressed heavy meromyosin (HMM)-like Myo10 construct consisting of the head, neck, and coiled-coil was imaged using electron microscopy (EM), approximately 90% of the molecules formed monomers and 10% formed dimers. Consistent with the hypothesized function of the SAH, the HMM Myo10 molecules that formed dimers had a greater distance between their heads than would be expected for a neck with three IQ motifs. Somewhat surprisingly, these dimers did not display a clearly visible region of coiled-coil and it was unclear if the dimers were parallel or anti-parallel. These data emphasize the importance of determining the properties and oligomerization status of *native full-length* Myo10. These data also raise the intriguing possibility that Myo10 may undergo regulated dimerization, as has been reported for myosin VI and the kinesin KIF1A (Klopfenstein et al., 2002; Park et al., 2006; Tomishige et al., 2002).

The coiled-coil region of Myo10 is followed by three PEST regions, which are rich in proline, glutamate, serine, and threonine. These sequences are associated with

increased susceptibility to cleavage by proteases such as the calcium-dependent protease calpain (Rechsteiner and Rogers, 1996). Indeed, Myo10 is a substrate for calpain *in vitro*, and it appears to be susceptible to cleavage at its PEST sequences (Berg et al., 2000). Cleavage of Myo10 in the PEST region would result in an HMM-like fragment as well as a fragment containing most of the tail. Cells may therefore generate multiple forms of Myo10: a full-length Myo10, an HMM-like-Myo10, and a tail fragment. Whether or not the Myo10 cleavage products have an important function *in vivo*, however, is not known.

Following the PEST region of Myo10 is a cluster of three pleckstrin homology (PH) domains. Indeed, this makes Myo10 unique, since Myo10 is the only known myosin with multiple PH domains. Although predictions based on initial genomic sequences suggested that chicken Myo10 contains five PH domains (Zhu et al., 2007), current genomic sequence indicates that chicken Myo10 contains only three PH domains and has an overall structure identical to other Myo10 proteins (a second Myo10-like sequence in chicken appears to be a pseudogene). The three PH domains have an unusual arrangement: the first PH domain of Myo10 (PH1) is split by the insertion of the second PH domain (PH2) (Figure 2.1). This insertion occurs precisely at the site of a highly variable surface loop where other PH domains have also been reported to contain large insertions (Macias et al., 1994; Musacchio et al., 1993). PH1 and PH2 show clear similarity to other known PH domains, most specifically to *Dictyostelium* protein kinase B homologs, whereas PH3 is not as well conserved (Berg et al., 2000). Analysis of the β 1- β 2 loop (Isakoff et al., 1998) reveals that PH2 and PH3 contain several conserved residues known to bind to phosphatidylinositol-3,4,5-

trisphosphate (PtdIns(3,4,5)P₃) (Berg et al., 2000; Tacon et al., 2004). Using a dot blot assay, a fusion protein consisting of all three PH domains bound with equal affinity to PtdIns(3,4,5)P₃ and PtdIns(3,5)P₂ and with 10-fold lower affinity to PtdIns(4,5)P₂ (Tacon et al., 2004). Additionally, PtdIns(3,4,5)P₃ is a product of PI3-kinase, and Myo10 PH2 has been shown to function downstream of PI3-kinase signaling in macrophage phagocytosis (Cox et al., 2002). Because signaling through PI3-kinase is important for numerous cell-biological processes, this result raises the possibility that Myo10 may function downstream of PI3-kinase in other cells as well. When expressed in cultured cells, GFP constructs consisting of the three PH domains are reported to localize to membrane ruffles, newly formed macropinosomes (Tacon et al., 2004), and dynamic sites of cell-cell contact (Yonezawa et al., 2003). Single-molecule imaging studies show that GFP-PH1-3 binds to the plasma membrane with a mean residence time of ~20s, indicating that the PH domains alone are sufficient for targeting to the plasma membrane (Mashanov et al., 2004).

The three PH domains in the tail of Myo10 are followed by a myosin tail homology 4 (MyTH4) domain. MyTH4 domains are relatively short – approximately 100 amino acids – but are well conserved. MyTH4 domains are present in several proteins including: 1) myosins of classes IV, VII, X, XII, and XV (Chen et al., 2001; Chen et al., 1996; Wang et al., 1998), 2) the plant kinesin protein KCBP (kinesin-like calmodulin-binding protein) (Reddy et al., 1996), and 3) a cytoplasmic protein implicated in axon guidance, known as MAX-1 (Huang et al., 2002). Although the precise functions of the MyTH4 domain are unclear, a portion of *Arabidopsis* KCBP containing the MyTH4 domain was found to bind to microtubules (Narasimhulu and Reddy, 1998). Excitingly,

the MyTH4 domain of *Xenopus* Myo10 was sufficient for binding to microtubules, although a longer construct that also contained the FERM domain appeared to bind more strongly (Weber et al., 2004). Myo10 may therefore provide a motorized link between the actin and the microtubule cytoskeletons.

The tail of Myo10 ends in a FERM domain, a domain originally discovered in Band 4.1, Ezrin, Radixin, and Moesin proteins. Although FERM domains exhibit relatively low overall protein sequence identity with one another (~20-50% identity between protein families), they have been identified in many proteins including talin, focal adhesion kinase (FAK), merlin (the neurofibromatosis 2 gene), and some tyrosine kinases and phosphatases. The FERM domain of Myo10 shares approximately 28% protein sequence identity to the FERM domain of talin. Several FERM domain-containing proteins serve as linkers between the actin cytoskeleton and integral membrane proteins (Chishti et al., 1998). Structural analysis of these proteins, such as radixin and moesin, reveals that FERM domains contain three subdomains: F1, F2, and F3. F1 shares similarity to the ubiquitin-like fold and F2 shares similarity to acetyl-CoA binding proteins. F3 is similar to the fold shared by PH, Ena-VASP homology (EVH1), and phospho-tryosine-binding (PTB) domains (Hamada et al., 2000; Pearson et al., 2000). This raises the possibility that the F3 subdomain may bind to ligands of these domains such as phosphoinositides, polyproline, or NPXY motifs. Importantly, two-hybrid experiments using the FERM domain of Myo10 revealed that it binds to the NPXY motif in the cytoplasmic domain of β_5 -integrin (Zhang et al., 2004). Moreover, mutations in the NPXY motif abolished this interaction. By immuno-precipitation and pull-down assays, the FERM domain of Myo10 also interacted with β_1 -integrin and β_3 -

integrin. Intriguingly, the well-characterized interaction between talin and β -integrins is mediated through the binding of the FERM domain of talin to the NPXY motif of the β -integrins (Campbell and Ginsberg, 2004). Although Myo10 binds β -integrins it shows little to no localization to focal adhesions; therefore, it is hypothesized to transport or anchor integrins in filopodia (Zhang et al., 2004). Importantly, it remains unknown if the FERM domain of Myo10, like that of talin, can activate integrins.

BIOCHEMICAL PROPERTIES OF MYOSIN X

Although the biochemical properties of full-length Myo10 have not yet been characterized, the properties of three truncated forms of Myo10 have been investigated. These baculovirus-expressed constructs include: 1) an HMM-like Myo10 construct consisting of the head, neck, and predicted coiled-coil (Homma et al., 2001), 2) a head+3IQ construct consisting of the head and three IQ motifs (Kovacs et al., 2005), and 3) a head+1IQ construct consisting of only the head and first IQ motif (Homma and Ikebe, 2005). *In vitro* motility assays with the HMM-Myo10 construct demonstrate that it is a barbed-end motor that translocates actin filaments at approximately 0.2-0.3 $\mu\text{m}/\text{sec}$ (Homma et al., 2001; Chen et al., 2001). Based on the surface concentrations required for sliding filament assays, the processivity of the HMM-Myo10 construct appeared to lie between non-processive myosins like skeletal muscle myosin II and highly processive motors like myosin Va. It should be noted, however, that the dimerization status of this construct was not shown and it is not clear if it exists as a monomer, a dimer, or a mixture of both species.

Two groups have recently performed detailed analyses of the kinetics of monomeric Myo10 constructs. Using a head+3IQ construct, Kovacs et al. measured an actin activated ATPase of $\sim 4 \text{ s}^{-1}$ at 25°C and calculated a duty ratio of $\sim 16\%$ (Kovacs et al., 2005). This duty ratio is intermediate between that of nonprocessive motors and highly processive motors. In addition, Kovacs et al. found that their Myo10 construct's "weak" actin-binding states exhibit surprisingly tight binding to actin. Given the high local concentration of actin filaments in filopodia, Myo10 would thus be expected to remain associated with actin much of the time. Under these conditions, formation of oligomers and/or tethering to the membrane via the tail might be expected to endow Myo10 with the ability to move forward in filopodia. Using a head+1IQ construct, Homma and Ikebe measured an actin activated ATPase of 13.5 s^{-1} and calculated a relatively high duty ratio of $\sim 60\%$ (Homma and Ikebe, 2005). The difference in the duty ratios reported by the two groups is puzzling given that there was general agreement in many of the other parameters, including the relatively high affinity of the weak binding states. An important goal for the future will thus be to resolve this difference and determine the single-molecule properties of Myo10 such as its processivity and step size.

Although *in vitro* experiments clearly show that calmodulin can bind to Myo10's IQ motifs and function as a light chain, the identity of the endogenous Myo10 light chains is less clear. In epithelial cells, calmodulin-like protein (CLP) has been identified as a light chain for Myo10 (Rogers and Strehler, 2001). CLP appears to bind most strongly to the third IQ motif (Rogers and Strehler, 2001). Importantly, both calmodulin and CLP bind to Ca^{++} , but CLP exhibits an approximate eight-fold lower

affinity for Ca⁺⁺. Homma et al. reported that increasing Ca⁺⁺ to 10 uM led to dissociation of one mole of calmodulin and inhibited the ATPase and motility of HMM-Myo10 (Homma et al., 2001). As with several other unconventional myosins, it is not yet clear if the Ca⁺⁺ regulation observed *in vitro* is a major form of regulation *in vivo*.

CELL BIOLOGICAL FUNCTIONS OF MYOSIN X

Myo10 is expressed at relatively low levels in most mammalian cells and tissues (Berg et al., 2000). Most human tissues express a ~9.2 kb transcript encoding full-length Myo10 (Berg et al., 2000), and a similar distribution of Myo10 transcripts is observed in mouse tissues (Yonezawa et al., 2000). In situ localization studies showed clear localization of Myo10 transcripts in the Sertoli cells of the seminiferous tubule and in the Purkinje cells of the cerebellum (Berg et al., 2000; Yonezawa et al., 2000). Based on immunoblotting, the Myo10 heavy chain is particularly abundant in testis and kidney. Lastly, proteomic analysis of bovine adrenal medulla tissue identified Myo10 as one of 71 proteins present in the adrenal medulla, with myosin II being the only other myosin identified (Jalili and Dass, 2004).

One of the most fascinating features of Myo10 is its striking localization to the tips of filopodia (Figure 2.2) (Berg et al., 2000; Berg and Cheney, 2002). Filopodia are long, slender cellular extensions consisting of a core of parallel bundled actin filaments surrounded by plasma membrane. Filopodia can dynamically extend and retract to interact with the extracellular environment and are widely hypothesized to function as organelles of exploration, adhesion, and signaling. The actin filaments within a filopodium are oriented with their barbed end – the site of actin polymerization –

located towards the tip of the filopodium. Although significant progress has been made in understanding the ARP2/3-dependent actin polymerization machinery responsible for lamellipodial extension (Pollard and Borisy, 2003), the mechanisms that regulate filopodial actin polymerization are unclear. Subsequently, there is much interest in the molecules present at the filopodial tip. Classic electron microscopy images of actin filaments in microvilli, which are structurally similar to filopodia, reveal that actin filaments insert into a dense “fuzz” at the tips of the microvilli (Mooseker and Tilney, 1975). Over thirty years later, the nature of ‘tip-complex’ components, such as Myo10, are being investigated for their role in filopodial actin polymerization, adhesion, and signaling.

How does Myo10 get to the tip of the filopodium? Since the actin filaments within the filopodium have their barbed ends oriented towards the tip, one might expect that Myo10 simply uses its motor activity to move along the filopodial actin filaments until it reaches the tip. Consistent with this hypothesis, a “head-less” construct lacking most of the motor fails to localize to the tips of filopodia, thus demonstrating that the head domain is necessary for tip localization (Figure 2.3) (Berg and Cheney, 2002; Sousa et al., 2006). Furthermore, an HMM-like Myo10 consisting of the head, neck, and coiled-coil is sufficient for localization to the tips of filopodia. Interestingly, a construct containing only the head and neck, which lacks the coiled-coil domain, does not localize to the tips of filopodia. This result demonstrates that the coiled-coil domain is necessary for tip localization and suggests that Myo10 can only localize to filopodia when it forms a dimer. Although the results of Knight et al show that only 10% of the species of HMM-Myo10 viewed by electron microscopy were

dimers (Knight et al., 2005), in cells, other factors such as high local concentrations or the presence of the tail might favor dimerization. Full-length Myo10 might also undergo regulated dimerization, as has been reported for the kinesin KIF1A (Klopfenstein et al., 2002; Tomishige et al., 2002). KIF1A dimerization is regulated through its PH domains, which bind to PtdIns(4,5)P₂ on membranous organelles to bring individual kinesins within close proximity. Perhaps different PtdIns densities throughout the cell facilitate Myo10 dimerization in select intracellular locations, such as in filopodia. Indeed, the precise dimerization status and mechanisms of regulation of Myo10 remain unclear, but are of great interest and importance.

In addition to Myo10, it is now known that Myo3a, Myo15a, and *Dictyostelium* myosin VII localize to the tips of filopodia-like structures (Belyantseva et al., 2003; Rzadzinska et al., 2004; Schneider et al., 2006; Tuxworth et al., 2001). How do these myosins selectively recognize filopodial actin, while others do not? One possibility is that filopodial actin filaments are associated with proteins that allow Myo10 to distinguish them from other actin filaments within the cell, or vice versa. The presence of the bundling protein fascin or the absence of specific tropomyosins, for example, might distinguish filopodial actin filaments from other filaments. It will thus be important to determine how Myo10 ‘recognizes’ filopodial actin filaments as well as how other myosins are excluded from filopodia

Live-cell imaging of GFP-tagged Myo10 expressed in cell culture reveals a remarkable phenomenon: punctae of GFP-Myo10 undergo fast, forward movements towards the tips of filopodia, as well as slower, rearward movements back towards the cell body collectively termed “intrafilopodial motility” (Figure 2.4) (Berg and Cheney,

2002). The average velocities of GFP-Myo10 within the filopodium are reported to be $\sim 0.1 \mu\text{m/s}$ for forward movements and $\sim 0.015 \mu\text{m/s}$ for rearward movements. The rearward movements of GFP-Myo10 occur at a rate similar to retrograde actin flow and the forward movements of GFP-Myo10 occur at a rate slightly slower than the average velocity reported from *in vitro* motility assays with HMM-Myo10 ($0.2\text{-}0.3 \mu\text{m/s}$) (Homma et al., 2001; Chen et al., 2001). The forward movements of GFP-Myo10 are thus hypothesized to be a result of the motor activity of Myo10 moving it along the filopodial actin filaments faster than the opposing retrograde flow, whereas the rearward movements are hypothesized to be a result of binding to actin filaments as they undergo retrograde flow (Berg and Cheney, 2002).

Since Myo10 shows such striking localization to and movements within filopodia, there is much interest in the role that Myo10 plays in the formation of these cellular extensions. Interestingly, deletion of myosin VII, a MyTH4-FERM myosin in *Dictyostelium*, results in inhibition of filopodia formation (Tuxworth et al., 2001). Initial studies examining filopodia formation in COS-7 cell, which normally extend few filopodia, revealed that over-expression of Myo10 results in ~ 4 -fold increase in the number of substrate-attached filopodia, as well as an increase in the average length of filopodia (Berg and Cheney, 2002). Importantly, the filopodia-promoting effect of Myo10 required both its tail and its head, since neither HMM-Myo10 nor head-less Myo10 were able to induce filopodia formation (see Figure 2.3). Although these results were quite striking, the experiments focused only on substrate-attached filopodia. By employing the technique of scanning electron microscopy (SEM), Bohil et al were able to visualize the filopodia on the dorsal surface of the cell. Consequently, they revealed

that over-expression of Myo10 in COS-7 results in a >500-fold increase in the number of dorsal filopodia produced (Figure 2.5) (Bohil et al., 2006). On the other hand, knockdown of Myo10 in HeLa cells, which normally produce many filopodia, resulted in a dramatic decrease in the number of dorsal filopodia produced from ~860/cell to ~200/cell. Additionally, the impressive filopodia-promoting activity of Myo10 appears to be: 1) independent of VASP (vasodilator-stimulated phosphoprotein) family proteins, which localize to the tips of and induce filopodia, and 2) downstream of Cdc42, which functions as a “master regulator” of filopodia formation (Bohil et al., 2006). Together, these experiments demonstrate that Myo10 has a central role in both dorsal and substrate-attached filopodia formation.

The intrafilopodial motility of Myo10 raises the question, why is Myo10 traveling to and from the tips of filopodia? One possibility is that Myo10 functions to carry specific cargos to the tips of filopodia, perhaps for filopodia formation, stabilization, or other filopodia-specific functions (Figure 2.6). In this regard, it has been reported that Myo10 can bind to, co-localize with, and exhibit co-transport with the filopodia-promoting proteins Mena and VASP (Quintero et al., 2003; Tokuo and Ikebe, 2004). Mena/VASP proteins bind to the barbed ends of actin filaments, thus antagonizing the function capping protein and promoting filament growth. While this raises the possibility that Myo10 may transport materials involved in filopodia formation, over-expression of Myo10 can promote filopodia in the absence of Mena/VASP proteins (Bohil et al., 2006). Thus, the significance of the Mena/VASP-Myo10 interaction remains unclear. Excitingly, another MyTH4-FERM myosin, Myo15,

has recently been shown to transport the PDZ protein whirlin, to the tips of stereocilia (Belyantseva et al., 2005).

Another possible cargo for Myo10 is β -integrins. The FERM domain of Myo10 can bind to the NPXY motif found on the cytoplasmic tails of several β -integrins (Zhang et al., 2004). This interaction may be similar to the well-characterized interaction between the FERM domain of talin and the NPXY motifs on several β -integrins (Campbell and Ginsberg, 2004; Calderwood et al., 2002; Ratnikov et al., 2005). Knockdown of Myo10 resulted in decreased integrin-mediated cell adhesion to the extra-cellular matrix, whereas mutation of the Myo10 FERM domain prevented integrin localization to filopodia and elongation of substrate-attached filopodia. The interaction between Myo10 and integrins allows tethering of the filopodial actin filaments to the extra-cellular matrix. Working as a “molecular clutch”, Myo10 may couple retrograde-flowing actin to integrin-mediated adhesions, thereby stabilizing the filopodial structure and aiding in elongation. Integrin localization to filopodial tips has been documented (Grabham et al., 2000) and filopodia are hypothesized to function as specialized sites of adhesion. Since filopodia formation and adhesion are an important part of several physiological phenomena such as neuronal outgrowth, angiogenesis, and phagocytosis, Myo10 might play a crucial role in these processes by transporting integrins and/or stabilizing adhesive structures during filopodia formation.

With its ability to carry cargos to the tips of filopodia, Myo10 may function as part of a ‘mobile polymerization complex’ as a means to promote filopodia formation and elongation. This is evidenced by the interaction of Myo10 with VASP, which facilitates actin polymerization, as well as with integrins, which provide stabilization by

binding to the ECM. As an alternative to carrying cargos to the tips of filopodia that are necessary for their formation, Myo10 may provide mechanical forces that directly facilitate filopodial actin polymerization at the tip. Using its motor activity, Myo10 could potentially push the plasma membrane away from the barbed end to create space to allow for the addition of actin subunits at filopodial tips.

Besides its role in filopodia formation, Myo10 appears to have several other cell biological roles. Using mouse and bovine macrophages, Cox et al showed that Myo10 is a downstream effector of PI3-kinase during phagocytosis (Cox et al., 2002). During phagocytosis, macrophages use cellular extensions such as filopodia, pseudopodia, and cup-like structures to contact and engulf foreign particles. Myo10 localizes to the phagocytic cup in macrophages and this localization is disrupted in the presence of the PI3-kinase inhibitor wortmannin. PI3-kinase and its lipid products are required for phagocytosis (Cox et al., 1999; Marshall et al., 2001), and Myo10's tail contains PH domains capable of binding to those lipid products. Although inhibition of Myo10 by antibody injection reduced phagocytic ability by over 50%, it is still unclear precisely what Myo10 is doing in phagocytosis. Myo10 may play a role in receptor localization, particle binding, filopodia/pseudopodia/cup formation and extension, or phagosome closure. Additionally, whereas Cox et al. examined Myo10 function during Fc-receptor-mediated phagocytosis, they did not examine if Myo10 plays a role in complement-mediated phagocytosis, which is mediated by β_2 -integrins. Since Myo10 is already known to interact with β_1 -, β_3 -, β_5 -integrins, it will be interesting to determine if Myo10 also participates in complement-mediated phagocytosis. Lastly, *Dictyostelium* myosin

VII, a MyTH4-FERM myosin found in *Dictyostelium*, is required for phagocytosis (Titus, 1999).

Research with *Xenopus* oocytes indicates that Myo10 can also interact with microtubules (Weber et al., 2004). Interactions between actin and microtubules are important for a variety of cell-biological processes, particularly during mitosis (Rodriguez et al., 2003). Weber et al found that *Xenopus* Myo10 associates with microtubules both *in vitro* and *in vivo*, and localizes to the meiotic spindle in oocytes. Myo10 staining in oocytes was most intense at areas where the spindle-microtubules contacted the F-actin rich cell cortex. Importantly, Weber et al demonstrated that Myo10 is required for both microtubule-dependent, asymmetric anchoring of the oocyte nucleus, and F-actin-meiotic spindle association. The disruption of Myo10 in *Xenopus* oocytes recapitulated the phenotypes displayed by disrupting microtubules or F-actin. Inhibition of Myo10 did not disassemble either cytoskeletal system, suggesting that Myo10 serves to link the microtubules and F-actin.

Recent experiments indicate that Myo10 is also necessary for spindle orientation in cultured mammalian cells (Toyoshima and Nishida, 2007). This work shows that in nonpolarized cells, integrin-mediated adhesion orients the mitotic spindle parallel to the substrate. Knockdown of Myo10 in cell culture results in spindle misorientation, whereas knockdown of myosin IIa and/or myosin IIb does not. In this system, as in *Xenopus*, disruption of Myo10 recapitulates the spindle phenotype presented following F-actin disruption. It appears that Myo10 is necessary for proper actin reorganization during mitosis and may provide a link between integrins, actin, and microtubules. It will therefore be exciting to determine if Myo10 participates in other actin-microtubule

interactions such as those involved in directed cell migration, neuronal growth cone guidance, and cellular wound healing (Rodriguez et al., 2003).

Myo10 also appears to have important roles in brain and neurons. Interestingly, brain expresses a "headless" form of Myo10 that is identical to full-length Myo10 except that it lacks most of the motor domain (Sousa et al., 2006). Headless Myo10 lacks motor activity, is unable to localize to the tips of filopodia, and does not induce filopodia. Headless Myo10 does have a domain structure similar to that of MAX-1 (motor axon guidance-1), a protein that is required for proper guidance of motor neurons via netrin signaling (Huang et al., 2002). In mouse cerebrum, full-length and headless Myo10 show dramatic developmental regulation, with peak expression of both occurring early in postnatal development when cortical neurons elaborate numerous filopodia and form synapses. Myo10 is also up-regulated approximately eight-fold following crush injuries to peripheral nerves, which suggests a possible role in nerve regeneration (Tanabe et al., 2003).

Exciting recent research has revealed that Myo10 interacts with the netrin receptors DCC (deleted in colorectal cancer) and neogenin (Zhu et al., 2007). Netrin is an extracellular guidance cue that is thought to work through DCC and neogenin to regulate axon path-finding during development. Myo10 binds to the cytoplasmic tails of both these receptors, and the FERM domain of Myo10 is required for this interaction. Over-expression and knockdown studies of Myo10 indicate that Myo10 may be involved in targeting DCC to neurites, thus influencing neurite outgrowth. Additional experiments revealed that DCC, which has attractive effects, and neogenin, which has

repulsive effects, may differentially regulate Myo10 function. Importantly, expression of a motor-less Myo10 in chicken embryos impaired neuronal axon projection.

Interestingly, Myo10 has been reported to be dramatically up-regulated in several different settings. In macrophages challenged with *Mycobacterium*, Myo10 expression is up-regulated more than twenty-fold (Blumenthal et al., 2005). Myo10 is also up-regulated 10- to 40-fold in mouse epidermal neural crest stem cells (Hu et al., 2006). Additionally, Myo10 is reported to be up-regulated 12-fold in acute lymphoblastic leukemia (Ross et al., 2003). These changes in expression suggest important roles for Myo10 in many physiological processes.

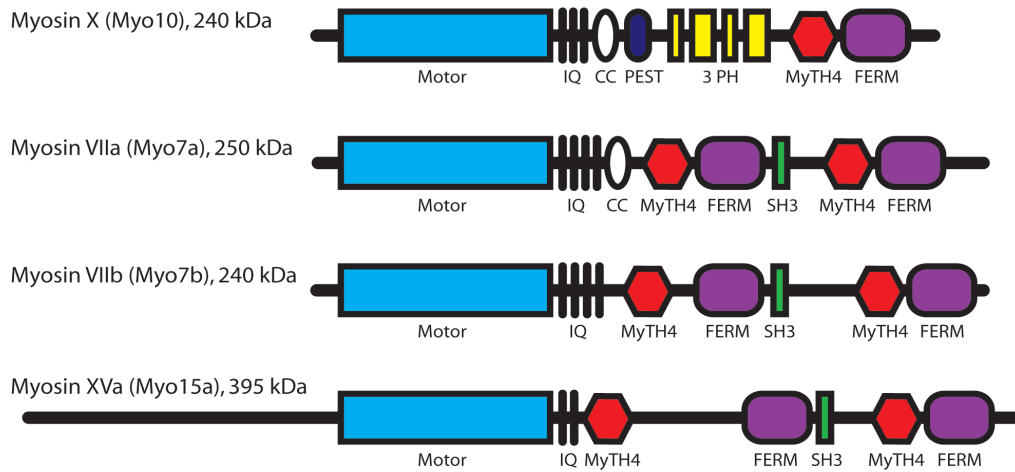
OUTSTANDING QUESTIONS

Since the initial identification of Myo10, interest in this unique myosin continues to grow. Although the basic properties and functions of Myo10 are beginning to come to light, many important and exciting questions surround Myo10. First, what are the single-molecule properties of Myo10? Is it a dimer? Can it move processively? Does the full-length molecule have unique properties? Second, how does Myo10 promote filopodia and what components are required? It will be critical to pick apart both the signaling pathways and cellular machinery that lead to filopodia formation and determine how Myo10 fits in. Third, what is the structure of the MyTH4 domain and what abilities does this bestow upon Myo10? It will be important to determine if, via its MyTH4 domain, Myo10 is responsible for coordinating the actin and microtubule cytoskeletons for a variety of cellular phenomena. Lastly, what are Myo10's roles in physiological processes such as immune function, wound healing, and cancer

progression? From the molecular details of Myo10, to its cellular and physiological functions, there is much to explore about this molecular motor at the cell's fingertips.

The text and figures in this chapter were reproduced with kind permission of Springer Science and Business Media from the following book: *Myosins: A Superfamily of Molecular Motors*, "Chapter 14: Myosin-X", pages 403-416, figures 14.1, 14.3, 14.5, 14.5, and 14.6, written by Melinda M. DiVito and Richard E. Cheney, edited by Lynne M. Coluccio, Copyright 2008 Springer.

(A) MyTH4-FERM myosins in humans



(B) Working model of Myo10 structure

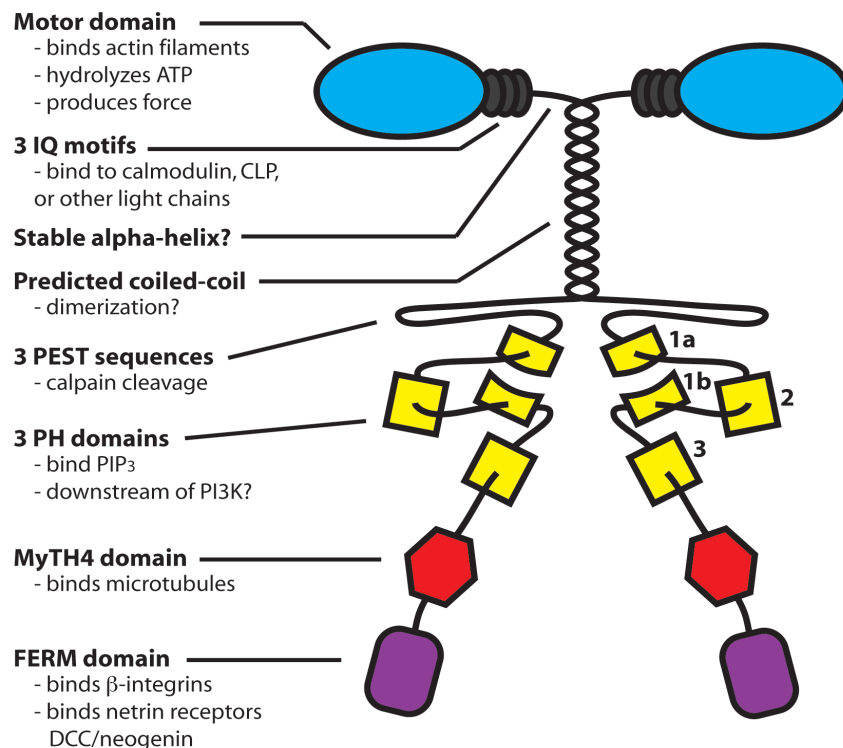


Figure 2.1. Myo10 is a MyTH4-FERM myosin. (A) The primary structures of the four MyTH4-FERM myosin proteins in humans. MyTH4-FERM myosins are defined by the presence of a Myosin Tail Homology 4 (MyTH4) domain followed by a band 4.1, Ezrin, Radixin, Moesin (FERM) domain. Myo10 is unique among MyTH4-FERM myosins in that it contains three PH domains. (B) Working model of Myo10 depicting the domain arrangement as well as the domain functions described in the text. Although the Myo10 heavy chains are shown here as parallel dimers, the actual structure of native Myo10 is not yet known.

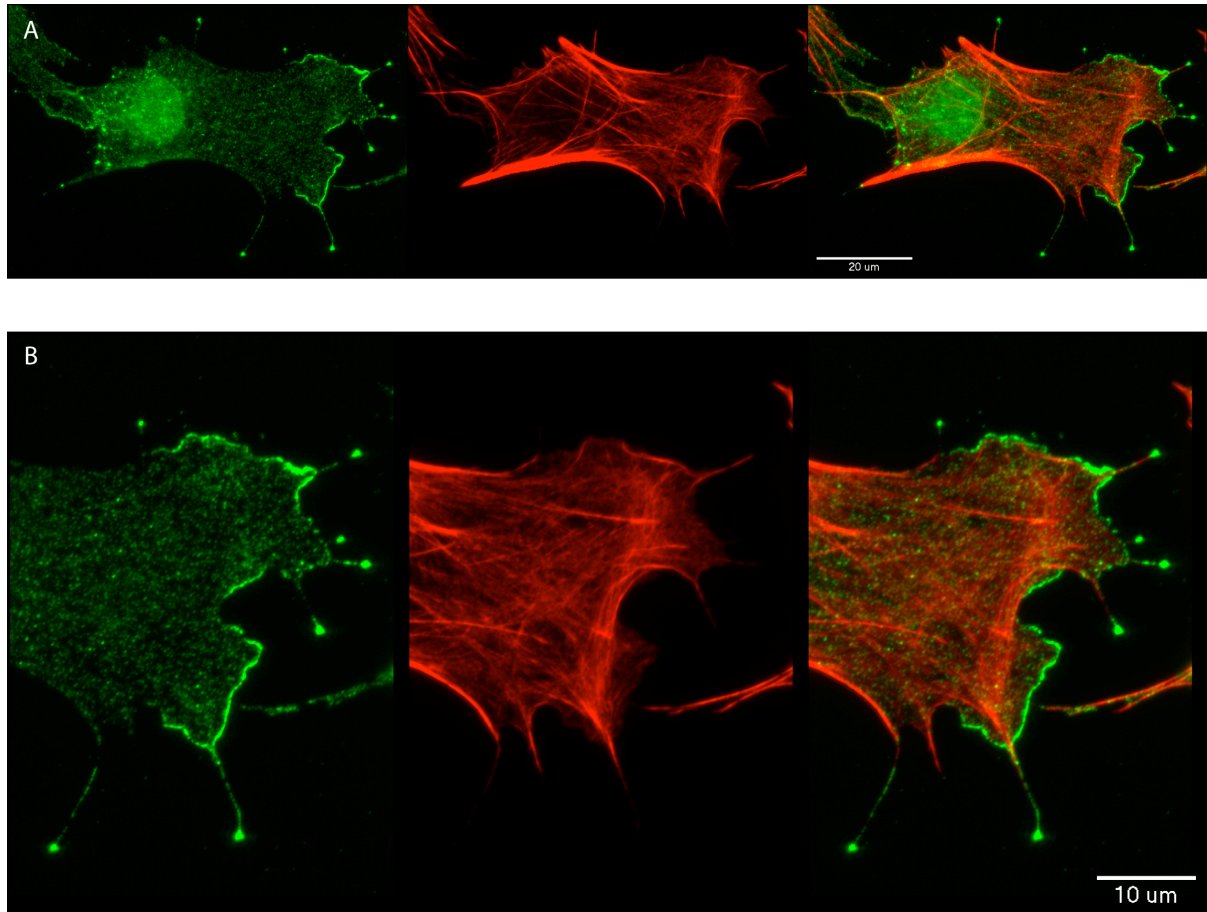


Figure 2.2. Myo10 localizes to the tips of filopodia. (A) Immunostaining of endogenous Myo10 (green) and phalloidin staining of actin (red). In this BAEC cell, Myo10 is present at the tips of filopodia and also at the edges of some lamellipodia. Endogenous Myo10 generally localizes to the tips of filopodia as well as other regions of dynamic actin such as membrane ruffles, the leading edge of lamellipodia, and phagocytic cups. A close-up of the right half of the cell is shown in (B).








Myo10 construct		Tip localization	Filopodia induction
Full-length		+	+
"FERM-less"		+	+
"MyTH4-FERM-less"		+	-
"HMM"		+	-
Head-neck		-	-
Coiled-coil		-	-
Head-less isoform		-	-

Figure 2.3. Myo10 domains required localization to filopodial tip and induction of dorsal filopodia. This chart summarizes the results of expression studies with a series of Myo10 deletion constructs. Note that the motor domain is necessary for tip localization and that the HMM construct is sufficient for tip localization. The "coiled-coil" region is also necessary for tip localization since the head-neck construct fails to localize to filopodial tips. Deletion of either the motor or the MyTH4-FERM region blocks the ability to induce dorsal filopodia.

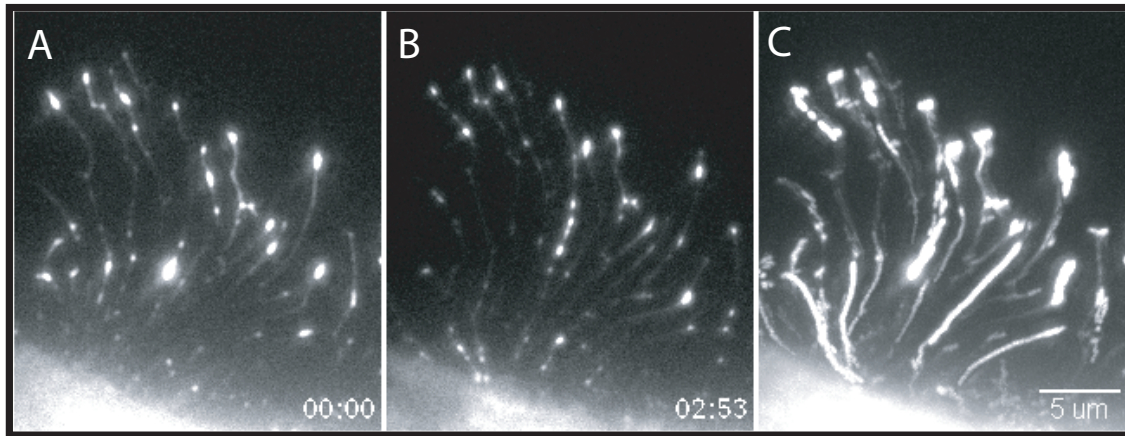


Figure 2.4. GFP-Myo10 undergoes intrafilopodial motility. HeLa cells expressing a GFP-tagged Myo10 were imaged by time-lapse microscopy to reveal the striking movements of GFP-Myo10 to and from the tips of filopodia. In this example of intrafilopodial motility, the first (A) and last (B) frames from a 2 minute and 53 second time-lapse experiment are shown. To highlight the forward and rearward movements of puncta of GFP-Myo10 within substrate-attached filopodia shown here, a maximum projection of all of the frames of the time-lapse movie is shown in (C). The streaks of fluorescence signal in the maximum projection represent the paths that punctae of Myo10 traveled throughout the time-lapse experiment. A copy of the time-lapse movie used to make this figure is available on the supplementary DVD as Movie 2.1.

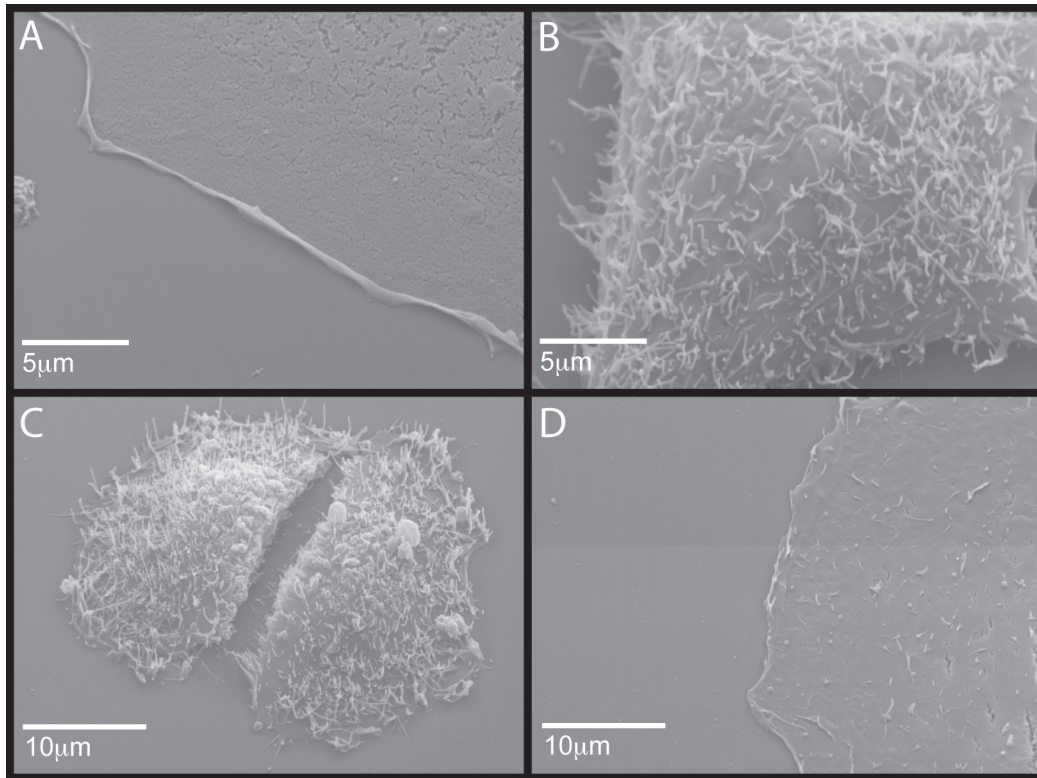


Figure 2.5. Myo10 is a potent regulator of filopodia formation. (A) Scanning electron micrograph of a control COS-7 cells expressing GFP. (B) Scanning electron micrograph of a COS-7 cells expressing GFP-Myo10. Control COS-7 cells are essentially 'bald' and extend very few dorsal filopodia. Expression of GFP-Myo10 leads to a massive increase in dorsal filopodia formation. (C) Scanning electron micrograph of a control HeLa cell treated with non-specific siRNA. (D) Scanning electron micrograph of a HeLa cell treated with Myo10-specific siRNA. In HeLa cells, a cell type that normally extends numerous filopodia, knockdown of Myo10 suppresses dorsal filopodia formation. Images courtesy of Aparna Bohil.

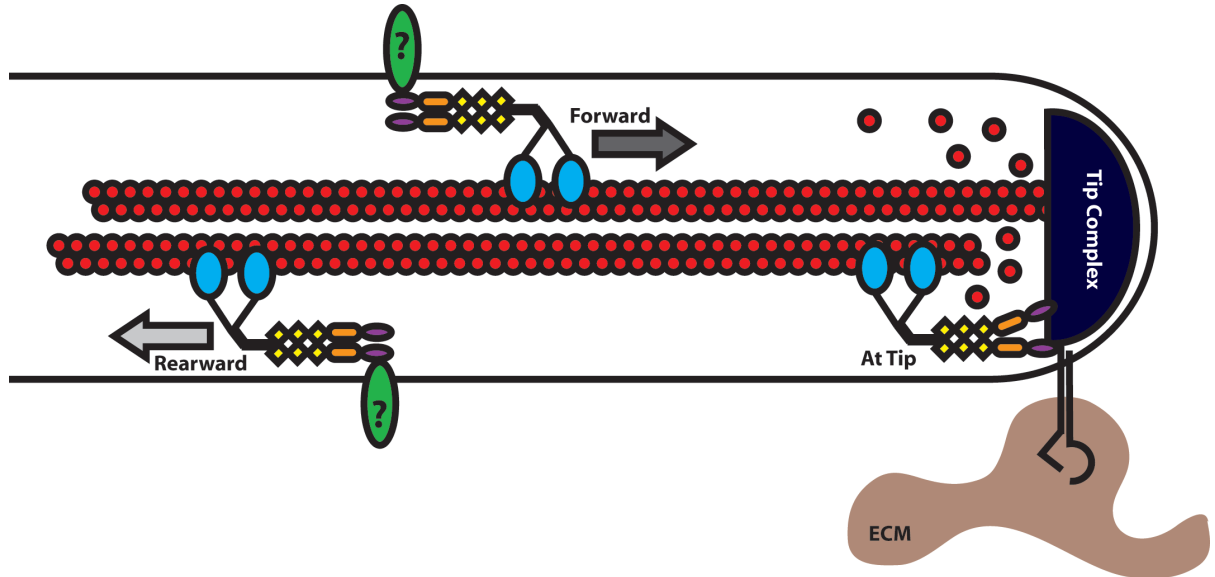


Figure 2.6. Schematic representing intrafilopodial motility of Myo10. In this model, actin filaments within the filopodium polymerize at their barbed ends, which are oriented towards the tip of the filopodium. The actin filaments within filopodia undergo constant rearward movement towards the cell body. This continuous flux of actin is known as retrograde flow. To overcome retrograde flow and travel to the tips of filopodia, it is hypothesized that Myo10 activates its motor activity and moves forward ('forward' arrow). Conversely, to travel rearward within the filopodium, it is hypothesized that Myo10 simply binds to actin and 'piggybacks' back to the cell body with retrograde flow of actin ('rearward' arrow). Candidate cargoes such as integrins and VASP proteins are indicated by question marks. Myo10 is also shown as part of a putative filopodial tip complex that may also provide a linkage between filopodial actin filaments, integrins, and the extracellular matrix (ECM).

CHAPTER 3
POINTING FINGERS: HOW THE CELL CREATES, MAINTAINS, AND EMPLOYS
FILOPODIA

FILOPODIA FUNCTIONS

Filopodia are long, slender cellular protrusions that dynamically extend and retract to interact with the extracellular environment. These finger-like extensions have a core of parallel bundled actin and contain various actin-binding, cell-signaling, and trans-membrane proteins. Filopodia are widely hypothesized to function as organelles of exploration, adhesion, and signaling, as evidenced by their participation in a diverse range of physiological processes. For example, during cell adhesion and spreading, integrin-rich filopodia are responsible for making the initial contacts between the cell and the extracellular matrix (Partridge and Marcantonio, 2006). Furthermore, some cell types appear to use these primary filopodial contacts as a guide for focal adhesion assembly; these cells assemble focal adhesions directly behind the initial filopodial adhesions, near the base of the filopodium (Steketee and Tosney, 2002; Schafer et al., 2009). Integrin-rich filopodia can also play a role in cell migration, where lamellipodia and filopodia with active, but unliganded, integrins at their tips probe the surrounding environment for adhesive migratory cues (Galbraith et al., 2007).

The participation of exploratory filopodia in cell adhesion and migration is critical to many processes during development and has been most extensively studied in neurons. During neuronal migration and path finding, growth cone filopodia dynamically survey the extracellular environment for migratory guidance cues and orient towards gradients of these factors (Davenport et al., 1993; Zheng et al., 1996; Rajnicek et al., 2006). Filopodia orientation towards a chemoattractant gradient is a key signal for extension, turning, or branching of the growth cone in the direction of the gradient to (Lowery and Van Vactor, 2009). In addition to neuronal path finding, filopodia are also crucial for neurite formation (Smith, 1994); in the absence of filopodia formation, cultured neurons could not initiate neurites, the precursors of axons and dendrites (Dent et al., 2007). Last, filopodia appear to function as precursors in the formation of dendritic spines (Yoshihara et al., 2009).

Filopodia participate in developmental processes outside of the brain as well. During angiogenesis, “tip cells” lead chains of migrating endothelial cells towards VEGF gradients (Gerhardt et al., 2003). These endothelial pioneers extend long filopodia that contain VEGF receptors at their tips. Akin to growth cone filopodia, tip cell filopodia sense VEGF gradients and dictate the direction of cell migration (De Smet et al., 2009). In addition to their role during development in endothelial cells, filopodia are key to the function of epithelial cells as well. Moreover, the adhesive nature of filopodia is not limited to cell-substrate interactions, as cadherins are reported to associate with filopodia tips to mediate epithelial cell-cell adhesions. Cadherin-rich filopodia from opposing epithelial cells make contact and interdigitate to facilitate a process known as “adhesion zippering” during *Drosophila* embryo dorsal closure (Wood et al., 2002;

Millard and Martin, 2008). Similarly, epithelial sheet fusion in *C. elegans* (Raich et al., 1999) and in cultured epithelial cells (Vasioukhin et al., 2000) display filopodia dependent behaviors.

Outside of development, filopodia have many other important physiological functions. In the immune system, macrophages have been observed using filopodia to survey the environment for infectious particles. Once bound, a macrophage filopodium can “wrangle in” the particle, bringing it closer to the cell body for phagocytosis (Kress et al., 2007; Vonna et al., 2007). Other immune cells such as monocytes, neutrophils, and lymphocytes are covered with short filopodia that dynamically interact with the endothelium (von Andrian et al., 1995). These filopodia-mediated interactions are important for the rolling, adhering, and migrating stages that culminate in trans-endothelial migration (Barreiro and Sanchez-Madrid, 2009; Shulman et al., 2009). Furthermore, there are several reports of a reciprocal interaction of the endothelium with leukocytes, in which endothelial cells uses adhesion-rich filopodia to grasp a leukocyte and direct it towards a favorable site for transmigration (Barreiro et al., 2002; Carman et al., 2003; Carman and Springer, 2004). Excitingly, more recent research has implicated filopodia in the transmission of several types of viruses from an infected cell to neighboring uninfected cells (Sherer et al., 2007; Kolesnikova et al., 2007; Mercer and Helenius, 2008; Zamudio-Meza et al., 2009).

FILOPODIA ARCHITECTURE AND DYNAMICS

Filopodia typically consist of a core of approximately 10-40 parallel bundled actin filaments sheathed in plasma membrane and are approximately 100 nanometers

in diameter (Lewis and Bridgman, 1992; Katoh et al., 1999). The actin filaments within a filopodium are oriented with their barbed ends – the site of actin polymerization – located towards the tip of the filopodium (Lewis and Bridgman, 1992; Mallavarapu and Mitchison, 1999). As visualized by electron microscopy, the barbed ends of filopodial actin filaments terminate in the filopodia tip complex, an electron-dense aggregation, whereas the actin at the base of the filopodium is often rooted and entangled within the web of lamellapodial actin (Figure 3.1.A) (Svitkina et al., 2003). Filopodial dynamics are mediated by the opposing actions of actin bundle extension, powered by actin polymerization at the filopodial tip (Okabe and Hirokawa, 1991), and actin bundle retraction, powered by retrograde flow of the actin filaments towards the cell body (Mallavarapu and Mitchison, 1999). The actin filaments within the filopodium are constantly undergoing a myosin-dependent rearward flow (Lin et al., 1996), so the rate at which polymerization occurs effects whether a filopodium is extending, retracting, or maintaining a stable length. These filopodial dynamics can vary significantly between organisms and cell types, as rates of filopodia extension ranging from 0.03-1.0 $\mu\text{m/s}$ have been reported (Mallavarapu and Mitchison, 1999; Svitkina et al., 2003; Medalia et al., 2007; Schirenbeck et al., 2005; Lebrand et al., 2004).

CLASSIFICATION OF FILOPODIA AND RELATED ACTIN STRUCTURES

Filopodia and related thin actin structures are broadly produced and participate in a range of physiological processes, which has led to an assortment of designations for these finger-like protrusions. Comparing reports detailing filopodia, microspikes, cytonemes, and myopodia, to name a few, can often reveal structures with seemingly

high similarity, both molecularly and morphologically. Additionally, the highly specialized, actin-based protrusive structures known as microvilli and stereocilia have been described in detail and share likeness with filopodia. Figure 3.2 depicts these thin, actin-based extensions and lists some important similarities and differences between them.

Microvilli are found on the apical surface of many epithelial cells of the intestine and kidney (Mooseker and Tilney, 1975). They are typically short ($\sim 2\mu\text{m}$), densely packed, and of uniform height. Microvilli contain a core of parallel bundled actin that terminates into a dense network of actin, myosin-II, and spectrin called the 'terminal web' (Hirokawa and Heuser, 1981; Hirokawa et al., 1982). Actin filaments in microvilli are bundled by the proteins villin and fimbrin and are tethered to the membrane by myosin-I and ezrin (Fath and Burgess, 1995).

Stereocilia are found on the apical surface of epithelial hair cells of the inner ear. They are arranged on the cell surface in order of increasing height, with heights ranging from $1\mu\text{m}$ to $120\mu\text{m}$ (Manor and Kachar, 2008). Stereocilia contain a core of parallel bundled actin that terminates into a dense network of actin known as the cuticular plate. The stereocilia on one cell comprise a hair bundle, with membranous links connecting adjacent stereocilia. The adhesion proteins cadherin-23 and protocadherin-15, the PDZ-domain protein whirlin, and the actin cross-linking proteins espin and fimbrin are all known to participate in stereocilia formation (Manor and Kachar, 2008; Nayak et al., 2007).

Whereas microvilli and stereocilia clearly have structural details and molecular components that distinguish them from filopodia, there are other slender actin-based

protrusions that do not appear so distinct. First, in *Drosophila*, long cellular extensions known as cytonemes extend from cells in the developing wing imaginal disc to the anterior/posterior-signaling compartment (Ramirez-Weber and Kornberg, 1999). Cytonemes contain a core of actin and can reach lengths of 10s of microns. Next, during neuro-muscular junction formation in *Drosophila*, actin-based protrusions know as myopodia extend from the muscle cell towards the innervating neuron and intermingle with neuronal filopodia (Ritzenthaler and Chiba, 2003). While cytonemes and myopodia are filopodia-like protrusions born on specific cell types, other extensions such as microspikes and retraction fibers have been described on several cell types. The term microspike is sometimes used interchangeably with filopodia, but other times used to describe short, stubby, nascent filopodia barely extending beyond the edge of the lammelipodium (Small et al., 2002). Lastly, retraction fibers are produced by a different mechanism than the rest of the protrusions discussed in this section – cell body retraction. Whereas filopodia are generated by active protrusion away from the cell, retraction fibers are the remnants of the cell pulling away from an area. They can contain a core of actin, but unlike filopodia, retraction fibers often appear branched. Together, these slender, actin-based protrusions comprise a group of morphologically similar cellular structures, often with related functions and molecular components.

KEY MOLECULES IN FILOPODIA FORMATION

The dynamic nature and distinct structure of the filopodium raise interesting questions about the mechanisms that regulate filopodia formation and maintenance. Several fundamental proteins have been identified, some common to both lamellipodia

and filopodia and others filopodia-specific, which comprise the filopodia formation machinery. This machinery must perform several tasks including, signaling for filopodia induction, actin nucleation and extension, anti-capping of barbed end, filament bundling, and movement along actin. Here we discuss some key proteins (depicted in figure 3.1.B), signaling pathways, and proposed models.

Fascin. A distinguishing feature of the filopodium is its bundled parallel actin fibers. Establishing such an arrangement of actin requires the work of actin bundling proteins, with fascin being the actin cross-linking protein most commonly associated with filopodia (Vignjevic et al., 2006). Fascin was first described in sea urchine coelomocyte filopodia where it was shown to localize to filopodia and bundle actin filaments (DeRosier and Edds, 1980; Otto et al., 1979). Subsequent research has demonstrated that fascin is necessary for filopodia formation and stiffness, as fascin knock-down cells display fewer filopodia with less rigid actin bundles (Vignjevic et al., 2006). Furthermore, the high density and fast dynamics of fascin association with filopodia bundles suggest a model where fascin is easily released from bundles to diffuse towards the tip of a growing filopodium to incorporate along with new actin monomers (Aratyn et al., 2007).

Ena/VASP Proteins. Members of the Ena/VASP family of proteins, Mena, VASP, and EVL, promote actin filament assembly and modulate lamellipodia and filopodia formation (Bear and Gertler, 2009). Ena/VASP proteins can be found at focal adhesions, the edges lamellipodia, and the tips of filopodia. VASP stably associates with the distal tips of filopodia, even as new actin monomers are added (Applewhite et al., 2007). The role of Ena/VASP in filopodia formation is seemingly multifaceted, as

Ena/VASP is reported to promote actin filament clustering and bundling and has anti-branching and anti-capping properties (Applewhite et al., 2007; Bear et al., 2002; Barzik et al., 2005). Importantly, several studies have shown that Ena/VASP function is required for filopodia formation (Dent et al., 2007; Lebrand et al., 2004).

Formins. Formins comprise a large family of proteins that mediate actin assembly with 15 identified formins in mammals, including the Diaphanous formins mDia1, mDia2, and mDia3 (Goode and Eck, 2007). Formins induce the formation of unbranched actin filaments by processive barbed-end nucleation and elongation and inhibit capping protein from blocking barbed-end growth (Paul and Pollard, 2009). Knock-down experiments in either *Dictyostelium* (Schirenbeck et al., 2005) or mammalian (Yang et al., 2007) cells demonstrate that Dia2 is required for filopodia formation and maintenance. Interestingly, formins may cooperate with VASP to form filopodia, as these two proteins were shown to interact in *Dictyostelium* (Schirenbeck et al., 2006), although similar evidence is lacking in mammalian cells.

Myosin-X. Myosin motor proteins bind to F-actin and use energy from ATP-hydrolysis to move along actin filaments. Myosins participate in a wide range of processes such as organelle movement and tethering, cell division, and cell migration (Coluccio, 2008). Myosin-X (Myo10), a member of the MyTH-FERM superclass of myosins, localizes to the tips of filopodia (Berg et al., 2000) and undergoes intra-filopodial motility (Berg and Cheney, 2002; Kerber et al., 2009). The striking localization and movements of Myo10 in filopodia raised questions about its participation in filopodia formation and/or maintenance. Using scanning electron microscopy, Bohil et al. showed that Myo10 acts as a regulator of filopodia production,

as knock-down of Myo10 blocked formation and over-expression of Myo10 enhanced formation of filopodia (Bohil et al., 2006). Additionally, studies using regulated dimerization of a tail-less Myo10 demonstrated that dimerization of Myo10 motors is critical for filopodia initiation, possibly by bringing together actin filaments at the cell periphery (Tokuo et al., 2007). Furthermore, Myo10 motility is highest on bundled actin, suggesting a cooperation between Myo10 and fascin in organizing actin filaments for incorporation into filopodia (Nagy et al., 2008; Brawley and Rock, 2009). Interestingly, through its tail domains, Myo10 binds to VASP (Tokuo and Ikebe, 2004) and integrins (Zhang et al., 2004), both of which can be found at the filopodia tip and participate in filopodia formation and stabilization. It appears that Myo10 is involved throughout the life of a filopodium, during regulation, initiation, and maintenance; it will be important to more precisely determine how Myo10 participates in each of process.

Cdc42, Rif, and other GTPases. Rho superfamily small GTPases participate in many aspects of cell migration through regulation of actin dynamics and membrane protrusions (Ridley, 2006) (Heasman and Ridley, 2008). Downstream of these GTPases, actin polymerization can be stimulated via two mechanisms: 1) activation of WASP/WAVE proteins, which induce Arp2/3 complex-mediated actin filament nucleation, or 2) activation of Diaphanous-related formins. Early studies demonstrated that activation of Cdc42 induced filopodia formation (Nobes and Hall, 1995) and subsequent research identifying WASP and N-WASP as downstream targets of Cdc42 (Machesky and Insall, 1998; Rohatgi et al., 1999) suggested that Cdc42's filopodia-inducing activity was through actin filament nucleation by the Arp2/3 complex. However, WASP and N-

WASP knock-down cells were still able to form filopodia (Snapper et al., 2001), indicating that an additional pathway downstream of Cdc42 existed for filopodia formation. Indeed, Cdc42 was shown to induce filopodia through IRSp53 (Krugmann et al., 2001), which may be due to its ability to associate with WAVE2 and Mena, or by the intrinsic membrane tubulation and F-actin bundling activities of its I-BAR domain (described below) (Scita et al., 2008).

Interestingly, it was discovered that Cdc42-null cells are still capable of forming filopodia (Czuchra et al., 2005). This suggests that signaling via other GTPases leads to filopodia formation; in fact, several other GTPases have been shown to promote filopodia. For example, RhoF/Rif (Rho in filopodia) over-expression stimulates filopodia formation in a Cdc42-independent manner (Ellis and Mellor, 2000). Moreover, Rif binds to the formin mDia2 and the filopodia-inducing activity of Rif depends on the presence of mDia2 (Pellegrin and Mellor, 2005). Other GTPases such as RhoD, RhoT, TC10, and Wrch1, have also been shown to induce filopodia formation (Aspenstrom et al., 2004; Murphy et al., 1999; Abe et al., 2003; Ruusala and Aspenstrom, 2008).

Convergent elongation versus formin-mediated models of filopodia formation.

Several models for filopodia formation have been proposed, with two at the forefront of discussion. The first model involves reorganization of the dendritic network via actin filament elongation and convergence at the barbed ends (Svitkina et al., 2003), whereas the second depends on formin-mediated formation of actin bundles in an unbranched network (Paul and Pollard, 2009; Pellegrin and Mellor, 2005; Mellor, 2009). In the convergent elongation model of filopodia formation, actin filaments arise by Arp2/3

mediated nucleation in the dendritic lamellar network. A subset of these filaments, possibly marked by Ena/VASP at their barbed end, converge at the cell periphery to initiate a filopodium. Ena/VASP is proposed to protect these filaments from capping and promote polymerization and bundling. As the initial actin filaments coalesce, the binding of fascin stabilizes the growing filopodium, allowing it to lengthen. Conversely, in the formin-mediated model of filopodia formation, mDia2 appears to perform most of the activities necessary to initiate filopodia. mDia2 nucleates actin filaments, protects barbed ends from capping, and bundles F-actin. Cdc42 activation can lead to either of these pathways, as Cdc42 activates Arp2/3 through the actin-regulatory protein N-WASP (Machesky and Insall, 1998; Rohatgi et al., 1999), but also activates mDia2 through direct interaction (Peng et al., 2003). Alternatively, the formin-mediated pathway can be stimulated by the GTPase Rif, which directly activates mDia2 (Pellegrin and Mellor, 2005).

THE FILOPODIA TIP COMPLEX: AT THE FOREFRONT OF FILOPODIA FORMATION AND FUNCTION?

Classic electron microscopy images of microvilli, a highly specialized relative of filopodia, revealed that their cores of parallel-bundled actin filaments insert into a dense “fuzz” at the tips of the microvilli (Mooseker and Tilney, 1975). More recent platinum replica EM studies of filopodia formation have also revealed an electron dense concentration of material at the tips of filopodia (Figure 3.1.A) (Svitkina et al., 2003). Despite its identification over thirty years ago, the nature of the “tip-complex” and its

components are still being investigated for their role in filopodia formation, maintenance, and function (Mellor, 2009; Gupton and Gertler, 2007).

The tips of filopodia contain a numerous proteins that participate in processes such as actin polymerization and dynamics, adhesion, and signaling (Table 3.1). It would seem obvious that many of the proteins implicated in filopodia formation would be found at the tips of filopodia and in the putative tip complex. Indeed, the filopodia-promoting proteins Myo10, VASP, mDia, and IRSp53 localize to the tips of filopodia (Peng et al., 2003; Berg et al., 2001; Krause et al., 2003; Nakagawa et al., 2003). Interestingly, these proteins can often be seen associating with budding filopodia, indicating the possibility that the filopodial tip complex, or a portion of it, is assembled prior to actin filament protrusion beyond the edge of the cell. Furthermore, these proteins remain at the tips of mature filopodia, perhaps maintaining filopodia length or mediating stable interactions with other tip complex components.

In addition to actin-associated proteins, several trans-membrane receptors are reported to localize to the tips of filopodia. These include integrins (Partridge and Marcantonio, 2006; Steketee and Tosney, 2002; Galbraith et al., 2007; Grabham and Goldberg, 1997; Letourneau and Shattuck, 1989; Rabinovitz and Mercurio, 1997; Wu et al., 1996), epidermal growth factor receptor (EGFR) (Lidke et al., 2005), vascular endothelial growth factor receptor 2 (VEGFR-2/Flk-1) (Gerhardt et al., 2003), netrin-1 receptor/DCC (Shekarabi and Kennedy, 2002), and bone morphogenic protein 6 receptor (ALK6) (Pi et al., 2007). Certainly, the presence of such receptors endows filopodia with the tools necessary to perform their exploratory function. However, it is unclear whether, like other tip complex components, these receptors are present in the

nascent tip complex or if they are trafficked to the tips of mature filopodia. Moreover, if these tip-complex receptors are delivered to the tips of established filopodia, then by what mechanism is this accomplished? Myo10 is an attractive candidate to perform this task, as is discussed below.

Although many proteins that localize to the tips of filopodia have been identified, little is known about how these proteins come together to form the electron dense tip complex. It will be important to determine the physical association between residents of the filopodia tip. Isolation and purification of filopodia, as has been performed on pseudopodia (Cho and Klemke, 2002), would certainly provide an opportunity to examine associations between tip complex proteins, as well as to identify new components of the tip complex. Additionally, it will be interesting to ascertain the similarities and differences between tip complexes from filopodia produced by different cell types. Multiple pathways are implicated in filopodia formation and various trans-membrane receptors can localize to the tips of filopodia; therefore it seems likely that different cell types would have specialized tip complexes to suit the needs of the cell.

INTRA-FILOPODIAL TRANSPORT

As a filopodium increases in length, it seems unlikely that a component not present in the nascent tip complex could easily diffuse from the base of the filopodium out to the tip. Several groups have recognized this issue and have used modeling to ask about the limitations of diffusion in a long, narrow filopodium (Mogilner and Rubinstein, 2005; Lan and Papoian, 2008; Zhuravlev and Papoian, 2009). For example, using modeling, it has been reported that G-actin diffusion to the tips of filopodia is

significantly hindered in filopodia longer than 1-2 μm . This would suggest that diffusion is an ineffective means of transport to the tips of filopodia, which are often observed to reach lengths of 10 μm and greater. How, then, do molecules get to the filopodial tip? This question is not without a related predecessor, as a similar cell biological scenario exists in flagella and cilia – long, thin, cellular projections containing a core of microtubules. Much research on these structures has uncovered a system of intra-flagellar transport, which uses kinesin and dynein motors to traffic flagellar or ciliary components along the axoneme (Scholey, 2008; Silverman and Leroux, 2009). As filopodia share a similar “long and thin” morphology to cilia, but are actin-based, myosin motors are strong candidates for facilitating intra-filopodial transport. Indeed, several myosins are known to localize to the tips of and travel within filopodia, microvilli, and stereocilia. Furthermore, increasing evidence of cargo co-transport with these myosins supports the idea of a myosin-mediated form of intra-filopodial transport.

Filopodia, stereocilia, and microvilli grow by polymerization of actin at the tip of the protrusion. Additionally, the actin filaments within these structures constantly undergo retrograde flow back towards the cell body. Although related to filopodia, stereocilia and microvilli are highly specialized and thus contain a particular set of proteins. Likewise, each of these protrusions appears to contain a distinct myosin profile. Stereocilia have been shown to contain several myosins, including Myo3a (Schneider et al., 2006), Myo15a (Belyantseva et al., 2003; Rzadzinska et al., 2004), and Myo7a, whereas microvilli have been shown to contain Myo7a (Wolfrum et al., 1998) and Myo7b (Dai, 2001). In contrast, Myo10 has been localized to filopodia from many

different tissues and cell types (Coluccio, 2008). Although Myo10 is ubiquitously expressed, no studies have been published that examine its localization in stereocilia or microvilli.

With several motors situated at the tips of slender, actin-based protrusions, what purpose are they serving? Several groups have published compelling evidence that these myosins are functioning to carry cargos to and from the tips of filopodia and related structures. Myo3a binds to and co-localizes with the actin bundling protein, espin-1, at the tips of stereocilia (Salles et al., 2009). When over-expressed in hair cells, Myo3a increases stereocilium length and when over-expressed in fibroblasts, Myo3a co-transportes espin-1 in filopodia. Also in inner ear hair cells, Myo15a co-localizes with whirlin, a protein necessary for stereocilia elongation. When expressed in COS-7 cells, Myo15a co-transportes with whirlin in filopodia (Belyantseva et al., 2005). Interestingly, the *Drosophila* Myo15 homolog, Sisyphus, was shown to localize to the tips of epithelial filopodia during dorsal closure and zippering (Liu et al., 2008). Several binding partners were indentified, including DE-cadherin and EB-1, and knock-out of Sisyphus lead to aberrant localization of these proteins. Myo7a binds to and co-localizes with twinfilin-2, an actin binding protein that prevents barbed end polymerization, in stereocilia (Rzadzinska et al., 2009). Furthermore, when expressed in fibroblasts, Myo7a increases the amount of twinfilin-2 that localizes to the tips of filopodia. Lastly, Myo10 undergoes intra-filopodial motility (Berg and Cheney, 2002) and has been shown to bind to VASP (Tokuo and Ikebe, 2004), BMP-6 receptor/ALK6 (Pi et al., 2007), the netrin receptor/DCC (Zhu et al., 2007), and integrins (Zhang et al., 2004). As Myo10

is the most widely expressed myosin that localizes to filopodia, it is likely to mediate intra-filopodial motility in most cells.

Intra-filopodial motility is clearly a means to traffic molecules to the tips of filopodia, but it may also function as a way to carry cargo back to the body of the cell. By tightly binding the filopodial actin filaments, barbed-end directed motors can hitch a ride back to the cell body via retrograde actin flow. This mode of movement is likely to play an important role during receptor recycling and endocytosis. For example, EGFR observed at the tips of filopodia was shuttled back along the filopodium to the base of the cell once it was bound to its ligand EGF (Lidke et al., 2005). Only when the receptor-ligand complex reached the cell body, was it endocytosed. In another interesting illustration of retrograde filopodial movements, several research groups have shown that filopodia mediate transmission of viral particles from one cell to its neighbors (Sherer et al., 2007; Kolesnikova et al., 2007; Mercer and Helenius, 2008; Zamudio-Meza et al., 2009). Although the viral particles can make initial contact with a cell on a filopodium, they must travel rearward toward the cell body where they can be endocytosed and cause infection (Mercer and Helenius, 2008). By linking to retrograde actin flow through filopodial myosin, various molecules and particles, like EGF and viruses, can be received at the filopodial tip and trafficked back to the cell to elicit a response.

While myosin-based transport in slender actin protrusions is intriguing, there are still some important questions to answer. First, are the cargo-carrying abilities of these myosins necessary for filopodia formation? It would seem so, but for Myo10, which is necessary for filopodia formation in several cell types, a tail-less version is still

capable of initiating filopodia (Tokuo et al., 2007). However, it is unclear whether the filopodia produced in cells expressing tail-less Myo10 can reach lengths of those put forth by wild-type cells. Therefore, it is likely that Myo10, and possibly other filopodial myosins, participate in filopodia formation by both affecting actin organization and transporting filopodial cargos. Next, how are these movements regulated? Are there constitutive forward and rearward movements of tip proteins? Or do particular cell signals dictate when a protein is shuttled to or from the filopodial tip? Lastly, it will be interesting to see to what detail we can observe myosin-mediated filopodial transport. As microscope and imaging techniques advance, observing these movements in additional scenarios, such as in the organism or at near single-molecule levels, will be fascinating and informative.

EMERGING TOPICS AND OUTSTANDING QUESTIONS IN FILOPODIAL BIOLOGY

As the literature on filopodia biology continues to flourish, two intriguing new topics have recently emerged. First, characterization of filopodia-like extensions known as nanotubes (also called tunneling or membrane nanotubes/nanotubules) is a young addition to the field. These long, thin protrusions make connections between cells and are thought to serve as compartment for exchanging cellular material such as calcium, cell surface receptors, vesicles, organelles, and other particles (Gerdes and Carvalho, 2008). They have been observed on a variety of cell types, but have mostly been studied in neuronal and immune cells. F-actin has been detected in all nanotubes and their integrity depends on its presence, whereas microtubules have rarely been observed in nanotubes (Davis and Sowinski, 2008). Interestingly, one observed

mechanism of nanotube birth involves filopodia. Nanotubes can arise from extension, contact, and fusion of either one filopodium with the body of a second cell, or two filopodia originating from different cells (Rustom et al., 2004). It remains unclear, though, if blocking filopodia formation will prevent formation of nanotubes.

Additionally, it is unclear how material is transferred between two cells connected by a nanotube. It will be interesting to determine if the mechanism of nanotubular transport shares common myosin machinery with intra-filopodial transport.

A second exciting emerging topic in filopodia biology is the involvement of I-BAR (Inverse Bin-Amphipysin-Rvs167) domain containing proteins in the formation of membrane protrusions. The Cdc42 effector IRSp53 was shown to induce filopodia formation by coordinating actin dynamics, through interacting with Mena/VASP, mDia2, Eps8, or N-WASP, with membrane curvature, through its IMD (IRSp53 and Missing-in-metastasis Domain) (Scita et al., 2008; Lim et al., 2008; Disanza et al., 2006; Krugmann et al., 2001). A member of the larger family of BAR domains, the IRSp53 IMD/I-BAR domain has an intrinsic curve to its protein structure, upon which it can bind lipids on the inner face of the plasma membrane to produce an outward curvature of the cell membrane (Mattila et al., 2007; Saarikangas et al., 2009). Interestingly, the IMD alone of IRSp53 can produce membrane deformations and small protrusions independent of actin (Mattila et al., 2007; Suetsugu et al., 2006). Although IRSp53 clearly participate in filopodia formation, it is unclear if IRSp53 is necessary for filopodia formation. It will be important to determine if all filopodia require the presence of a membrane curving protein such as IRSp53.

Finally, many outstanding questions in filopodia biology still exist. One of the most important questions being: What are filopodia like *in vivo*? Although several studies have examined filopodia in model systems such as *Drosophila* and *C. elegans*, much of our understanding of filopodia biology is based off of work performed with cultured cells on glass coverslips. The formation and behavior of filopodia in a 3-D environment, as exists *in vivo*, may differ from what has been observed in cell culture models. Next, it will be interesting to determine more precisely the nature of the filopodia tip complex. Can the tip complex be purified? What is the complete set of proteins that comprise the filopodia tip complex? Do these vary from one cell type to another? The tip complex is clearly an integral structure within the filopodium and it is crucial to establish its role in filopodia formation, maintenance, and function. Additionally, as described above, it will be important to elucidate the details of intra-filopodial motility – what molecules are involved and how is transport regulated. Lastly, questions remain regarding the seemingly multiple mechanisms of filopodia formation. Are the convergent elongation and formin-mediated nucleation models mutually exclusive? Although multiple pathways lead to filopodia formation, it remains unclear if, under knock-out conditions, the other pathways can compensate. Moreover, which components, if any, are shared between these pathways? It will be important to determine how the key molecules and pathways in filopodia formation are interconnected. Surely, continuing to explore these and other questions about filopodia will continue to reveal fascinating information about the cell's fingers.

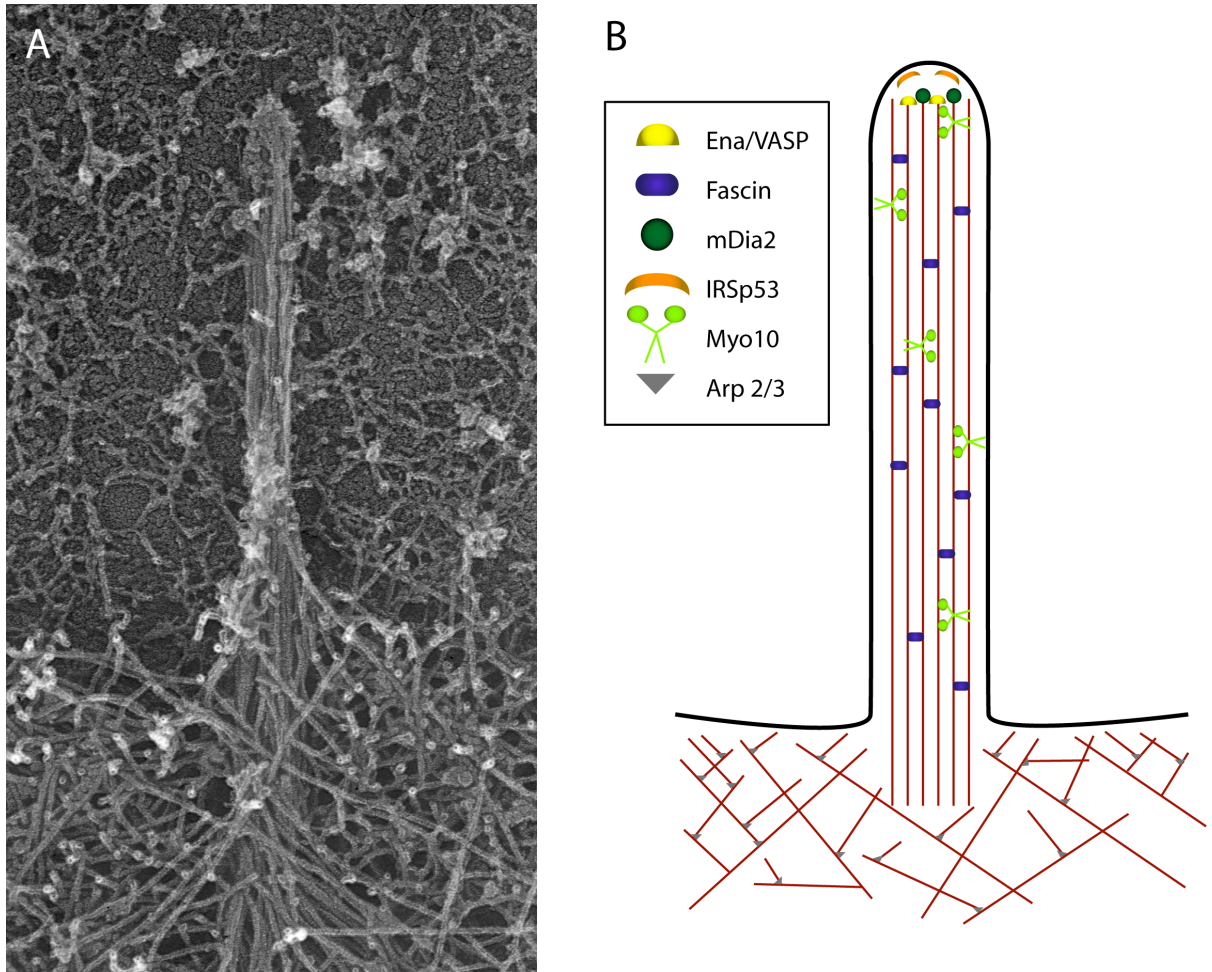


Figure 3.1. Architecture and molecular components of filopodia. (A) Platinum replica electron micrograph of a filopodium produced by a B16 cell. Note the parallel bundle of actin that originates from within the lamellipodium and the electron dense tip complex. Image courtesy of Tanya Svitkina, University of Pennsylvania. (B) Cartoon diagramming key components in filopodia formation and maintenance.

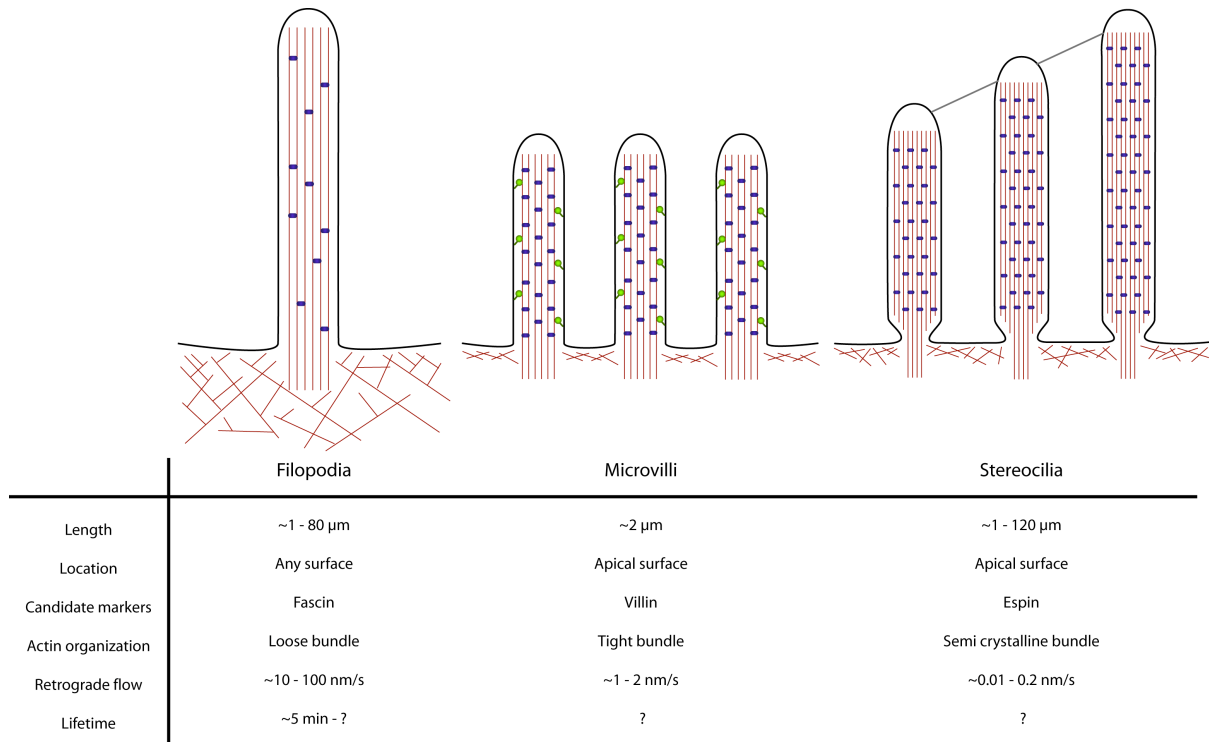


Figure 3.2. Classification of filopodia, microvilli, and stereocilia. In this diagram, general structural features of related slender actin structures are shown along with a table of distinguishing characteristics for each.

Table 3.1. Proteins that localize to the tips of filopodia

Protein	Function	Reference
Ena/VASP	Promotes actin filament elongation, anti-capping, and bundling	(Krause et al., 2003)
mDia	Nucleates actin filaments	(Peng et al., 2003)
Myosin-X	Mediates intra-filopodial transport, initiates filopodia by converging actin filaments at the cell edge	(Berg et al., 2001)
IRSp53	Scaffolding protein, deforms membranes to promote protrusion	(Nakagawa et al., 2003)
Integrins	Mediate cell-substrate adhesion by binding to extracellular matrix proteins	(Galbraith et al., 2007; Grabham and Goldberg, 1997; Letourneau and Shattuck, 1989; Partridge and Marcantonio, 2006; Rabinovitz and Mercurio, 1997; Steketee and Tosney, 2002; Wu et al., 1996)
Cadherins	Mediate cell-cell adhesion through homotypic interactions	(Vasioukhin et al., 2000; Raich et al., 1999; Wood et al., 2002; Millard and Martin, 2008)
EGFR	Binds to epidermal growth factor and signals for cell growth, proliferation, and differentiation	(Lidke et al., 2005)
VEGFR-2/Flk-1	Binds to vascular endothelial growth factor and signals for vasculogenesis and angiogenesis	(Gerhardt et al., 2003)
Netrin receptor-1/DCC	Binds to netrin and directs axon guidance	(Shekarabi and Kennedy, 2002)
BMP-6 receptor/ALK6	Binds to bone morphogenic protein 6 and promotes bone formation, vasculogenesis, and angiogenesis	(Pi et al., 2007)

CHAPTER 4
DETERMINING THE FUNCTIONAL CONSEQUENCE OF THE MYOSIN-X – BETA
INTEGRIN INTERACTION

Filopodia participate in a number of adhesion-dependent processes such as development, wound healing, and cell signaling. Integrins localize to filopodia in various cell types and this localization is hypothesized to occur at a specialized type of adhesion specific to filopodia (Partridge and Marcantonio, 2006; Steketee and Tosney, 2002; Galbraith et al., 2007; Grabham and Goldberg, 1997; Letourneau and Shattuck, 1989; Rabinovitz and Mercurio, 1997; Wu et al., 1996). Although integrin-rich filopodia are involved in many cell biological processes, little is known about filopodia-specific integrin binding partners or the mechanism by which integrins localize to filopodia.

The cytoplasmic tail of β -integrins is a hub for interactions with various signaling, scaffolding, and cytoskeletal proteins. Some of the proteins that bind to the cytoplasmic tail of β -integrins do so through a FERM (4.1, Ezrin, Radixin, Moesin) domain. FERM domains are present in many proteins that mediate membrane-cytoskeleton interactions or bind to cytoplasmic tails of transmembrane receptors (Chishti et al., 1998; Bretscher et al., 2002). Proteins such as talin, radixin, kindlin, and FAK all bind to β -integrins through their FERM domains (Calderwood et al., 1999; Tang et al., 2007; Shi et al., 2007; Schaller et al., 1995).

Following initial characterization of Myo10, the Stromblad lab (Karolinska Institute, Sweden) informed us that in a yeast-two-hybrid screen to identify novel integrin interacting proteins, they had identified Myo10 as a candidate binding partner for integrins. Preliminary studies in our lab confirmed that Myo10 colocalized with integrins in filopodia (Figure 4.1) and subsequent collaboration with the Stromblad lab characterized the interaction between these two molecules. Using a combination of immunoprecipitation, yeast-two-hybrid, and GST-pulldown techniques, Zhang et al showed that the FERM domain of Myo10 binds to the cytoplasmic tails of integrins β_1 , β_3 , and β_5 (Zhang et al., 2004). Furthermore, the binding site of Myo10's FERM domain was specifically located to the β -integrin NPXY motif – a location in the β -integrin cytoplasmic tail known to bind to other FERM domain-containing proteins. Accompanying cell biological studies demonstrated that the interaction between the Myo10 FERM domain and β -integrin NPXY motif was necessary for β -integrin localization to the tips of filopodia and extension of filopodia on extracellular-matrix coated surfaces (Zhang et al., 2004).

Following the experiments that identified the interaction between Myo10 and integrins, the next question at hand was: What is the functional consequence of the Myo10 – β -integrin interaction? We hypothesize that this interaction might be playing a role in: 1) cell adhesion and spreading, 2) integrin activation, and/or 3) integrin transport.

KNOCK-DOWN OF MYOSIN-X IMPAIRS CELL ADHESION AND SPREADING

It is well known that integrins mediate adhesive interactions between the cell and the extracellular matrix. More recently, it has been reported that the initial adhesive interactions between a cell and its environment are mediated by integrin-rich filopodia (Partridge and Marcantonio, 2006). We therefore suspected that the Myo10 – integrin interaction might influence cell adhesion and spreading.

To test this hypothesis, I first developed a lentivirus-mediated shRNA strategy to knock-down Myo10 in HeLa cells. HeLa cells were infected with the pLL5.0-mCherry vector containing both the mCherry sequence and either an shRNA sequence directed against Myo10 or a non-specific (NS) sequence. Approximately 50 percent of the cells were infected, as determined by presence of mCherry fluorescence. Whole cell lysates prepared from Myo10 and NS shRNA infected cells and analyzed by Western blot revealed that Myo10 protein level was reduced by approximately 50 percent in the Myo10 shRNA infected cells. It is likely that this 50 percent reduction in protein reflects a near 100 percent knock-down of Myo10 in the positively infected cells, because the population of cells used here was heterogeneous (a mix of 50% infected, 50% uninfected). Thus, it is important to note that the magnitude of the results obtained using these cells could be increased if the cells are sorted into a pure mCherry-shRNA positive population.

Next, cell adhesion and spreading of NS and Myo10 knock-down cells was tested using a real-time cell electronic sensing (RT-CES) system (Atienza et al., 2005). In this system, cells are plated under different conditions on E-plates – plates with electrode-coated surfaces designed to measure local electrical impedance and thus allow for sensitive and quantitative detection of cellular attachment and morphology in real time.

Equal numbers of NS and Myo10 knock-down cells were plated on uncoated or fibronectin (FN)-coated E-plates in the presence or absence of serum. Impedance measurements were taken for each condition every two minutes for ten hours and used to calculate the cell index (CI) at each time point. The CI is a measure of cell attachment and spreading; therefore, a larger CI value means more cells are attaching and spreading. CI versus time plots for NS and Myo10 knock-down cells from one assay are depicted in Figure 4.2. These plots show that knock-down of Myo10 impaired cell adhesion and spreading when compared to NS cells plated under the same conditions. In this experiment, cells were plated on plastic (uncoated) or FN-coated wells in the absence of serum. Under these conditions, the rate of adhesion and spreading of Myo10 knock-down cells (cyan and magenta lines) was substantially slower than the rate of NS knock-down cells (dark blue and yellow lines). Additionally, Myo10 knock-down cells did not reach as large of a final spread area (final CI value) as NS knock-down cells plated on the same substrate did. This difference was greatest when comparing Myo10 knock-down cells plated on FN (cyan line) versus NS cells on FN (yellow line). Together, the decreased rate of adhesion and spreading and smaller final spread area of Myo10 knock-down cells suggests that Myo10 plays an important role in cell adhesion and spreading.

THE FERM DOMAIN OF MYOSIN-X DOES NOT ACTIVATE INTEGRINS

Next, to better understand the mechanism for the adhesion defects seen in Myo10 knock-down cells, we wanted to determine more specifically the role of Myo10's interaction with integrins. Our first approach was driven by the discovery that the

FERM domain of talin activates integrins (Calderwood et al., 1999; Calderwood et al., 2002). Through multiple pathways, integrins on the surface of the cell can be “activated” – the process by which integrins undergo a conformational change that increases their affinity for extracellular matrix ligands, thus increasing the adhesiveness of the cell (reviewed in)(Banno and Ginsberg, 2008; Askari et al., 2009). Talin binds to multiple β -integrins (Calderwood, 2004), links integrins to the actin cytoskeleton (Horwitz et al., 1986), and participates in integrin clustering into focal adhesions (Priddle et al., 1998). It was also reported that talin binding to the cytoplasmic tail of β -integrins is a common final step in several pathways of integrin activation (Tadokoro et al., 2003). Importantly, the talin- β -integrin interaction is mediated through binding of talin’s FERM domain to the NPXY motif of β -integrins. These observations lead us to ask the question: Does the FERM domain of Myo10 activate integrins?

To test the hypothesis that Myo10-FERM can activate integrins, we used an experimental setup very similar to that used by Calderwood *et al.* to determine that talin-FERM activates integrins. CHO cells stably expressing integrin $\alpha_{11b}\beta_3$ were transfected with GFP, GFP-talin-FERM, or GFP-Myo10-FERM. Transfected cells were immunostained using the PAC-1 antibody, which recognizes the activated conformation of $\alpha_{11b}\beta_3$, and analyzed by flow cytometry to measure the amounts of PAC-1 antibody bound. GFP alone and GFP + $MnCl_2$ were used to determine the range of minimum and maximum PAC-1 staining values, as $MnCl_2$ treatment strongly stimulates integrin activation (Chen et al., 2003). Histograms displaying PAC-1 intensity for cells expressing GFP, GFP + $MnCl_2$, GFP-talin-FERM, or GFP-Myo10-FERM are shown in Figure 4.3. In this experiment, the control for minimum $\alpha_{11b}\beta_3$ activation, GFP alone,

gives an average PAC-1 staining intensity of 96, whereas the control for maximum $\alpha_{IIb}\beta_3$ activation, GFP + MnCl₂, gives an average PAC-1 intensity of 506. Cells expressing the FERM domain of talin revealed an average PAC-1 staining intensity of 190 – a value that lies in between the minimum and maximum controls for integrin activation.

Interestingly, when cells expressing the FERM domain of Myo10 were stained with PAC-1, the average staining intensity was 94 – a value essentially the same as that of the GFP-alone cells. From these results, we conclude that the FERM domain of Myo10, unlike the FERM domain of talin, does not activate integrins.

Recent research further investigating the interaction between the FERM domain of talin and the cytoplasmic tail of β_3 integrin revealed key structural elements within the talin FERM domain that are necessary for talin to activate integrins (Garcia-Alvarez et al., 2003; Vinogradova et al., 2002; Ulmer et al., 2003; Wegener et al., 2007). FERM domains contain three subdomains named F1, F2, and F3 (Chishti et al., 1998) and the F3 subdomain of talin shows the highest binding affinity for β tails and is sufficient for integrin activation (Calderwood et al., 2002). Using a combination of x-ray crystallography, NMR spectroscopy, and mutational analysis, these studies collectively determined that the talin F3 subdomain interacts with the membrane-proximal region of the β cytoplasmic tail to induce a conformational change in the integrin heterodimer. This conformational change begins by disrupting the “handshake” between the α and β integrin cytoplasmic tails and then is transmitted to the extracellular portions of the receptor, where the conformational change increases ligand affinity. Furthermore, the ability to activate integrins was shown to be specific to talin’s ability to bind to the membrane-proximal β tail and not its ability to bind the membrane distal tail – a known

binding site for other β -integrin interacting proteins. Studies by Wegner *et al.* focused in on the specific residues and structural elements that mediate the membrane-proximal interaction and identified a loop in talin's F3 subdomain as critical to this interaction (Wegener et al., 2007). Loop 1-2, located between the first and second β strands of the talin F3 subdomain, makes critical contact with the membrane-proximal region of the β -integrin cytoplasmic tail (Figure 4.4.A). Moreover, mutational analysis revealed that leucine 325 of loop 1-2 is essential to bury two phenylalanine residues within the membrane-proximal β -tail, thus stabilizing the β -tail and inducing integrin activation.

These studies provide a mechanism for the ability of talin to activate integrins and distinguish talin's unique ability from other β -integrin tail binding proteins. Using this new information, I sought to strengthen my result of Myo10-FERM's inability to activate integrins by comparing the sequence of the F3 subdomain of Myo10-FERM to that of talin-FERM. I aligned the sequences of Myo10-F3 and talin-F3 using ClustalW2, as depicted in Figure 4.4. Myo10 and talin show high sequence identity and similarity throughout their F3 subdomains with the important exception of the loop 1-2 region. As denoted by the blue box in Figure 4.4.C, the sequence comprising loop 1-2 within talin F3 is essentially absent from the F3 subdomain of Myo10. This is important for our observation that the FERM domain of Myo10 does not activate integrins – without loop 1-2, Myo10 does not contain the necessary structural feature to stabilize the β -integrin cytoplasmic tail and ultimately activate the integrin heterodimer. Together, the structural comparison in combination with the activation assay results suggest that the

FERM domain of Myo10 can bind to β -integrins, but, unlike talin, this binding does not induce integrin activation.

MYOSIN-X CO-TRANSPORTS WITH INTEGRINS IN FILOPODIA

We next hypothesized that the spreading and adhesion defect observed in the Myo10 knock-down cells may be due to a filopodia-specific function of the Myo10 – integrin interaction. A large body of evidence supports the idea that Myo10 is a master regulator of filopodia production, maintenance, and function (reviewed in chapter 2) and filopodia rich in integrins are known to participate in the earliest stages of cell adhesion and spreading (Partridge and Marcantonio, 2006; Price et al., 1998).

Furthermore, forward and rearward movements of β_1 integrin have been observed in filopodia (Grabham et al., 2000) and are highly reminiscent of the intrafilopodial motility of Myo10. Consequently, we wondered if the interaction between Myo10 and β -integrins functioned as a mechanism to transport integrins to and from the tips of filopodia via Myo10's ability to undergo intrafilopodial motility.

To test if integrins undergo co-transport with Myo10 in filopodia, I used live-cell imaging of HeLa cells transiently expressing mCherry-Myo10 and GFP-tagged integrins. Cells were plated on ECM-coated coverslips and imaged after allowing the cells to spread for various amounts of time. Figure 4.5.A displays a montage of frames from a time-lapse movie of a HeLa cell expressing mCherry-Myo10 and GFP- α_5 . Several filopodia on this cell show characteristic tip and shaft localization of Myo10. In addition, GFP- α_5 localizes in puncta along the length of many filopodia and often co-localizes with puncta of Myo10. These co-localizing puncta also display synchronized

forward and rearward movement within filopodia at velocities previously reported for Myo10 (Berg and Cheney, 2002; Kerber et al., 2009). To more precisely determine if the movements of mCherry-Myo10 and GFP- α_5 were highly coordinated, we performed kymography on individual filopodia that displayed motile puncta. Figures 4.5.B and C show kymographs of the filopodia denoted by arrowheads in Figure 4.5.A. From this analysis, we can see that puncta of GFP- α_5 integrin do indeed co-transport with mCherry-Myo10 both forward and rearward within filopodia. Co-transport of Myo10 with other GFP-tagged integrins was also observed in HeLa cells. Figures 4.5.D-G show kymographs of mCherry-Myo10 movement along with GFP-tagged α_5 , β_3 , and β_1 integrin.

As an additional method to observe live co-transport of Myo10 and integrins, we labeled endogenous β_1 integrin using quantum dots conjugated to anti- β_1 antibodies. A similar approach was used by Lidke *et al.* to observe live movements of GFP-tagged ErbB1 receptor along with quantum-dot-conjugated EGF in filopodia (Lidke et al., 2005). We applied anti- β_1 -conjugated quantum dots to CAD cells expressing GFP-Myo10 and used time-lapse imaging to observe the movements of the two molecules. CAD cells are a brain-derived mouse cell line that can be differentiated into neurons. In their undifferentiated state, they produce short filopodia with thick actin bundles that originate from deep within the lamella. These bundles often move laterally at a slow velocity and are visible using phase-contrast microscopy. GFP-Myo10 localized to the tips of these short filopodia and displayed forward and rearward movements along the actin bundles, even on the parts of the bundles that are extended into the lamella. Figure 4.6 shows a montage of frames taken from a time-lapse movie of a CAD cell

expressing GFP-Myo10 and labeled with anti- β_1 quantum dots. In this cell, we observed several punta of GFP-Myo10 moving rearward along a filopodial actin bundle. The box in the phase-contrast image notes the bundle. We also observed synchronous rearward movements of quantum dots along the same path as the GFP-Myo10 puncta. When a kymograph was drawn along the actin bundle in question, we see that the paths taken by both the GFP-Myo10 and the quantum dot-tagged β_1 overlap. In addition, we can see one of the quantum dots rapidly change directions and switch from a slow, rearward trajectory to a fast, forward trajectory – a commonly observed behavior for Myo10 in filopodia. Furthermore, the fast forward movement of the quantum dot occurs at ~ 150 nm/s. This was exciting, as we recently discovered a previously undetected population of near single molecules of Myo10 that undergo fast forward movements that can reach velocities as high as 1000 nm/s (Kerber et al., 2009). We were able to uncover the fast forward movements of rather dim GFP-Myo10 molecules by using a TIRF microscopy system coupled with high frame rates. Because quantum dots are so bright, we were easily able to observe this fast forward movement of the anti- β_1 -conjugated quantum dot while using our standard wide field imaging mode with a frame rate of 1 frame every 3 seconds, whereas the dimmer GFP-Myo10 molecule presumably co-transporting with this quantum dot was not detectable during this forward trajectory. This was one of the first observations of a movement of a Myo10 binding partner in filopodia at the new, fast forward velocity. Now that we have a TIRF system set up to image these types of movements, repeating these experiments using TIRF may enhance our current slow forward and rearward co-transport data by revealing fast forward co-transport of Myo10 and integrins. Together, these experiments using either fluorescent

protein- or quantum dot-tagged Myo10 and β -integrins suggest that a functional consequence of the Myo10 – β -integrin interaction is to transport integrins to and from the tips of filopodia.

DISCUSSION

The notion that filopodia can function as specialized adhesive structures is an important idea supported by the numerous cell types that use filopodia to contact the ECM, other cells, and extra-cellular particles. In addition, the localization and transport of integrin adhesion receptors in filopodia provide a molecular mechanism to mediate their adhesiveness. Previous research revealing the role of Myo10 in filopodia formation as well as the interaction between Myo10 and β -integrins led us explore the functional consequence of this interaction in filopodia, as well as in the whole cell.

Previous research by Zhang *et al.* characterized the interaction between the FERM domain of Myo10 and the NPXY motif of integrins β_1 , β_3 , and β_5 (Zhang et al., 2004). This research also described some functional data regarding the interaction between Myo10 and integrins. First, deletion of the F2 or F3 subdomains in the FERM domain of Myo10 abolished localization of integrins to the tips of filopodia. Second, over-expression of the tail or FERM domain of Myo10 as a dominant negative approach decreased cell adhesion on vitronectin. Last, siRNA-mediated knock-down of Myo10 in CPAE cells decreased adhesion on collagen. Importantly, these adhesion assays were analyzed only at early time points of 15, 30, and 60 minutes. Our use of cells stably expressing shRNA against Myo10 in a real-time quantitative cell-spreading assay strengthens these preliminary observations that Myo10 plays a role in cell adhesion

and spreading. It is important to note that the cells used in our experiments were a heterogeneous population – approximately 50% of the cells were infected with the lentivirus containing the shRNA sequence. Therefore, removal of the uninfected cells via fluorescence activated cell sorting to obtain a 100% positive population of Myo10 shRNA cells would likely yield an even greater defect in adhesion and spreading when assayed. Additionally, it will be valuable to determine if knock-down of Myo10 results in a similar spreading defect on other ECM-coated surfaces. As Myo10 is known to bind to β_1 , β_3 , and β_5 integrins, we would expect to see spreading defects on surfaces coated with ligands to those integrins. Lastly, it will be important to monitor cell spreading beyond 10 hours. Previous research by Bohil *et al.* reported that the spread area of Myo10 siRNA-treated cells increased approximately 4-fold over that of non-specific siRNA-treated cells at times of 24 hours or greater post-plating (Bohil et al., 2006). In our ACEA RT-CES assay, although the spread area of Myo10 shRNA cells is still approaching that of NS shRNA cells at 10 hours, it may surpass that of NS shRNA cells at times greater than 10 hours. This would not be entirely surprising, as the pool of membrane previously used to sheath the large population of filopodia in the NS shRNA cells would need to be used up in a different manner in the filopodia-devoid Myo10 shRNA cells. Although the initial adhesion and spreading of Myo10 knock-down cells is retarded, spreading may continue for a longer period of time and result in a final spread area greater than that of control cells.

We next were interested to know if the FERM domain of Myo10, like that of talin, could activate integrins. This was an important question; until recently, no other FERM domains were known to participate in integrin activation. It is now known that the

FERM domain of radixin can specifically activate the leukocyte-specific $\alpha_m\beta_2$ integrin (Tang et al., 2007) and that the FERM domain-containing protein kindlin works cooperatively with talin to activate integrins (Moser et al., 2009). Although the FERM domain of Myo10 does not activate integrins, this information is still useful in elucidating the role of the Myo10 – integrin interaction. It will be interesting to determine if Myo10 binds to integrins regardless of their activation state, or if Myo10 only binds to inactivated or activated integrins. The possibility of selective binding could provide a way for integrins in a specific activation state to be carried out to or back from the tips of filopodia. Additionally, Myo10 could selectively bind active, ECM-engaged integrins to supply mechanical tension at filopodia tips or at anchor points along filopodia shafts. Such stable adhesions at specific points along the length of the filopodium have been reported previously (Steketee and Tosney, 2002) and we routinely observed stable puncta of both integrins and Myo10 at the tips and along the shafts of filopodia during our live-cell imaging studies (represented by vertical lines in kymograph analysis in Figure 4.5).

Testing our third hypothesis that Myo10 co-transport with integrins yielded exciting results. Previous reports highlighted the movements of integrins in filopodia (Grabham et al., 2000) and lamellipodia (Galbraith et al., 2007), but we show here that similar integrin movements coordinate with Myo10 in HeLa and CAD cells. Although the data here clearly show co-transport, we have not yet confirmed that the movements of integrins in filopodia depend on the presence of Myo10. It will be important to determine if integrins undergo forward and rearward movements in filopodia in Myo10 knock-down cells. These experiments will likely prove to be challenging, as knock-

down of Myo10 drastically reduces the number of filopodia that cells produce. It may be possible to bypass this obstacle by rescuing Myo10 knock-down cells with a FERM-less Myo10, which has been shown to retain its filopodia-promoting activity. FERM-less Myo10 still forms filopodia, but will be unable to bind to integrins, thus we would expect no delivery of integrins to filopodia using this strategy.

EXPERIMENTAL PROCEDURES

Constructs and reagents. pLL5.0 and helper vectors were a gift from Jim Bear (UNC-Chapel Hill). GFP-Myo10 construction was previously described (Berg and Cheney, 2002). GFP-Myo10-FERM was constructed by Jonathan Berg (UNC-Chapel Hill) and contains nucleotides 5452-6588 (amino acids 1744-2052) of bovine Myo10. mCherry-Myo10 was constructed by Michael Kerber (UNC-Chapel Hill). GFP-talin-FERM was a gift from Pietro De Camilli (Yale University). $\alpha 5$ -GFP was a gift from Rick Horwitz (University of Virginia). $\beta 1$ -GFP was a gift from Maddy Parsons (King's College, London). $\beta 3$ -GFP was a gift from Jonathan Jones (Northwestern University). Antibody 117 rabbit anti bovine Myo10 was previously described and used at 1 μ g/mL (Berg et al., 2000). Mouse anti human $\beta 1$ antibody clone HB1.1 used for immunostaining was used at 1 μ g/mL (Chemicon). Biotinylated hamster anti rat $\beta 1$ antibody clone Ha2/5 was conjugated to Qdots (BD Biosciences). PAC-1 mouse anti activated $\alpha_{11b}\beta_3$ was purchased from BD Biosciences. Mouse anti human $\beta 3$ antibody clone PM6/13 was used at 1 μ g/mL (AbD Serotec). Alexa 568-conjugated phalloidin and Qdot 565 streptavidin conjugate were purchased from Invitrogen. Fibronectin and laminin were

purchased from Sigma and used at a final concentration of 10 μ g/mL to coat cell culture surfaces.

Cell Culture. HeLa cells were grown in MEM supplemented with 10% FBS and 1% pen/strep. CHO-A5 cells stably expressing $\alpha_{11b}\beta_3$ were a gift from Mark Ginsberg (UCSD) and were grown in DMEM supplemented with 10% FBS and 1% pen/strep. CAD cells are a subclone of Cath-a cells that can be differentiated into a catecholaminergic neuronal phenotype by serum withdrawal (Qi et al., 1997) and were grown in Ham's-F12 supplemented with 10% FBS and 1% pen/strep. HEK293-FT cells were a gift from Jim Bear (UNC-Chapel Hill) and were grown in DMEM supplemented with 10% FBS and 1% pen/strep. All cells were grown at 37°C with 5% CO₂.

Lentivirus production. Lentivirus construction and production was performed as in (Rubinson et al., 2003). Briefly, shRNA sequences against Myo10 (target sequence: GTGCGAACGGCAAAAGAGA) or non-specific (target sequence: GATCGACTTACGACGTTATT) were cloned into pLL5.0 mCherry using HpaI and XhoI. pLL5.0 vectors were co-transfected along with pCMV-VSVG, pMDL-PRRE, and pRSV-REV helper vectors into HEK293-FT using Fugene6 (Roche) according to the manufacturers instructions. Virus-containing supernatants were collected after 3-4 days, spun down at 5000 rpm to remove contaminating HEK cells, and added to HeLa along with 4 μ g/ml polybrene. After 24 hours of virus exposure, media was replaced on HeLa and they were grown and passaged as usual. Knock-down of Myo10 protein was confirmed by Western blotting cell lysates of equal cell number using our rabbit anti bovine Myo10 antibody 117 (Berg et al., 2000).

Immunostaining. HeLa cells were plated onto fibronectin-coated coverslips and grown for 24-48 hours at 37°C with 5% CO₂. Coverslips were washed once with PBS, fixed in 4% paraformaldehyde for 10 minutes, washed once with PBS, permeabilized in 0.2% Triton-X 100 for 5 minutes, and washed 3 times with PBS. Next, coverslips were blocked in 5% goat serum for 1 hour, incubated with primary antibody for one hour, washed 3 times with PBS, incubated with secondary antibody for one hour, washed 3 times with PBS, and mounted. All steps were carried out at room temperature. Coverslips were imaged on a Nikon TE-2000U inverted microscope using a 60X 1.40NA phase-3 lens and an Orca ER CCD camera and run using MetaMorph software. Image cropping and coloration were performed in MetaMorph.

ACEA RT-CES cell spreading assays. A detailed explanation of the ACEA RT-CES system and the cell spreading protocols that were referred to for these experiments can be found in (Atienza et al., 2005). ACEA microplates were purchased from ACEA biosciences. Wells were coated with 10 µg/ml fibronectin for 2hs at 37°C, then washed 3 times with PBS. Myo10 shRNA or NS shRNA HeLa cells were trypsinized, spun down in trypsin neutralizing solution, and resuspended in serum-free MEM. Cell concentration was measured using the Nexcelom Cellometer. 2000-5000 cells were added to each well of the microplate. The microplate was inserted into the ACEA dock and incubated at 37°C with 5% CO₂. The ACEA software was used to acquire cell index readings for each well every 2 minutes for 10 hours. Raw data was imported into Excel to create plots of cell index versus time. Each line on the plot represents the average cell index value for 3 or 4 wells of identical conditions.

Integrin activation assays. Integrin activation assays were performed following the methods used by (Calderwood et al., 2002; Calderwood, 2004). Briefly, CHO-A5 cells were transfected with GFP, GFP-talin-FERM, or GFP-Myo10-FERM using Polyfect (Qiagen) following the manufacturers instructions. After 24-48 hours post-transfection, cells were trypsinized with 0.25% trypsin without EDTA, spun down in complete DMEM to neutralize trypsin, and resuspended in Tyrode's buffer (137mM NaCl, 2.7mM KCl, 12mM NaHCO₃, 5mM HEPES, 1mM MgCl₂, 0.5mM CaCl₂, pH7.4, 0.1% glucose and BSA added immediately before use). For the GFP + MnCl₂ positive control, cells were treated with 2mM MnCl₂ for 30 minutes prior to trypsinization. Cell number was counted using a hemocytometer and cells were resuspended to 5x10⁵ – 1x10⁶ in 40µl in Tyrode's buffer. Ten µl of PAC-1 antibody was added and cells were incubated on ice for 30 minutes. Cells were washed two times with Tyrode's buffer and resuspended in a final volume of 40µl. Alexa 633 goat anti mouse IgM was added at a final dilution of 1:50 and the cells were incubated on ice for 30 minutes. Cells were washed two times with Tyrode's buffer, resuspended in a final volume of 500µl, and analyzed using a Dako CyAn flow cytometer fitted with 405nm, 488nm, and 635nm excitation lasers. Forward and side scatter measurements were used to gate for single cells and exclude clumped or fragmented cells. GFP intensity measurements were used to gate for GFP-positive cells and exclude untransfected cells. Alexa 633 intensities were measured for the double-gated population of cells. Histograms were made using the CyAn Summit software. To control for non-specific staining, non-immune mouse IgM and secondary alone controls were analyzed. To confirm that CHO-A5 cells still retained expression of $\alpha_{11b}\beta_3$, staining with an anti- β_3 antibody was analyzed.

Live cell imaging. HeLa cells were co-transfected with mCherry-Myo10 and GFP-tagged integrin using Polyfect (Qiagen) and following the manufacturers instructions. 24 hours after transfection, cells were replated onto fibronectin-coated coverslips. Cells were imaged 3 or more hours after replating. Coverslips were mounted into rose chambers and filled with Opti-Mem minus phenol red (Gibco) for imaging. Imaging was performed on a Nikon-TE2000U inverted microscope fitted with a 60X 1.40 NA phase-3 lens and an Orca-ER CCD camera. Images were acquired at a frame rate of 1 frame every 3 seconds. Image acquisition was controlled using MetaMorph. Image manipulations and kymograph analysis were performed in MetaMorph. Velocity measurements were calculated from kymographs. For experiments using Qdot-labeling of integrins, streptavidin-conjugated Qdots were incubated with biotin-conjugated anti β_1 antibody Ha2/5 at a 1:1 molar ratio in PBS for 30 minutes at 4°C with rotating as described in (Lidke et al., 2005). Anti β_1 Qdots were added at a final concentration of 125pM to GFP-Myo10 transfected CAD cells plated on laminin-coated coverslips. In some experiments, Qdots were added to cells while they were on the microscope stage. For other experiments, Qdots were added to the cells and allowed to bind for 30 minutes at 37°C before imaging. As a control for non-specific interactions, naked Qdots were added to transfected cells and imaged. Very few Qdots appeared to bind to the surface of these cells and did not display intrafilopodial motility. Movies of CAD cells transfected with GFP-Myo10 and labeled with Qdots were taken and processed using the same conditions as movies of HeLa cells transfected with mCherry-Myo10 and GFP-integrins.

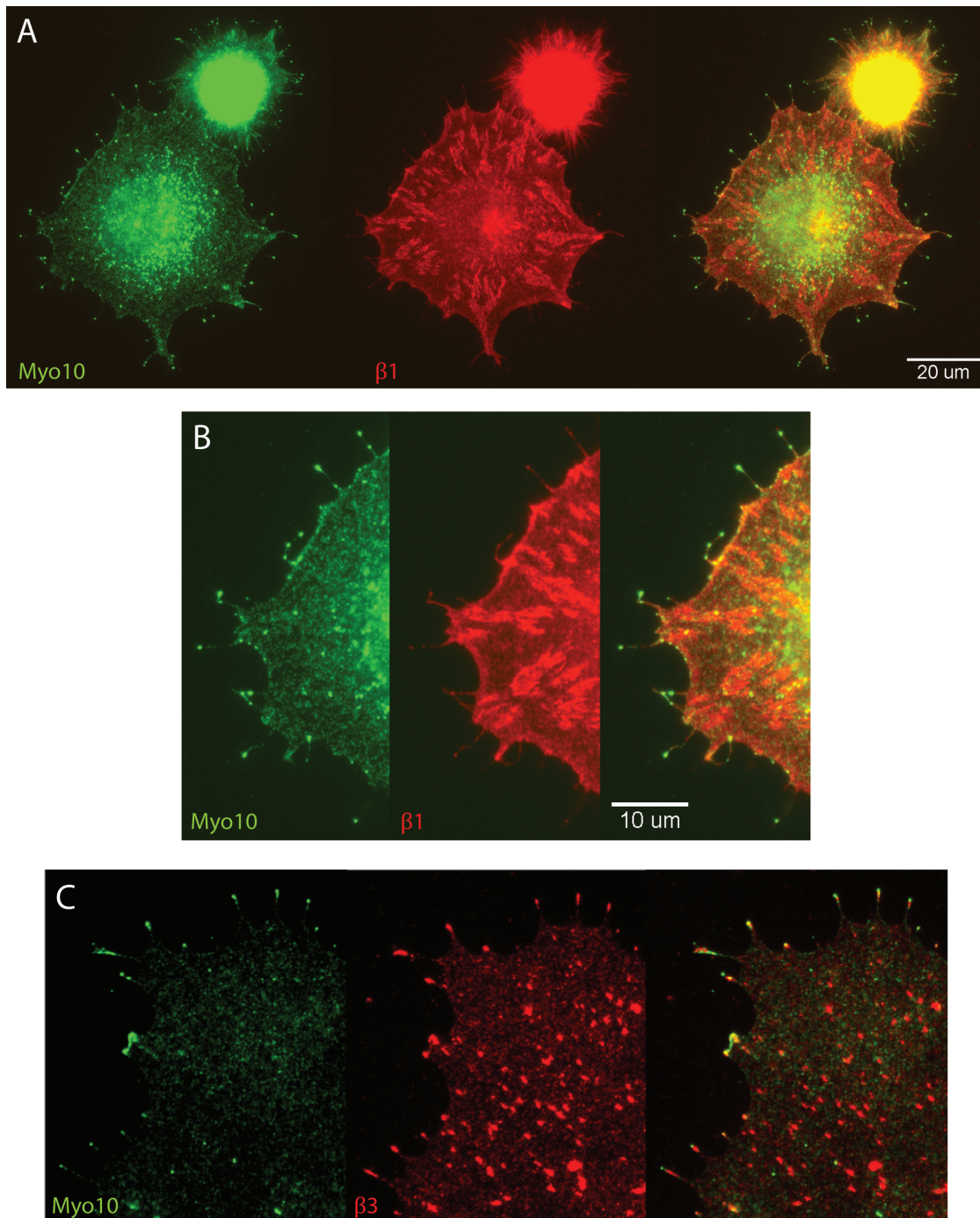


Figure 4.1. Endogenous myosin-X and integrins colocalize in filopodia. (A) Immuno-staining of endogenous myosin-X (green) and β_1 integrin (red) in HeLa cells. (B) Zoomed in view of the left half of the cell in (A). (C) Immuno-staining of endogenous myosin-X (green) and $\alpha_5\beta_3$ integrin (red) in CPAE cells. Image reproduced from {{13 Zhang,H. 2004;}}. Rabbit anti bovine myosin-X antibody 117 was used in these experiments. Myosin-X colocalizes with β integrins at the tips and along the shafts of filopodia. Small amounts of endogenous myosin-X are occasionally seen at focal adhesions, which stain brightly for integrins.

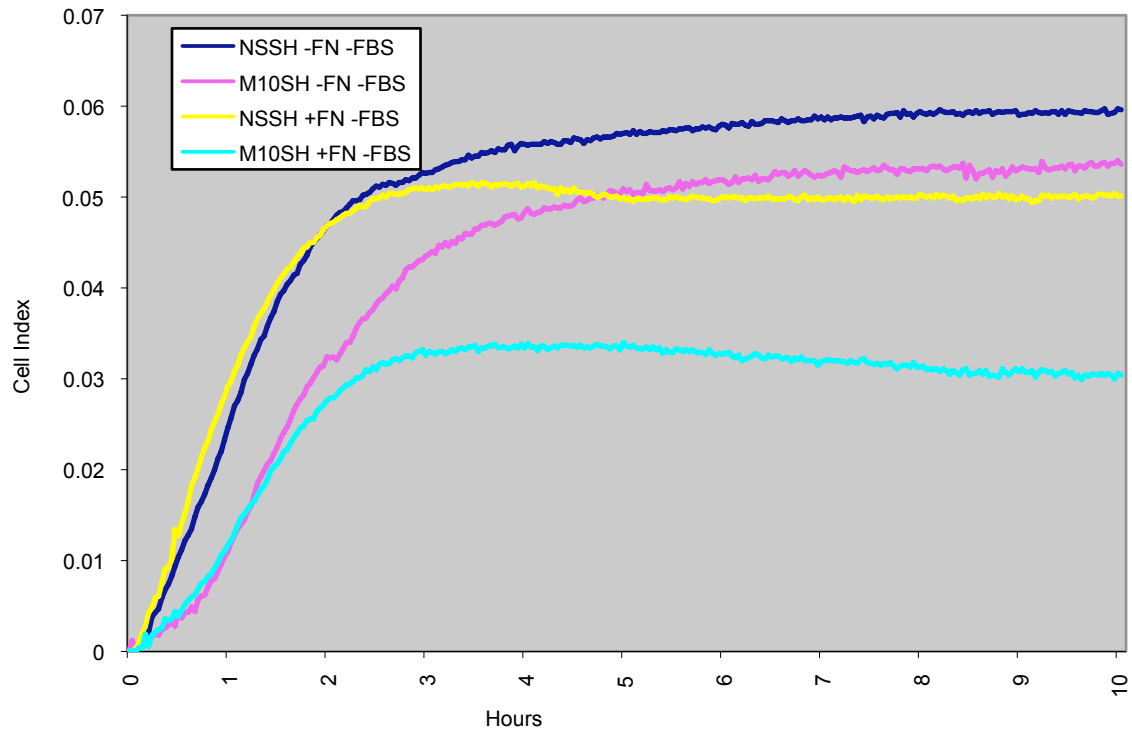


Figure 4.2. Knock-down of myosin-X impairs cell adhesion and spreading. HeLa cells treated with lentivirus containing a Myo10-specific (M10SH) or non-specific (NSSH) shRNA were used in an adhesion and spreading assay using the ACEA RT-CES system. Cells were plated in the absence of FBS on plastic/uncoated wells or fibronectin (FN) coated wells. Impedance values for each well were recorded every two minutes for 10 hours and used to calculate cell index – a measure of the cell spread area. The cell index for each condition is plotted above versus time. Each line represents the average of three identical wells for each condition. It is important to note that the shRNA-treated cells used in this experiment had ~50% infection efficiency and ~50% knock-down in Myo10 protein level. Thus, we would expect an even greater defect in cell spreading with a near 100% population of Myo10 knock-down cells.

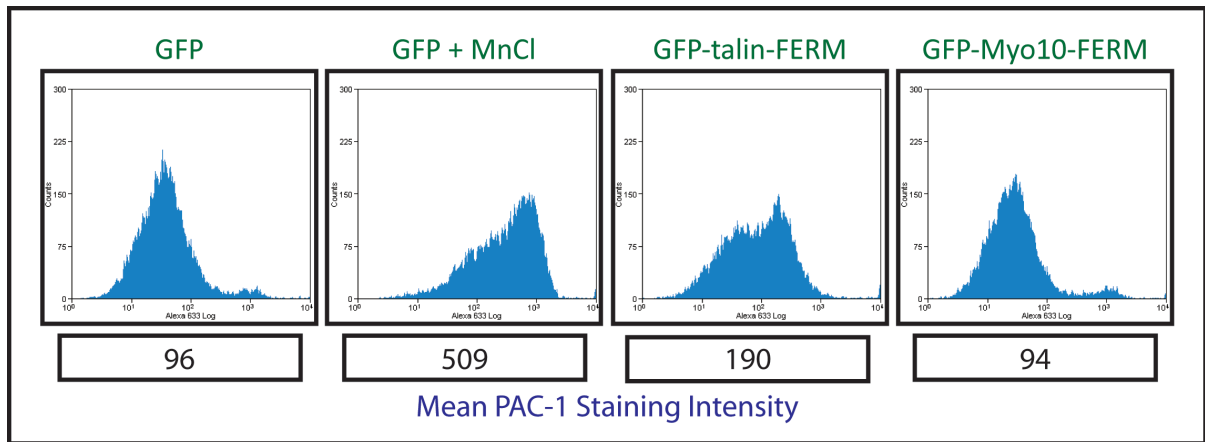


Figure 4.3. The FERM domain of myosin-X does not activate $\alpha_{IIb}\beta_3$. CHO cells stably expressing integrin $\alpha_{IIb}\beta_3$ were used to test various GFP-tagged constructs for integrin activation. Treatment with $MnCl_2$ was used to reveal a maximal level of integrin activation. The monoclonal antibody PAC-1, which recognizes the activated form of $\alpha_{IIb}\beta_3$, was applied to the cells and quantified using flow cytometry. Histograms representing the levels of PAC-1 staining are displayed along with the average PAC-1 staining for each condition. Note that GFP-talin-FERM, which is known to activate integrins, gives a mean PAC-1 staining intensity in between the positive (GFP + $MnCl_2$) and negative (GFP) controls, while GFP-Myo10-FERM gives a value similar to the negative control.

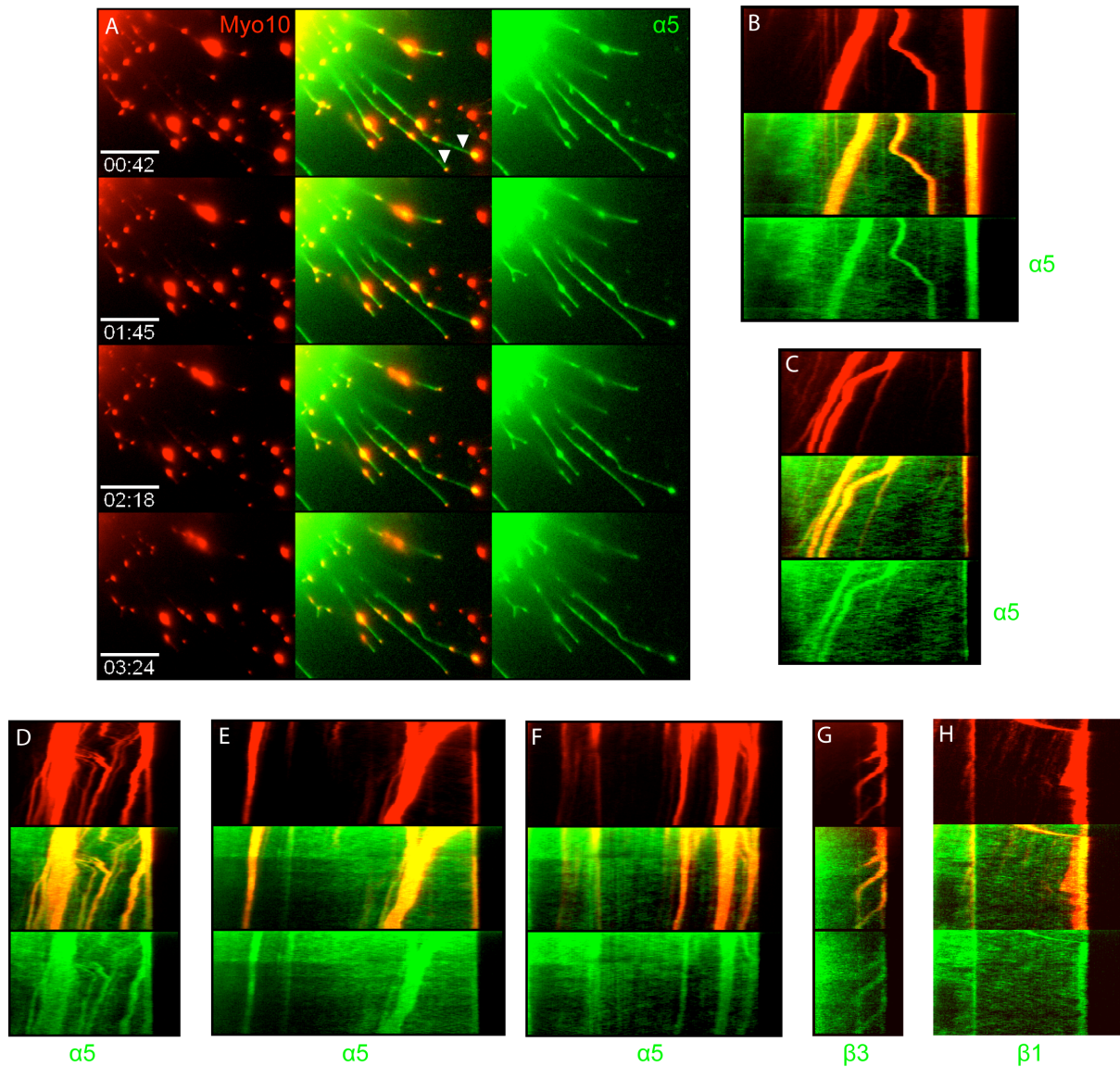


Figure 4.5. Myosin-X co-transport with integrins in filopodia. (A) Montage of selected frames from a time lapse movie of a HeLa cell transiently expressing mCherry-Myo10 and α_5 -GFP. (B) and (C) Kymographs of the filopodia noted by arrowheads in panel (A). (D), (E), and (F) Kymographs of filopodia from a HeLa cell transiently expressing mCherry-Myo10 and α_5 -GFP. (G) Kymograph of a filopodium from a HeLa cell transiently expressing mCherry-Myo10 and β_3 -GFP. (H) Kymograph of a filopodium from a HeLa cell transiently expressing mCherry-Myo10 and β_1 -GFP. Movies 4.1 to 4.4 correspond to the kymographs shown here and are found on the supplementary DVD.

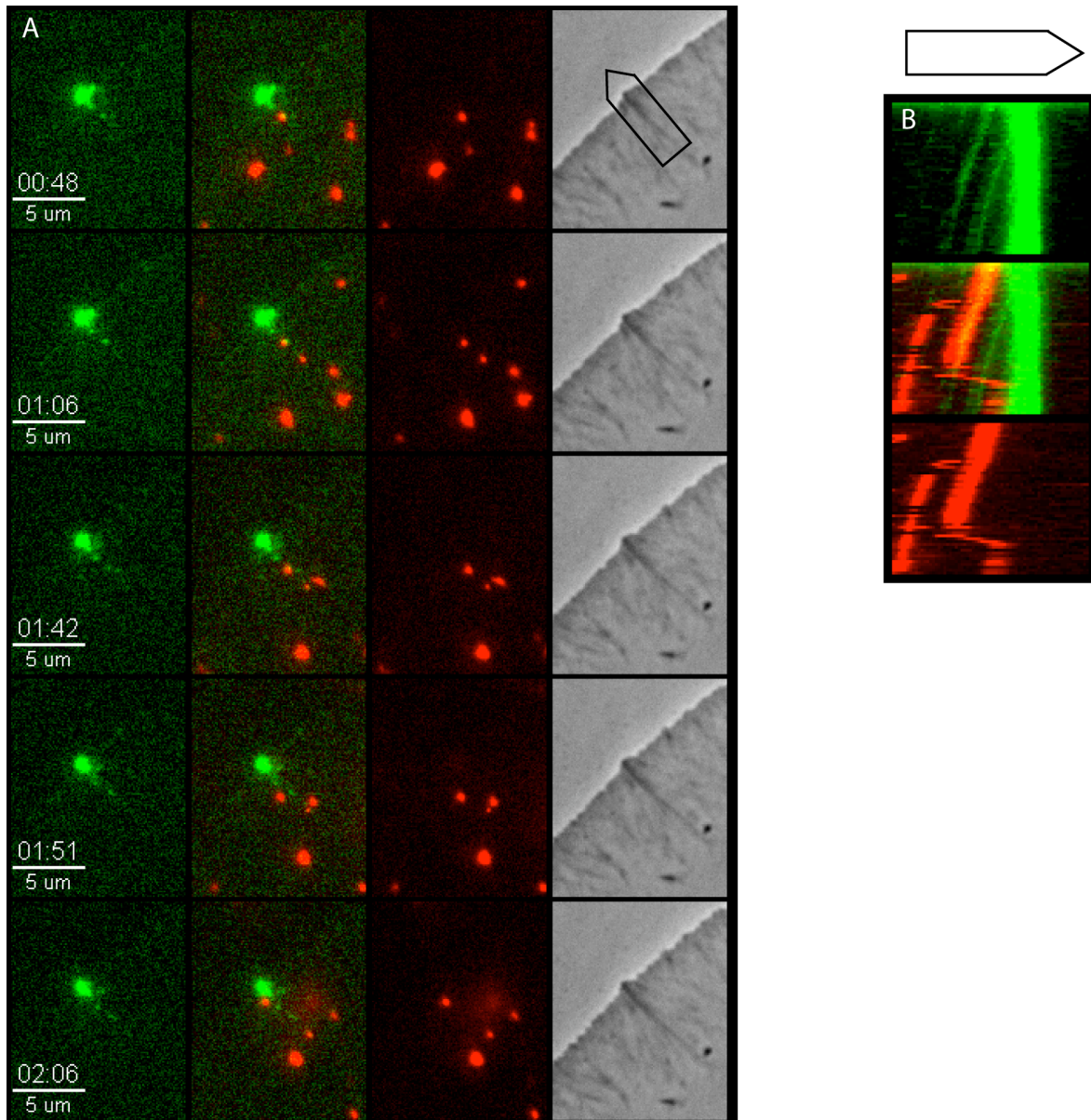


Figure 4.6. Myosin-X cotransports with integrins on actin bundles in CAD cells. (A) Montage of selected frames from a time-lapse movie of a CAD cell transiently expressing GFP-Myo10 and labeled with anti- β_1 -conjugated quantum dots. Note from the phase contrast images that filopodia in CAD cells are often short and contain bundles of actin that extend deeply into the lamella. Movie 4.5 corresponds to this montage and is found on the supplementary DVD. (B) Kymograph of the region denoted in panel (A).

CHAPTER 4 MOVIE LEGENDS

Movie 4.1. Time-lapse movie of a HeLa cell transiently expressing mCherry-Myo10 and α_5 -GFP. This movie corresponds to the montage shown in Figure 4.5.A and the kymographs shown in Figure 4.5.B and C. Note the faster forward movements of Myo10 and α_5 versus the slower rearward movements.

Movie 4.2. Time-lapse movie of a HeLa cell transiently expressing mCherry-Myo10 and α_5 -GFP. This movie corresponds to the kymographs shown in Figure 4.5.D-F.

Movie 4.3. Time-lapse movie of a HeLa cell transiently expressing mCherry-Myo10 and β_3 -GFP. This movie corresponds to the kymograph shown in Figure 4.5.G.

Movie 4.4. Time-lapse movie of a HeLa cell transiently expressing mCherry-Myo10 and β_1 -GFP. This movie corresponds to the kymograph shown in Figure 4.5.H.

Movie 4.5. Time-lapse movie of a CAD cell transiently expressing GFP-Myo10 and labeled with anti- β_1 -conjugated Quantum dots. This movie corresponds to the montage and kymograph shown in Figure 4.6. Note the initial slow, rearward movement of the bundle-associated Quantum dot followed by the fast, forward movement towards the tip of the short filopodia. Also note the random wiggling of Quantum dots attached to the surface of the cell. These are presumably bound to integrins on the dorsal surface of the cell that are diffusing in the plasma membrane.

CHAPTER 5

MYO19 IS A NOVEL MYOSIN THAT ASSOCIATES WITH MITOCHONDRIA

Mitochondria are organelles that have central roles in cell physiology. One of the first described and most fundamental functions of the mitochondrion is to carry out oxidative phosphorylation to generate ATP from energy-rich molecules. As the cell's "energy powerhouse", mitochondria are essential for providing ATP for a vast number of cellular functions. In addition to their critical role in energy production, mitochondria are key players in a wide range of cellular activities such as calcium homeostasis (Spat et al., 2008), apoptosis (Kuwana and Newmeyer, 2003), reactive oxygen species (ROS) production (Wallace and Fan, 2009), development (Van Blerkom, 2009), cell cycle progression and cell signaling (McBride et al., 2006).

As with any component of the cell whose function is fundamental to homeostasis, mutations that arise in these components can lead to disease. Several diseases have been identified that are caused by defective mitochondrial function. For example, mutations in mitochondria-associated proteins lead to skeletal muscle and brain pathologies such as MERRF syndrome (*myoclonic epilepsy associated with ragged-red fibers*), MELAS syndrome (*mitochondrial encephalomyopathy, lactic acidosis, and stroke-like episodes*), Charcot-Marie-Tooth disease, and Kjer's disease/autosomal dominant optic atrophy (Wallace and Fan, 2009; Chan, 2006a). Importantly, aberrant

mitochondrial function has been implicated other complex conditions such as the degenerative Alzheimer's, Parkinson's, and Huntington's diseases (Celsi et al., 2009), diabetes (Lowell and Shulman, 2005), aging (Balaban et al., 2005), and the progression of cancer (Gogvadze et al., 2008).

Mitochondrial dynamics and localization are central to mitochondria function in both normal and disease states and have been studied in detail. First, mitochondria fission and fusion are critical to maintaining an effective mitochondrial network. The cell maintains the overall size and shape of its mitochondria through the opposing processes of fission and fusion and imbalances in these processes lead to mitochondria fragmentation or elongation. The GTPases Mitofusin1, Mitofusin2, and OPA1 are known to participate in mitochondrial fusion, while dynamin-related protein 1 (Drp1), Fis1, and Endophilin B1 are known to participate in mitochondrial fission (Chan, 2006b; Liesa et al., 2009). Mutations in the genes for these proteins can lead to an imbalanced mitochondrial population and cause diseases such as Charcot-Marie-Tooth disease or dominant optic atrophy (Chan, 2006a).

Next, the dynamics of mitochondria transport along the cytoskeleton is a critical component of proper mitochondria function. Mitochondrial movements have been most intensively studied in neurons where research has revealed the transport of mitochondria along the axon (reviewed in (Hollenbeck and Saxton, 2005)). Several groups have observed anterograde and retrograde transport of mitochondria along the axon and mitochondria relocation to specific areas within the axon in response to intracellular calcium signals, local ATP needs, axon outgrowth, or other physiological stimuli. Many of these observed movements were demonstrated to occur along

microtubules via microtubule-based motors. Specifically, the kinesin-1 family member KIF5B and the kinesin-3 family member KIF1B associate with mitochondria and participate in anterograde transport (Nangaku et al., 1994; Tanaka et al., 1998), whereas cytoplasmic dynein has been implicated in retrograde transport (Martin et al., 1999; Waterman-Storer et al., 1997). In addition to the microtubule cytoskeleton, the actin cytoskeleton is involved in mitochondria transport. In studies using drug treatments to depolymerize the microtubule or actin networks, Morris and Hollenbeck found that disrupting the actin network reduced the velocity of both anterograde and retrograde mitochondria transport (Morris and Hollenbeck, 1995). Moreover, without an actin network, mitochondria spent 3-fold more time moving retrograde versus anterograde, thus imbalancing overall mitochondria trafficking and resulting in a decreased number of mitochondria that reached the distal axon. Until recently, no myosin motor was known to interact with mitochondria. Altmann et al reported that in budding yeast, Myo2 (mammalian Myo5) is involved in transporting mitochondria along actin cables during cell division (Altmann et al., 2008). This result was exciting, since it was the first account of a myosin motor participating in the transport of mitochondria, but it did not consequently reveal the myosin responsible for actin-based movements in mammalian cells; Myo5, the mammalian homolog of yeast Myo2, does not associate with mitochondria. Together these data suggest that a myosin motor may be involved in mitochondria transport in mammalian cells, but to date, no such myosin has been identified. Here we report the discovery of myosin-XIX (Myo19), the founding member of a novel class of myosin that associates with mitochondria in mammalian cells.

MYO19 ENCODES A NOVEL METAZOAN MYOSIN

Previous sequence analysis predicted an uncharacterized myosin gene on human chromosome 17q12 that appeared to represent a novel myosin class (Berg et al., 2001). Using the database sequence FLJ22865 (*myohd1*, GI:14286205), we generated PCR primers to clone the full-length coding region of this putative myosin from human pancreas cDNA. Sequence analysis of the PCR-amplified clone revealed a 970aa coding region consisting of a myosin motor domain, a neck region containing three IQ motifs, and a short tail (Figure 5.1). The Myo19 motor domain shares ~35% sequence identity with the motor domains of human skeletal muscle myosin, Myo5a, and Myo6. Additionally, the motor contains the conserved GESGAGKT sequence from the P-loop, DXXGFE sequence from switch-2 (DVYGF), and a slightly divergent MEAFGNACTLRNNSRFGK in the switch-1 region (Supplemental Figure 5.1.A, reviewed in (Cope et al., 1996)). Myo19 has a glutamine at the TEDS position, indicating that it is not regulated by heavy-chain phosphorylation at this site (Bement and Mooseker, 1995). The three IQ motifs in the neck region are expected to bind calmodulin or calmodulin-like light chains (Cheney and Mooseker, 1992). The 146aa tail domain of Myo19 is basic (pI ~9.2) and is not predicted to form a coiled-coil (Lupas et al., 1991). Interestingly, the tail has no obvious sequence homology with other proteins in the databases, except for other Myo19 orthologs (Figure 5.1.B). Clear orthologs of human Myo19 are present in multiple vertebrate species including mouse (GI:56206893), chicken (GI: 118100337), *Xenopus laevis* (GI:62185680), and zebrafish (GI:189519181). Furthermore, at the amino acid level, human Myo19 (970aa) exhibits

82% identity to mouse Myo19 (963aa) and 56% identity to *Xenopus laevis* Myo19 (971aa). Although Myo19 arose early in metazoan evolution, it appears to have been lost from lineages leading to *Drosophila* and *C. elegans* (Odrionitz and Kollmar, 2007).

MYO19 IS EXPRESSED IN MULTIPLE TISSUES AND CELL LINES

To determine the tissue expression pattern of Myo19, we probed a Northern blot using a sequence from the 3' non-coding region. A band of approximately 4.2kb was detected in multiple tissues (Figure 5.2.A). Although the sample from human brain did not react strongly with this probe, analysis of ESTs and the Allen Brain Atlas (<http://www.brain-map.org>) indicate that Myo19 is broadly expressed in vertebrate tumors, cells, and tissues, including brain. Antibodies raised against the human Myo19 peptide AKELDGVVEEKHFS (aa 829-841) detected a protein of the expected size of ~109kD in western blots of human and other primate cell lines (Figure 5.2.B). We also detected Myo19 in mouse cell lines (B16-F1 and CAD) using this antibody, but the signal was weaker, likely due to sequence differences in the antibody target (SKELDGMEEKPMP in mouse). To study mouse Myo19 in addition to human, we raised 2 antibodies against bacterially expressed and purified mouse Myo19 tail sequence. The anti-mMyo19 antibody #42 (Ab42) recognized a protein of the expected size of ~109kD in mouse cells (B16 and CAD), but not in human cells (A549) (Figure 5.2.C). When mouse cells were transfected with either full-length hMyo19 or the tail of hMyo19, Ab42 could only detect endogenous mMyo19, whereas anti-mMyo19 antibody #43 (Ab43) could detect either endogenous mouse or exogenous human Myo19 (Figure

5.2.D). Together, our antibodies detected a protein of predicted size in several cell types from different species and tissues.

MYO19 LOCALIZES TO MITOCHONDRIA

To reveal the cellular localization of Myo19, we immunostained multiple cell lines (B16, NIH3T3, A549, HeLa, and COS-7) with anti-Myo19 antibodies. Colocalization with mitochondrial markers revealed clear and striking localization of endogenous Myo19 to mitochondria (Figure 5.3). Next, we performed differential centrifugation on NIH3T3 homogenates to determine if Myo19 separated into fractions along with a known mitochondrial marker. With increasing centrifugal force, endogenous Myo19 indeed followed the mitochondria marker porin from supernatant to pellet (Figure 5.4). To determine the region of Myo19 required for mitochondrial localization, we generated a series of GFP-constructs containing different regions of the human Myo19 protein. When expressed in A549 (Figure 5.5.A) or B16 cells (not shown), full-length GFP-Myo19 and a “tail” construct containing amino acids 801-970 both clearly localized to mitochondria. However, a construct containing the motor domain and IQ motifs (amino acids 1-828) did not localize to mitochondria and exhibited punctate cytoplasmic staining (Figure 5.5A). To test if Myo19 is anchored to the mitochondrial outer membrane via insertion of a c-terminal transmembrane helix (Borgese et al., 2003), we added GFP to the c-terminus of our constructs (Horie et al., 2002). Expression of either a Myo19 tail or a full-length Myo19 construct GFP-tagged at the c-terminus resulted in mitochondrial localization. Taken together, these data indicate

that the tail domain of Myo19 is necessary and sufficient for mitochondrial localization via a mechanism that is likely not a c-terminal transmembrane helix (Figure 5.5.B).

EXPRESSING GFP-MYO19 ALTERS MITOCHONDRIAL DYNAMICS

Due to its striking endogenous localization to mitochondria, we next wondered if Myo19 functions in actin-based mitochondrial motility. To test Myo19's role in mitochondrial dynamics, we used time-lapse imaging to monitor the movements of mitochondria in GFP-Myo19 transfected cells versus Mito Tracker labeled or fluorescently-tagged mitochondrial targeting sequence transfected control cells. In control cells, the vast majority of mitochondria remained largely in place with only small "jostling" movements (Movie 5.1). The rare mitochondria that underwent long-range, end-on movement in these cells traveled with a velocity of 102 ± 7 nm/s (n=27 mitochondria, 6 cells). Expressing GFP-Myo19, however, led to a dramatic increase in mitochondrial motility (Movie 5.2 and Figure 5.6). In approximately 40% of the cells expressing GFP-Myo19, the majority of mitochondria moved continuously for many microns with one end of the mitochondrion leading. The leading end was often wider than the trailing end, resulting in a tadpole-like appearance (Figure 5.6.B, Movie 5.3). Unlike microtubule-dependent movements, these mitochondria did not follow linear tracks and their movements were not obviously directed towards or away from the cell center (Figure 5.6.A). The mitochondria in GFP-Myo19 cells that were moving continuously had an average velocity of 73 ± 3 nm/s (n=125 mitochondria, 8 cells).

To quantify the increase in mitochondrial motility induced by GFP-Myo19, we measured the average velocities of randomly selected mitochondria in control A549

cells and A549 cells transfected with GFP-Myo19. The velocities of control mitochondria formed a broad peak centered at relatively low values, while the velocity distribution for GFP-Myo19 mitochondria was shifted to the right and had an additional small peak in the 50-75 nm/s range (Figure 5.6.C). The average velocity of randomly selected mitochondria in the control cells was 16 ± 1 nm/s ($n=122$ mitochondria, 12 cells). Expressing GFP-Myo19 resulted in an average velocity of 28 ± 2 nm/s ($n=163$, 8 cells; $p < 4 \times 10^{-8}$), a 75% increase over control cells. Since these measurements included mitochondria from all GFP-Myo19 cells, including those that exhibited little movement, the average velocity from only the ~40% of A549 cells that exhibited overall increased mitochondrial motility would be even greater.

As an additional measure of mitochondrial dynamics, we also determined a "Displacement Index" (D.I.) by dividing the area over which mitochondrial network moved in a 3:20 (min:sec) time-lapse by the area occupied by mitochondria in the first frame of the recording (Figure 5.7). If the mitochondrial network remained perfectly stationary, then D.I.=1. Control A549 cells had a D.I. of 1.2 ± 0.1 ($n=10$, $p < 5 \times 10^{-5}$, Figure 5.7.A), whereas the D.I. in GFP-Myo19 cells increased by 75% to 2.1 ± 0.7 ($n=28$), again demonstrating that expression of GFP-Myo19 dramatically increases mitochondrial motility.

GFP-MYO19 INDUCED MITOCHONDRIAL MOTILITY IS LIKELY DUE TO MYO19 MOTOR ACTIVITY

We hypothesize that the movements of mitochondria we observed are powered by Myo19 moving on randomly organized actin filaments. To test if these movements

are in fact actin-based, live cells expressing full-length GFP-Myo19 were treated with 15 μ M nocodazole to disrupt microtubules or 500nM latrunculin B to disrupt F-actin. This dose of nocodazole was sufficient to disrupt the distribution of the endoplasmic reticulum within 5 minutes (data not shown). Mitochondrial movements induced by GFP-Myo19 were insensitive to nocodazole treatments lasting as long as least twenty minutes (Figure 5.8, Movie 5.4). These mitochondria continued to display movement over many microns and the tadpole shape remained. However, upon addition of latrunculin B to nocodazole-treated cells, the end-on, directed movements ceased (Figure 5.8, Movie 5.4). In addition, the mitochondria lost their asymmetric shape within 2 minutes of latrunculin B treatment (Figure 5.8.C). Treatment of cells with latrunculin B without nocodazole pretreatment also resulted in a prompt cessation of end-on mitochondrial movement and a rapid loss of the asymmetric shape, demonstrating that both the motility and altered shape are dependent on the presence of F-actin (Movie 5.5).

siRNA OLIGOS DIRECTED AGAINST MYO19 EFFECTIVELY KNOCK-DOWN MYO19 PROTEIN

The discoveries that Myo19 localizes to mitochondria and that over-expression of Myo19 led to a dramatic increase in mitochondrial dynamics were quite intriguing and raised an obvious next question: what is the function of endogenous Myo19? To address this question, we sought to examine the loss of function phenotype in Myo19 knock-down cells. Numerous previous attempts to perform such experiments in human cells using siRNA and morpholino strategies proved unsuccessful. This was in large

part because the chicken anti-human antibody used to screen for knock-down gave a low signal and high background in Western blotting. Therefore, I began characterizing the rabbit anti-mouse Myo19 antibodies (as shown in figures 5.2, 5.3, and 5.4). With the reproducible success of these antibodies, I decided to test for the Myo19 loss of function phenotype in mouse cells. To achieve this aim, I designed five siRNAs against mouse Myo19 (Figure 5.9.A) and used B16 cells to test several concentrations and lengths of exposure for each siRNA (Figure 5.9.B). Within the conditions I tested, all of the siRNA sequences knocked-down Myo19 to some extent, although sequence #2 appeared most effective. Overall, I was able to achieve maximum knock-down of Myo19 protein in the range of 50-90%, as detected by Western blot. These results were exciting, as now we have a strategy to examine the effects of endogenous Myo19 knock-down.

Next, I used my siRNA protocol to perform some preliminary loss of function studies. I first was interested to know if Myo19 knock-down affected mitochondrial shape, size, or distribution. Changes in mitochondria shape and/or size would suggest that Myo19 may participate in mitochondria fusion or fission, as knock-down of proteins that participate in mitochondria fusion and fission result in fragmented or elongated mitochondria populations, respectively (Chen and Chan, 2004; Detmer and Chan, 2007). Alternatively, the increase in mitochondrial dynamics following Myo19 over-expression suggests that Myo19 may play a role in mitochondria positioning; therefore Myo19 knock-down could result in an abnormal distribution of mitochondria. To begin testing these possible functions for Myo19, I treated B16 cells with non-specific or Myo19-specific siRNA for four days, labeled mitochondria with Mitotracker,

fixed, and imaged the cells. In these preliminary experiments, I did not see an obvious qualitative defect in mitochondrial shape, size, or distribution (not shown). Although these initial experiments using my Myo19 knock-down strategy did not reveal an obvious phenotype, we now have the tools and methods necessary to uncover the endogenous role of Myo19 by testing its function in a number of different assays, as discussed below.

MYO19 IS A NOVEL MITOCHONDRIA-ASSOCIATED MYOSIN THAT IS LIKELY TO FUNCTION IN ACTIN-BASED MITOCHONDRIA DYNAMICS

Taken together, our data strongly suggest that Myo19 is a broadly expressed mitochondrial myosin involved in actin-mediated mitochondria movement and positioning. Endogenous Myo19 localizes to mitochondria, as revealed by immunostaining and differential centrifugation, and truncation analyses indicate that this localization is via Myo19's tail. Expression of full-length GFP-Myo19 protein induces a dramatic increase in mitochondrial motility in A549 and B16 cells and we observed similar increases in mitochondrial motility in COS-7 cells (data not shown). As predicted for myosin-driven movements, these movements are indeed actin based, as GFP-Myo19-induced movements cease upon destabilization of the actin network. Since the striking increase in mitochondrial motility was not observed in 100% of the cells expressing GFP-Myo19, it is likely that additional factors regulate Myo19 function and/or mitochondrial movement. Whether those conditions are related to the amount of Myo19 on the mitochondrial surface or activation state of Myo19 motor has yet to be determined.

Although our over-expression data revealed an obvious gain of function for Myo19, our initial knock-down results were not clear. Preliminary analysis of Myo19 knock-down cells did not display a defect in mitochondria shape, size, or distribution. Investigating these mitochondrial attributes was quite difficult, as mitochondria are known to be heterogeneous and pleiomorphic (Collins et al., 2002; Rube and van der Bliek, 2004), but qualitative analysis did not reveal the gross defects seen in knock-down of fusion or fission proteins. Additionally, we did not observe obvious changes in the distribution of mitochondria when Myo19 was knocked-down in B16 cells; however, mitochondria distribution in wild-type B16 cells is heterogeneous. It is possible that B16 cells are not the ideal model to test for changes in mitochondria position following knock-down of Myo19. A cell type such as neurons or polarized epithelial cells, which require spatially disparate energy needs, may normally have a less heterogeneous mitochondria distribution. Knock-down of Myo19 in such a cell type could reveal a role for Myo19 in mitochondrial positioning and distribution.

An alternative possibility for a Myo19 null phenotype, as implicated by the gain of function phenotype of increased mitochondrial dynamics, is that knock-down of Myo19 will result in decreased mitochondrial motility. Unfortunately, the normally low level of mitochondrial dynamics in B16 cells makes it difficult to assess how knock-down of Myo19 effects mitochondrial movements in our current system. Just as described above for mitochondria positioning and distribution, it may be important to find a cell type that normally exhibits a high degree of mitochondrial dynamics. In addition, it may be possible to identify drugs or cellular conditions that induce an increase in mitochondria movements. For example, decreasing calcium levels with

treatment with either the calcium chelator BAPTA-AM or activation of protein kinase C with phorbol myristate acetate can increase mitochondrial motility (Saotome et al., 2008; Wang and Schwarz, 2009; Nekrasova et al., June 2007). Treatment of control versus Myo19 knock-down cells with these drugs may reveal a defect in mitochondrial dynamics that is not otherwise apparent in untreated cells.

While it is possible that we could see dramatic changes in mitochondrial dynamics following Myo19 knock-down, perhaps Myo19 plays a more subtle role in mitochondria movements. In wild-type B16, A549, and HeLa cells, we routinely observe a constant “jostling” movement of the mitochondria. These movements may represent a form of perpetual interaction with the surrounding actin cytoskeleton powered by Myo19. Furthermore, transient Myo19-mediated interactions with the actin cytoskeleton may play an important role in conjunction with microtubules-based mitochondrial movements. As mitochondria move across long distances via microtubule-based motors, pauses along the journey could be the result of Myo19 interacting with the surrounding actin as it passes by. These more subtle roles for Myo19 could be important not so much for transporting mitochondria, but for anchoring them in specific cellular locations.

Lastly, it is important to note that although we suggest several possible roles for Myo19 in mitochondria function, defects in these processes may not be apparent in knock-down cells with only a 50% reduction in Myo19 protein. If very low amounts of Myo19 are sufficient to sustain a functioning mitochondria system, we may need to reduce the levels of Myo19 protein by 90% or more to reveal a Myo19-null phenotype. To address this concern, we are currently creating a Myo19-shRNA construct for use

with the pLL lentivirus system (Rubinson et al., 2003). With this system, the shRNA directed against Myo19 will be stably inserted into the genome, allowing for a longer period and higher percentage of Myo19 knock-down. Under these conditions, it will be more feasible to determine in which of the duties described above Myo19 is participating.

The localization and dynamics of mitochondria are critical to mitochondrial function and disruption of these processes leads to human disease (Zuchner et al., 2004; Delettre et al., 2002). Mitochondrial localization and dynamics have been shown to involve both microtubules and actin (Nangaku et al., 1994; Tanaka et al., 1998; Altmann et al., 2008; Boldogh et al., 2001; Minin et al., 2006). However, the mechanism of actin-based mitochondrial movements in vertebrates remains unclear (Hollenbeck and Saxton, 2005). Here we report the discovery of a novel mitochondria-associated myosin, Myo19. Myo19 is the founding member of a novel class of myosins and is the last uncharacterized myosin in humans. We show that Myo19 exhibits striking localization to mitochondria and that this localization is mediated through its tail. Additionally, we demonstrate that over-expression of Myo19 results in a remarkable gain of function phenotype, in which mitochondria become more motile and dynamic. Finally, we developed an siRNA strategy to knock-down Myo19 in mouse cells, which can be used in the future to uncover the endogenous role of Myo19. Our discovery of a novel class of myosin that localizes to mitochondria provides a possible molecular mechanism for actin-based mitochondrial movements.

EXPERIMENTAL PROCEDURES

PCR cloning. The full-length human Myo19 construct was cloned from a QUICK-Clone pancreas cDNA mix (Clontech) using the primers listed in Quintero et al, 2009. The 3.7 kb band (as visualized by agarose gel electrophoresis) was then extracted and cloned into the pCR 2.1-TOPO cloning vector (Invitrogen) as per the manufacturer's protocol. After the verification of the fragment's sequence by direct sequencing, this clone was used to generate all subsequent GFP constructs of Myo19 by adding restriction sites that would allow insertion into the correct pEGFP expression vector (Clontech). All clones were verified by sequencing.

Northern blotting. A 433 bp oligonucleotide probe to the 3'-untranslated region of the predicted human Myo19 mRNA was generated by PCR (forward primer 5'-TGCCTCAGGGATCGATAAAG-3' and reverse primer 5'-CATGACTGCTGCTGAGTTTGA-3') from a previously generated PCR clone of the Myo19 mRNA. The probe was end-labeled with ³²P using Ready To Go DNA labeling beads (Amersham), according to the manufacturer's directions, and unincorporated counts were removed by ProbeQuant G-50 Micro Column (Pharmacia Biotech). The probe was added to the hybridization solution to a final concentration of 2 x 10⁶cpm/mL, and a human multiple tissue blot (BD Biosciences) was hybridized under stringent conditions and washed according to the manufacturer's directions. The blot was then exposed using a phosphorimager.

Antibody production. For biochemical studies and immunolocalization, antibodies were raised in chickens against a synthetic peptide sequence consisting of amino acids 829-841 of human Myo19 (AKELDGVEEKHFS). Two chickens were immunized and the antibodies specific to the peptide were isolated by affinity

chromatography using the immobilized peptide (Aves Labs). Additional antibodies were raised in rabbits against a bacterially-expressed and purified His-tagged mouse Myo19 tail sequence (Qiagen PQE vector system). Two rabbits were immunized and the antibodies specific to the Myo19 tail sequence were isolated by affinity chromatography using the immobilized protein.

Cell culture. HeLa carcinoma cells and COS-7 kidney epithelial cells were obtained from the Lineberger Comprehensive Cancer Center, UNC-Chapel Hill. A549 pulmonary epithelial cells and B16F1 melanoma cells were obtained from Dr. Jo Rae Wright (Duke University Medical Center) and Dr. Gary Borisy (Northwestern University Medical School), respectively. HeLa cells were maintained in MEM medium supplemented with 10% fetal bovine serum and 100U penicillin-streptomycin. A549 cells were maintained in F12K medium supplemented with 10% fetal bovine serum and 100U penicillin-streptomycin. COS-7 and B16F1 cells were maintained in DMEM medium supplemented with 10% fetal bovine serum and 100U penicillin-streptomycin. Cells were passaged using 0.25% trypsin-EDTA (Invitrogen) and plated onto the required substrate (cell culture flasks or glass slides) depending upon the requirements for the experiment.

Immunoblotting. For western blots to determine the presence of Myo19 protein, cells from 100mm cell culture dishes that were 80% confluent were scraped directly into 1mL of lysis buffer (10mM HEPES, 2mM EDTA, 10% sucrose, Sigma protease inhibitor cocktail, pH7.4), mixed with 5x SDS-PAGE sample buffer, and boiled at 95°C for 5 minutes prior to loading on a 4-20% Tris-glycine SDS-PAGE gel. Samples were then transferred to nitrocellulose at 150 V-hr in transfer buffer (25 mM Tris, 192 mM

glycine, 20% methanol, 0.02% SDS). Affinity purified antibodies were used at 0.3-1 $\mu\text{g}/\text{ml}$ with 1:10,000 donkey anti-chicken or donkey anti-rabbit (Jackson) secondary antibody conjugated to horseradish peroxidase. Immunoblots were developed using SuperSignal West Pico chemiluminescent substrate (Pierce).

Immunostaining. HeLa, A549, or COS7 cells were plated onto acid-washed coverslips or B16 cells were plated onto laminin-coated coverslips in a 6-well cell culture dish in their appropriate media overnight. For cells labeled with Mitotracker to stain mitochondria, cells were incubated with 1-5nM Mitotracker CMX-Ros for 10 minutes, and then washed three times for 10 minutes with the appropriate cell culture medium. The cells were fixed with 3.7% paraformaldehyde in PBS for 7 minutes, permeabilized with 0.5% Triton X-100 for 2 minutes, and blocked in 5% goat serum in PBS for 1 hour. Coverslips were incubated with specific antibodies at 0.5-5 $\mu\text{g}/\text{ml}$ for 1 hour, rinsed three times for 15 minutes in PBS, incubated with Alexa488- and/or Alexa568-conjugated secondary antibodies (Molecular Probes) at 1 $\mu\text{g}/\text{ml}$ for 60-90 minutes, and rinsed three times in PBS for 10 minutes. Coverslips were mounted using 90% glycerol containing 0.5% N-propyl gallate or GelMount (BioMedia) and examined using a Nikon fluorescence microscope with a 60x/1.4NA phase objective. Images were obtained using an Orca ER cooled CCD digital camera (Hamamatsu) or a Coolsnap ES cooled CCD digital camera (Photometrics) and Metamorph software (Universal Imaging).

Live cell imaging of GFP-Myo19 constructs. HeLa, A549, or COS7 cells were plated onto acid-washed coverslips in a 6-well cell culture dish in their appropriate media overnight. The cells were then transfected with the appropriate GFP-Myo19 construct,

either alone or in combination with pDsRed2-Mito (Clontech) using Polyfect transfection reagent (Qiagen) according to the manufacturer's protocol. For B16 cells, cells were transfected overnight, replated onto laminin-coated coverslips, then imaged the following day. The coverslips were transferred to imaging chambers containing Imaging Medium (Optimem medium without phenol red supplemented with 5% fetal bovine serum and 100U penicillin-streptomycin). For drug treatments, coverslips were mounted in perfusion chambers and the cells were treated with Imaging Medium supplemented 15 μ M nocodazole, or Imaging Medium supplemented with 500nM latrunculin B. Time-lapse images were collected using a Nikon fluorescence microscope with a 60x/1.4NA phase objective. Images were obtained using an Orca ER cooled CCD digital camera (Hamamatsu) or a Coolsnap ES cooled CCD digital camera (Photometrics) and Metamorph software (Universal Imaging). During imaging, the cells were maintained at approximately 35°C.

siRNA. Target sequences against mouse Myo19 were identified used the siDESIGN Center by Dharmacon. Non-specific, siGLO, and Myo19-specific oligos were ordered from Dharmacon. B16 cells at 30-50% confluency were transfected with siRNA oliogs using Lipofectamine 2000 (Invitrogen) according to the manufacturers instructions and following previously reported conditions (Dalby et al., 2004). Twenty-four hours after transfection, those cells transfected with siGLO were imaged to determine transfection efficiency. For experiments in which siRNA-treated cells would be imaged, cells were replated on coverslips three days after transfection. Imaging assays and Western blots were performed four or five days after siRNA transfection.

Data analysis and software used. Pair-wise sequence alignments were performed using BLAST (<http://blast.ncbi.nlm.nih.gov/bl2seq/>) (Tatusova and Madden, 1999). Sequence alignment was accomplished using ClustalW2 (<http://www.ebi.ac.uk/clustalw/>) (Larkin et al., 2007). Mitochondrial velocities were calculated by manually tracking individual mitochondria (moving with a leading end) frame-by-frame and calculating average velocity by dividing distance moved by elapsed time. In the experiments where mitochondria were selected at random, mitochondria to track were selected in the first frame of the time-lapse, prior to viewing the movie. Mitochondria that could not be tracked for the entire movie were not included. In the experiments where the velocities of moving mitochondria were measured, moving mitochondria were identified by viewing the time-lapse and choosing individual mitochondria that were moving end-on for at least 5 frames (25 seconds of elapsed time). Displacement Index (D.I.) was calculated by dividing the cellular area where mitochondria had been present during a 3:20 time-lapse (as calculated by maximum projection) by the cellular area that contained mitochondria in the first image of the series. Run length was defined as the distance traveled by a mitochondrion before an apparent pause of two or more frames. Data were compared using Minitab 12 software by Student's t-test for unpaired samples or analysis of variance and a Tukey test when appropriate. Data are expressed as mean \pm standard error of the mean. All images were prepared for publication using Metamorph, Photoshop, or a combination of both software packages.

Portions of this chapter were reprinted from *Current Biology*, Volume 19, Issue 23, Omar A. Quintero, Melinda M. DiVito, et. al, "Human Myo19 is a Novel Myosin that Associates with Mitochondria", pages 2008-2013, Copyright 2009 Elsevier, with kind permission from Elsevier.

A

1-MLQQVNGHNP GSDGQAREYL REDLQEFLGG EVLLYKLLDDL TRVNPVTLET VLRCLQARYM-60

61-ADTFYTNAGC TLVALNPFKP VPQLYSPELM REYHAAPQPQ KLKPHVFTVG EQTYRNVKSL-120

121-IEPVNQSIIV SGESGAGKTW TSRCLMKFYA VVATSPASWE SHKIAERIEQ RIILNSNPVME-180
 {P-loop} {Loop 1} {

181-AFGNACTLRN_NSSRFKFI QLQLNRAQQM TGAAVQTYLL EKTRVACQAS SERNFHIFYQ-240
 Switch 1 }

241-ICKGASEDER LQWHLPEGAA FSWLPNPERS LEEDCFEVTR EAMLHLGIDT PTQNNIFKVL-300

301-AGLLHLGNIQ FAASEDEAQP CQPMDDAKYS VRTAASLLGL PEDVLL~~EM~~VQ IRTIRAGRQ-360
 {HCM

361-QVFRKPCARA ECDTRRDCLA KLIYARLFDW LVSVINSSIC ADTDSWTFI GLLDVYGFES-420
 loop } {Switch 2

421-FPDNSLEQLC INYANEKLOQ HEVAHYLRAQ QEYAVEGLE WSFINYQDNQ PCLDLIEGSP-480
 } missing from FLJ22865 (in italics)

481-ISICSLINEE CRLNRPSAA QLQTRIAL AGSPCLGHNK LSREPSFIVV HYAGPVRYHT-540

541-AGLVEKNKDP IPPELTRLLQ QSQDPLMGL FPTNPKEKTO EPPGOSRAP VLTVVSKFKA-600
 {Loop 2} }

601-SLEQLLQVLH STTPHYRCI KPNSQGQAQT FLQEEVLSQL EACGLVETIH ISAAGFPIRV-660
 SH2 SH1

661-SHRNFVERYK LLRRLHPCTS SGPDSPYPAK GLPEWCPHSE EATLEPLIQD ILHTLPVLTQ-720

721-AAAITGDSAE AMPAPMHCGR TKVFMTDSML ELLECGRARV LEQCARCIQG GWRRHRHREQ-780
 {IQ core#1 }

781-ERQWRVAMLI QAAIRSWLTR KHIQRLHAAA TVIKRAWQKW RIRMACLAAK ELDGVEEKHF-840
 {IQ core#2} {IQ core #3 }

841-SQAPCSLSTS PLQTRLLEAI IRFWPLGLVL ANTAMGVGSF QRKLVVWACL QLPRGSPSSY-900

901-TVQTAQDQAG VTSIRALPQG SIKFHCRKSP LRYADICPEP SPYSITGFNQ ILLERHRLIH-960

961-VTSSAFTGLG-970

B

Human	821- <u>MACLAAKELDG</u> -VE-- <u>EKHSQAPCSLSTS</u> SPL---QT-----RLEEAIIRLWPL <u>GLVLA</u> -871
Cow	<u>MAFLASEELDG</u> -VE-- <u>EKHS</u> PHAPCSPGSSPLPPAQT-----RLQGAIIRLWPL <u>GLLALA</u>
Mouse	<u>MACLASKELDG</u> -ME-- <u>EKPMPQAPGTLR</u> -SSMSPAHT-----RFLGAIHHLWPLGLVLA
Opossum	<u>MDSLVSIELDN</u> -VE-- <u>ESCVSRVPEPPLSTTLP</u> -----WPPRSTVQLWPL <u>GLVLS</u>
Chicken	<u>MAALAAAELDE</u> -ND-- <u>EKTPFSAMSAKSPCSLET</u> --A-----WPLSAIIQFWPL <u>GLVLS</u>
X_laevis	<u>MEALAAAELDD</u> STEDV <u>ESTLFS</u> SMLASPVKLSLESSKTNLPDKIMTQSAILRFGTL <u>GLVLY</u>
Zebrafish	<u>MDALAEAELDD</u> AEDLV <u>EEEA</u> EASLMPNLLKERGVSQ LCS----VPEPVPVRGWP <u>GLAMA</u>
Human	872-NTA-----MGVGSFQ <u>RKLVVWACLQ</u> LPRGSPSSYTVQT-AQDQAG <u>VTSIRALPQGS</u> IKF-924
Cow	NAA-----VGVHGFG <u>RKLVVFA</u> CLQLPVGSPRSCAVQT-AQEQA <u>GVL</u> SIRALPQGSIRF
Mouse	NSA-----DGVRFQ <u>RKLVVA</u> CLRLPSDRP-SNKVQTPQQDQAG <u>ITSIRALPQGS</u> IKF
Opossum	NSP-----VGVGTGMR <u>NLSLQA</u> CLQIPCHSN-TYKVEATQHDQAG <u>ITSIRALPQGS</u> HQV
Chicken	AAP-----VTIVGLFR <u>RELSLLA</u> CLKVLQIG-CYKMS-SFLGC <u>GITSV</u> RALPQGSVRF
X_laevis	GAPAIRKYIVETDELK <u>RNQNILM</u> CLNMLHRNN-RYKVTV-NREBP <u>GITSIRAP</u> QGSIRF
Zebrafish	SAPSITVS-LTASGFQ <u>RIMS</u> IMTCINIPFRHG-QYKVTNQFDQ-G <u>VASIRAP</u> RGSIKM
Human	925- <u>HCRK</u> SPLRYADICPEPSPYSITGFNQ <u>ILLERHRLIH</u> VTSSTFTGLG-970
Cow	<u>HCRK</u> SPLRYADTCPPSPDSV <u>TGFNQILLERHR</u> PGHV-----
Mouse	<u>HCRK</u> SPLQYADICPPSASCVTGFNQ <u>ILLES</u> HRPVQV-----
Opossum	<u>HCKK</u> SPLLYANISPETQNCDI <u>TGFNQILLDRHRL</u> IEV-----
Chicken	<u>HCKK</u> SPLHYANVSPHTAAYSTGFNQ <u>ILLDRKELL</u> PT-----
X_laevis	<u>HYKR</u> SPLHFANICPGKINCGITGFNE <u>ILLEKT</u> -----V-----
Zebrafish	<u>HLQR</u> SPLLYADMHPAHKTEVV <u>TGFNQILLERD</u> -----

C

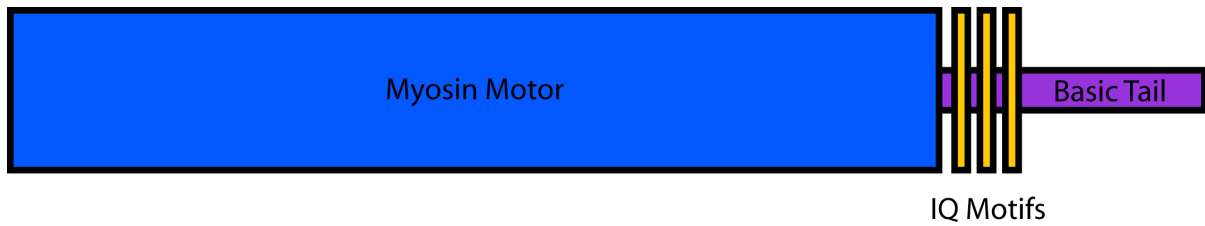


Figure 5.1. Myo19 is myosin motor protein with a novel tail domain. (A) Sequence analysis of Myo19 shows that it contains highly conserved sequences present in myosin motors (underlined) and the IQ motifs present in myosin lever arms. It is important to note that database entry FLJ22865 corresponds to a 770aa Myo19 sequence lacking 4 sequential exons from the core motor domain and is thus likely to represent either an aberrant cDNA or a splice form with a non-functional motor. The 200aa region of the motor domain missing from hypothetical protein FLJ22865 is represented in blue italics. (B) Although the tail domain of Myo19 does not contain obvious homology to other proteins or domains, sequence alignment of the Myo19 tail domain indicates regions of conservation exist. Mouse GI:81862507, cow GI:194675806, opossum GI:75750490, chicken GI:118100337, X. laevis GI:62185680, zebrafish GI:189519181. (C) Human Myo19 is predicted to consist of a motor domain, neck region with three IQ motifs, and a short tail domain.

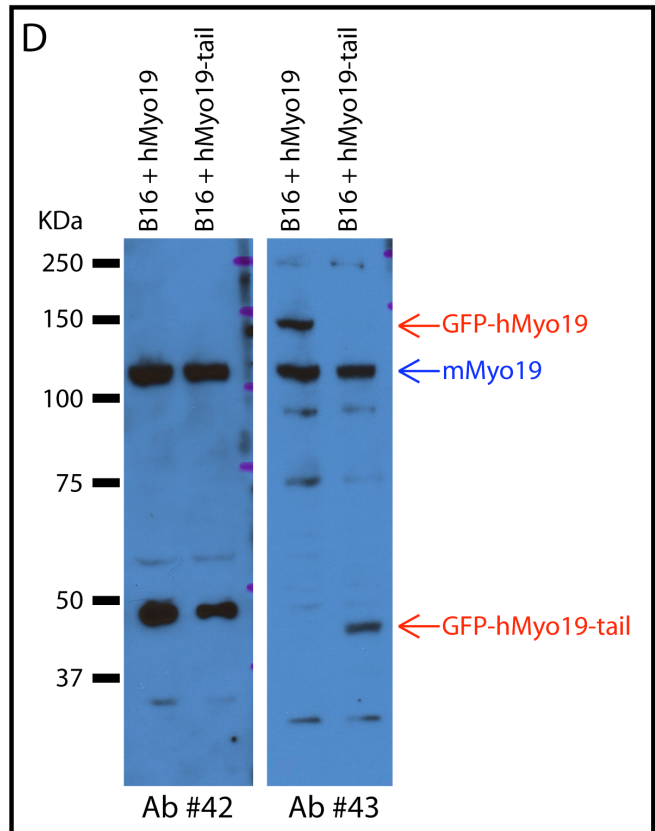
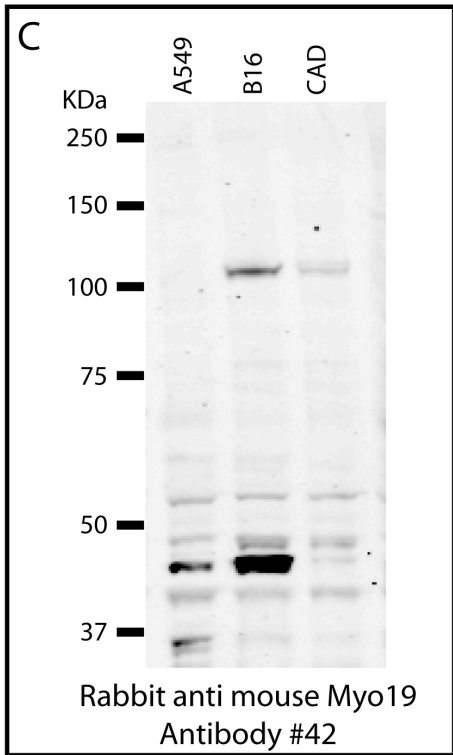
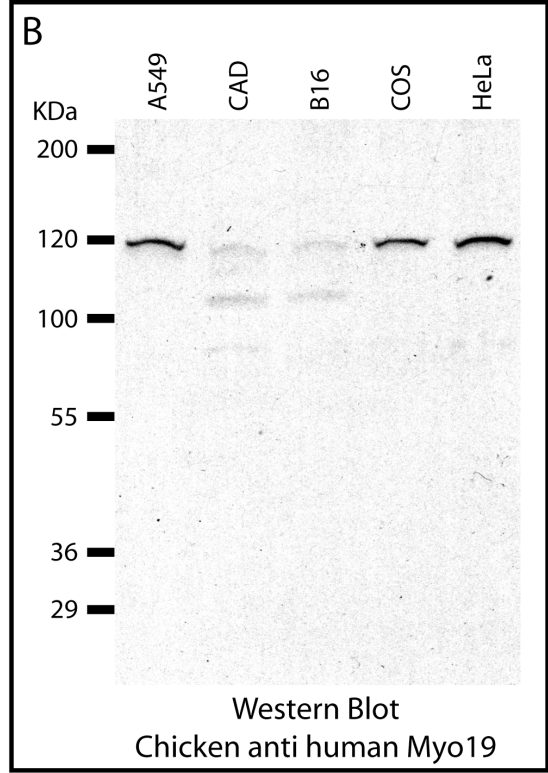
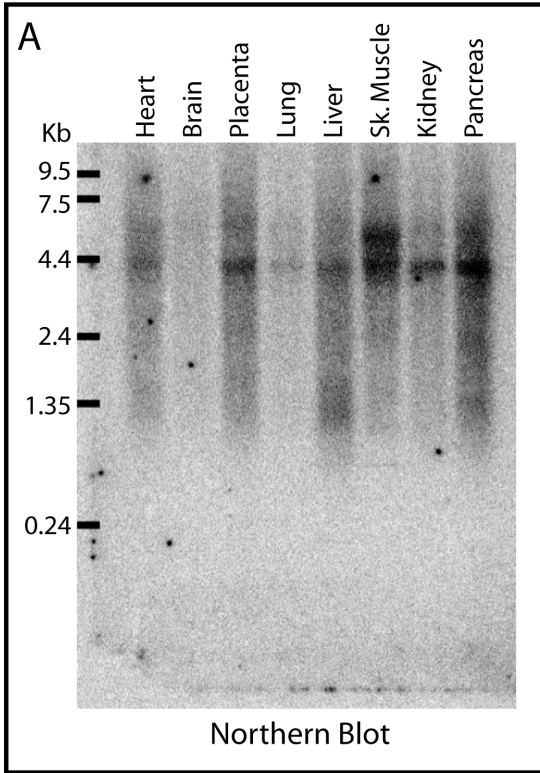


Figure 5.2. Myo19 is expressed in multiple tissues and cell lines. (A) A 4.2kb messenger RNA encoding for the Myo19 protein was detected by Northern blot analysis in multiple human tissues at varying levels. In skeletal muscle, a larger mRNA also appeared to react with the probe. Although the brain sample in this blot did not show strong reactivity, EST databases do indicate that Myo19 is expressed in brain. Ladder indicates sizes of molecular weight markers in kilobases (Kb). **(B)** Using an antibody raised against a peptide from the tail sequence of human Myo19, a protein of approximately 109kD was detected by western blot. This antibody cross-reacted poorly with rodent cell lines (B16 and CAD), but was able to detect Myo19 in human (HeLa and A549) and monkey cell lines (COS-7). Ladder indicates sizes of molecular weight markers in kiloDaltons (KDa). **(C)** Using an antibody raised against bacterially expressed and purified tail of mouse Myo19, a protein of approximately 109kD was detected by western blot. This antibody (Ab #42) detected Myo19 in mouse cell lines (B16 and CAD), but did not detect human Myo19 (A549). Additionally, Ab #42 reacted non-specifically with a band of approximately 45 KDa in several cell lines. **(D)** Two antibodies against mouse Myo19 (Ab #42 and Ab #43) have different cross-reactivity. In B16 cells transfected with human Myo19 constructs, Ab #42 only detects endogenous mouse Myo19, whereas Ab #43 can detect either mouse or human Myo19. Although Ab #43 can detect both mouse and human Myo19, its overall reactivity is weaker than Ab #42.

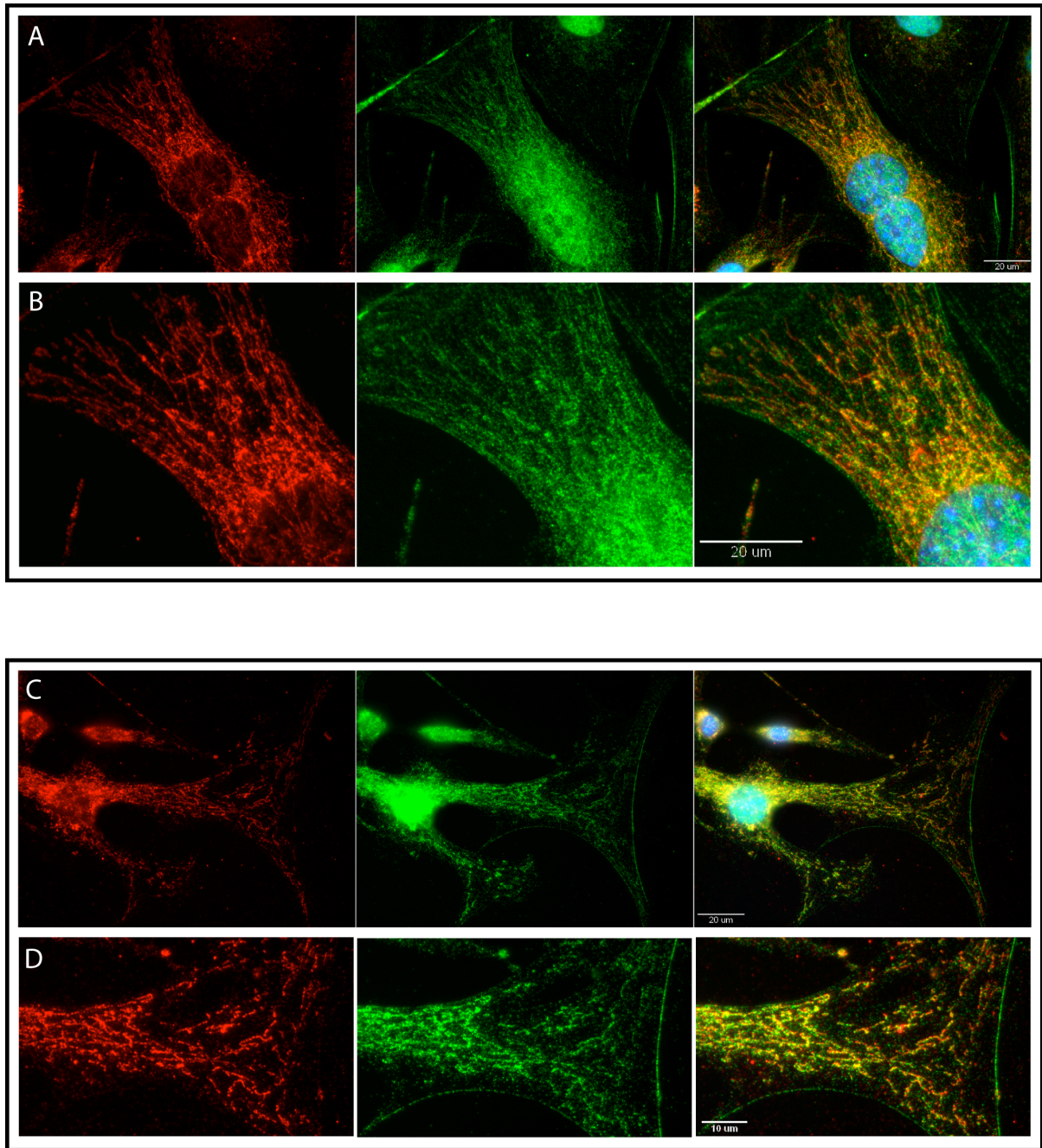


Figure 5.3. Myo19 localizes to mitochondria. Antibody #42 against mouse Myo19 (green) strongly colocalizes with anti-OxPhos complex IV subunit I stained mitochondria (red) in B16 cells. Nuclei are revealed with DAPI (blue). Chicken anti-human Myo19 antibody also labels mitochondria in HeLa and COS-7 cells (not shown).

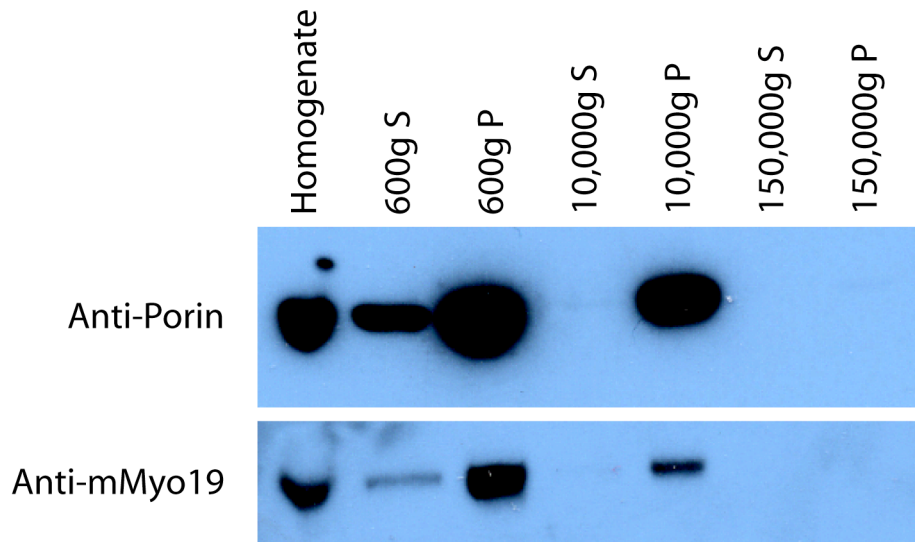


Figure 5.4. Myo19 co-sediments with mitochondria. NIH3T3 cells were homogenized and subjected to differential centrifugation. Samples of the supernatant and pellet from each centrifugation step were separated by SDS-PAGE and Western blotted. The presence of mitochondria in was detected using antibodies against the mitochondrial membrane protein, porin. Myo19 was detected using antibody #42. As revealed by anti-porin staining, a large portion of the mitochondria pellet out at 600g, indicating that the homogenate contained many cells still intact. The rest mitochondria released by homogenization pellet at 10,000g. Importantly, the Myo19 staining closely mirrors the porin staining, with a large portion of Myo19 in the 600g pellet and the remainder in the 10,000g pellet. Little to no porin or Myo19 protein is detectable in the 150,000g supernatant or pellet. This data suggests that Myo19 is found in cellular fractions containing mitochondria.

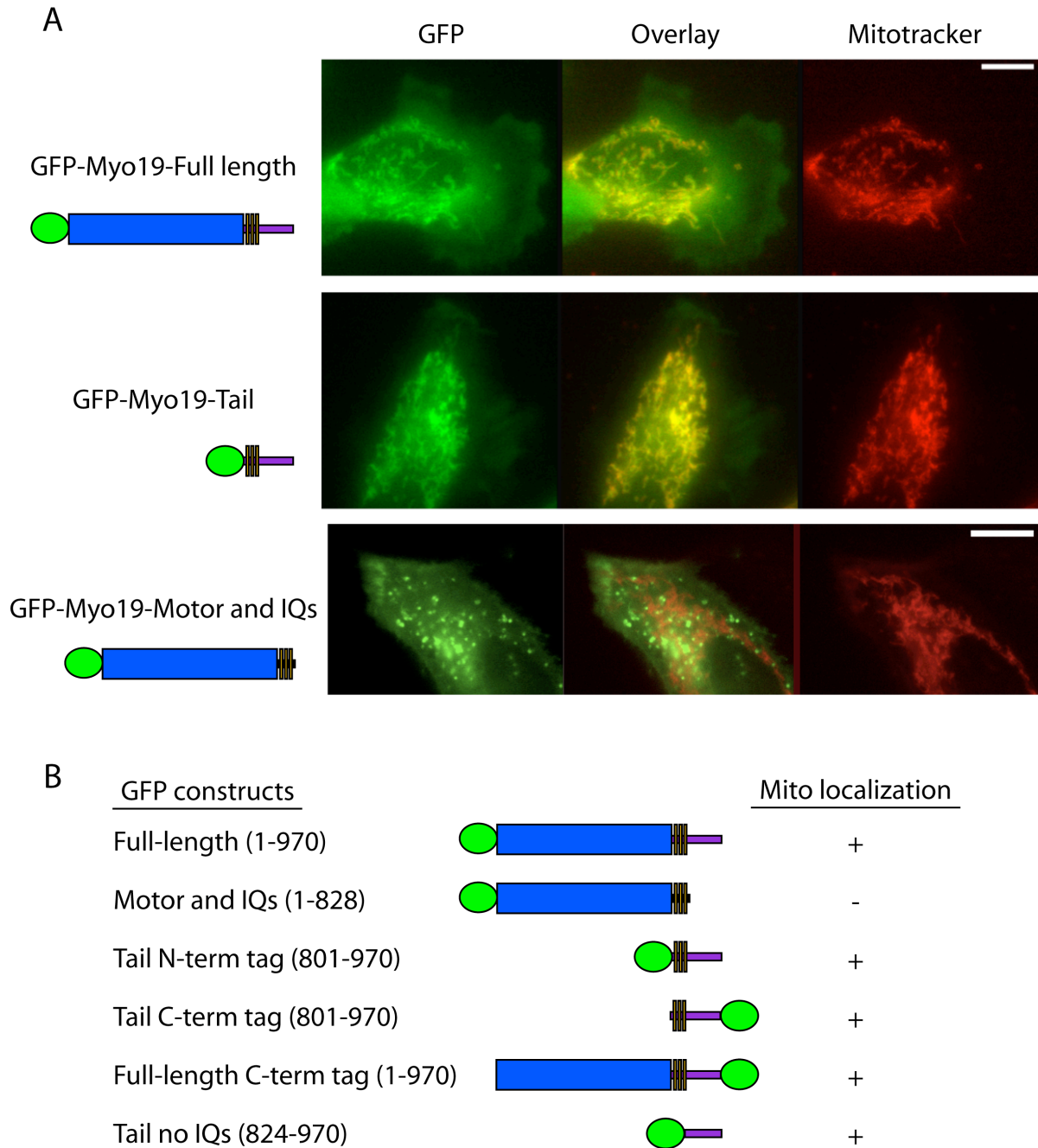


Figure 5.5. GFP-Myo19 localizes to mitochondria through its tail domain. (A) Both full length GFP-Myo19 and a GFP-Myo19-tail construct (green) colocalize with Mitotracker-labeled mitochondria (red) in HeLa (shown), A549, COS-7, and B16 cells. Constructs consisting of the motor domain and IQ motifs do not localize to mitochondria. **(B)** Amino acids 824-970 are necessary and sufficient for mitochondrial localization, as GFP constructs consisting of only this sequence of amino acids localize to mitochondria. GFP is represented by a green oval in the domain diagrams of the constructs in panels (A) and (B). Scale bars in (A) equal 10 μ m.

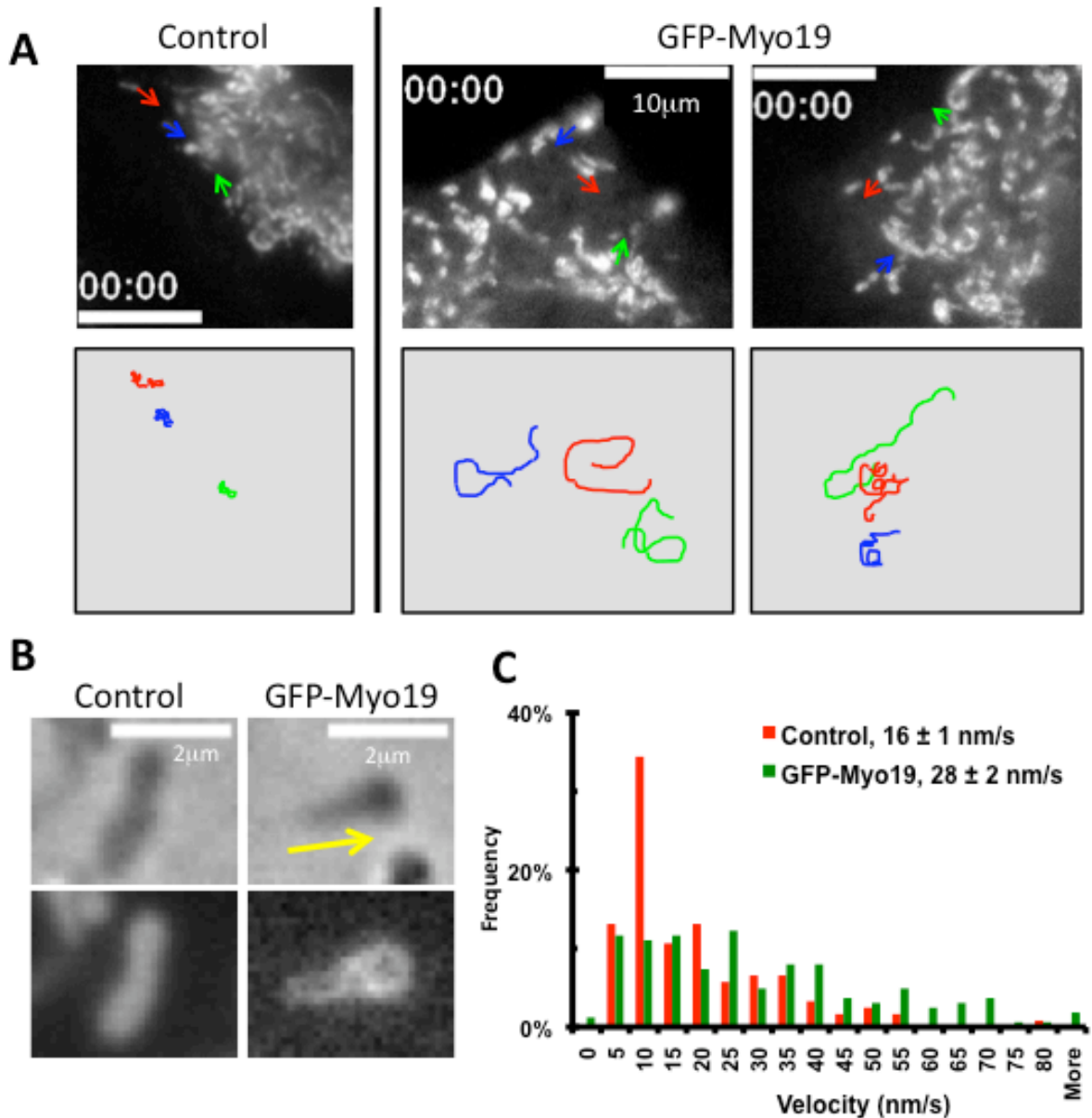


Figure 5.6. Expressing GFP-Myo19 increases mitochondrial motility. (A) Mitochondria in control A549 cells expressing pDsRed2-Mito showed little movement. Expression of GFP-Myo19 led to a vast increase in the number of mitochondria that moved and the lengths of those movements. These movements were often non-linear and did not necessarily correspond to movements towards or away from the nucleus. Arrows in the top panels represent the initial direction of movement for the indicated mitochondria and the paths taken by those mitochondria during a 4-minute recording are depicted in the bottom panel. (B) In addition to inducing motility of mitochondria in A549 cells, expression of full-length GFP-Myo19 often led to mitochondria with an obvious taper, where the trailing end was narrower than the leading end, as can be seen by phase contrast imaging or fluorescence imaging. Tapered mitochondria were rarely

observed in cells not expressing GFP-Myo19. Arrow indicates the direction of movement. **(C)** A histogram of velocities of randomly selected mitochondria shows that expression of full length GFP-Myo19 led to a 75% increase in mitochondrial velocity ($*p < 4 \times 10^{-8}$). For pDsRed2-Mito (control) cells, n=122 mitochondria (12 cells). For GFP-Myo19 cells, n=163 mitochondria (8 cells). Velocities in legend are mean \pm SEM.

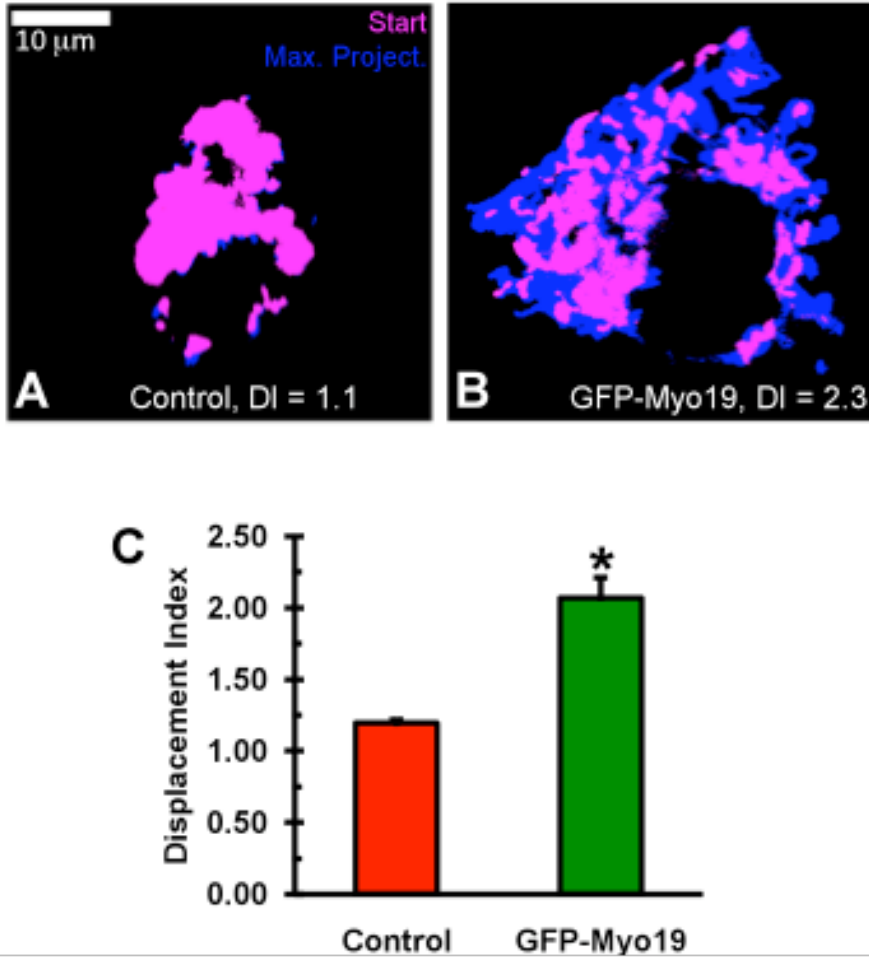


Figure 5.7. Expression of Myo19 increases mitochondrial dynamics. Displacement Index (D.I.) for a 3:20 time-lapse was calculated by dividing the cellular area where mitochondria had been present during the time-lapse (as calculated by maximum projection, blue) by the cellular area that contained mitochondria in the first image of the series (red) for **(A)** pDsRed2-Mito expressing (control) A549 cells and **(B)** GFP-Myo19 expressing A549 cells. Expression of GFP-Myo19 led to a dramatic increase in mitochondrial dynamics **(C)**, as indicated by the 75% increase in D.I. compared to control cells (* $p < 5 \times 10^{-5}$, $n = 28$ cells for GFP-Myo19, $n = 10$ cells for pDsRed2-Mito). Data are mean D.I. \pm SEM.

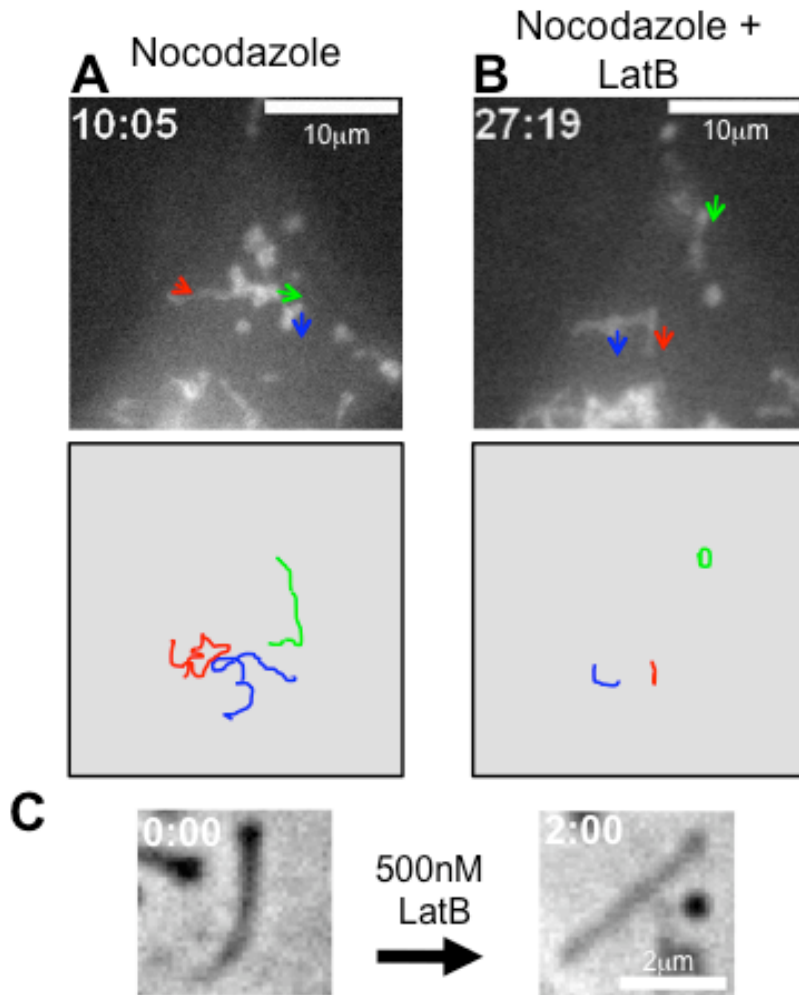


Figure 5.8. GFP-Myo19 induced movements in A549 cells are actin-dependent. (A) As can be seen in Movie 5.4, microtubule disruption with 15µM nocodazole failed to inhibit mitochondrial movements or shape change in GFP-Myo19 expressing A549 cells (drug added at 1minute, 40 seconds). Arrows in the top panels represent the initial direction of movement and the corresponding tracks over the next four minutes are shown in the bottom panels. **(B)** Disruption of actin with the addition of 500nM latrunculin B halted mitochondrial movements (drug added at 26:19). **(C)** Latrunculin B also disrupted the tapered mitochondrial shape within two minutes of addition, as visualized by phase contrast microscopy.

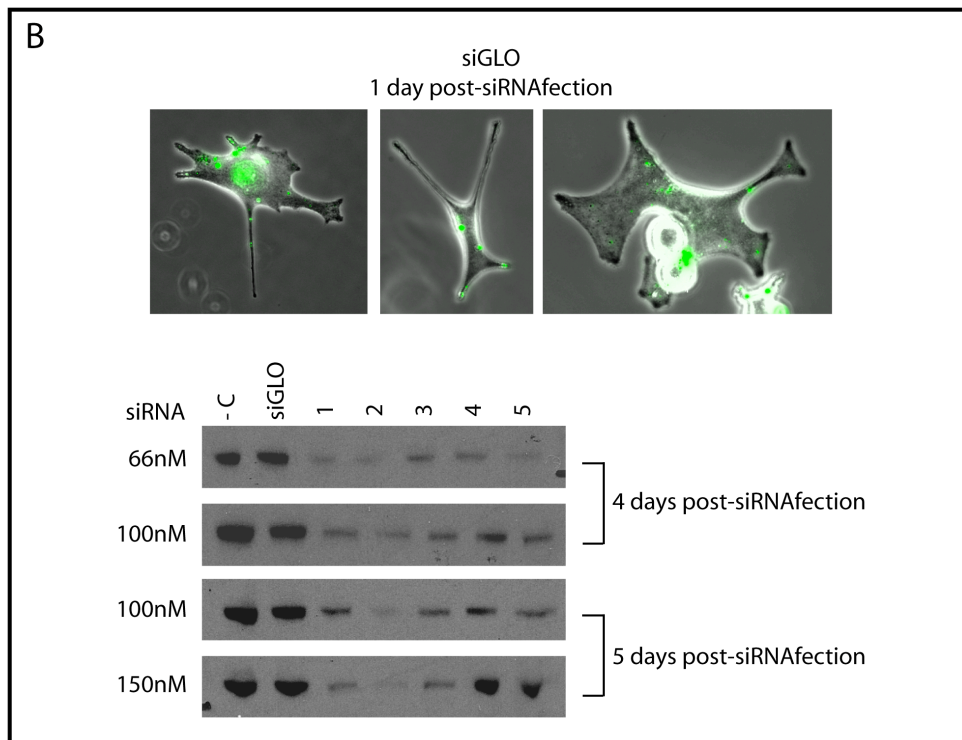
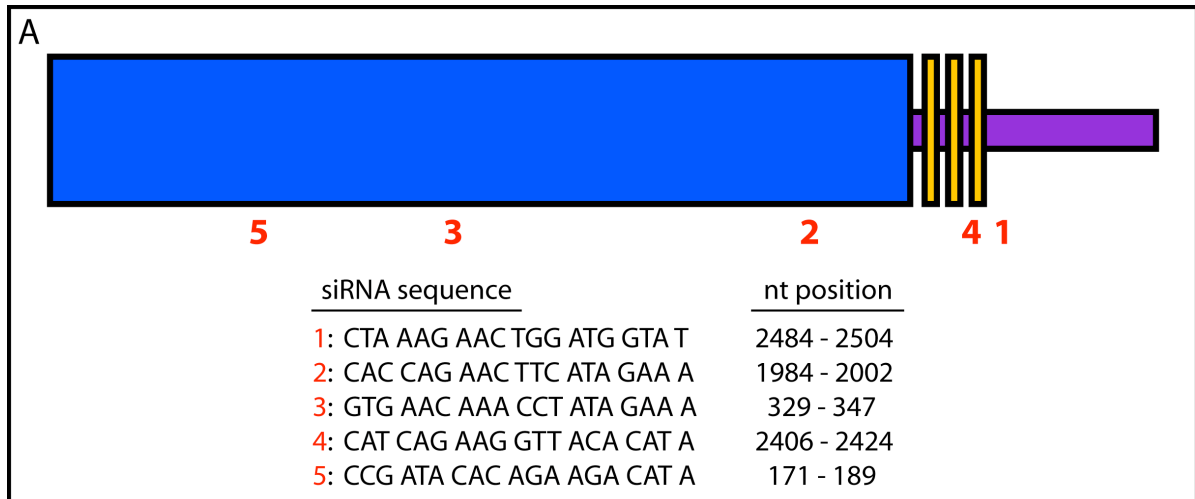


Figure 5.9. siRNA sequences directed against mouse Myo19 knock-down endogenous protein. **(A)** Five siRNAs were designed against mouse Myo19 and named siRNA #1-5. The nucleotide targets of each siRNA are listed along with the location of each target on the Myo19 protein bar diagram. **(B)** B16 cells transfected with fluorescently-labeled control siRNA oligos (siGLO) are positive for fluorescence one day after transfection. Visualizing presence of siGLO revealed a >90% transfection efficiency of siRNA oligos. Western blot analysis of B16 cells treated with non-specific (-C or siGLO) or Myo19-specific siRNA reveals knock-down of Myo19 protein levels. siRNA dose (nM) and length of exposure (days) were varied to determine an optimal siRNA treatment. Under these conditions, siRNA #2 appeared most effective versus the other siRNA sequences. Protein knock-down ranged from approximately 50-90%.

CHAPTER 5 MOVIE LEGENDS

Movie 5.1. Mitochondria in B16 cells are mostly stationary. Live-cell imaging of a B16 cell labeled with Mito Tracker revealed that although mitochondria exhibited small "jostling" movements, most did not undergo long-range movements. Images were captured once every 5 seconds. Timestamp represents min:sec.

Movie 5.2. Expressing GFP-Myo19 results in a dramatic increase in mitochondrial motility. B16 cells transiently transfected with GFP-Myo19 were imaged via time-lapse fluorescence microscopy. Expression of GFP-Myo19 caused majority of the mitochondria in the cell to become motile. These mitochondria moved with a leading end, but not in straight lines. Images were captured once every 5 seconds. Timestamp represents min:sec.

Movie 5.3. Expressing GFP-Myo19 often results in mitochondria with an asymmetric shape. B16 cells transiently transfected with GFP-Myo19 were imaged via time-lapse microscopy. Expression of GFP-Myo19 caused majority of the mitochondria in the cell to become motile. Moving mitochondria often displayed a characteristic "tadpole" shape where the leading end of the organelle was wider than the trailing end and brightly labeled with GFP-Myo19. The distorted shape can be seen in both the fluorescence (left) and phase contrast (right) images. Images were captured once every 5 seconds. Timestamp represents min:sec.

Movie 5.4. GFP-Myo19-induced mitochondrial movements are not microtubule-dependent, but are actin-dependent. A549 cells were transiently transfected with GFP-Myo19 and imaged via time-lapse fluorescence microscopy. Cells expressing full-length GFP-Myo19 were treated with cytoskeleton destabilizing drugs to identify which filaments are involved in Myo19-mediated mitochondrial movements. Media containing 15 μ M nocodazole was perfused into the imaging chamber at 1:40 (min:sec). The mitochondria maintained their tadpole shape and continued to move. Perfusion of media containing 500nM latrunculin B at 26:19 resulted in a cessation of the mitochondrial movements and a loss of the asymmetric mitochondrial shape. Prior to nocodazole treatment, the average velocity of moving mitochondria in this cell was 120 \pm 12nm/s (n=13). Following nocodazole treatment, the average velocity of moving mitochondria increased slightly to 148 \pm 7nm/s (n=22). Following addition of LatB, end-on mitochondrial movements ceased. As can be seen in the phase images, LatB treatment triggered some blebbing but the treated cell remained spread. Images were captured once every 5 seconds. Scale bar equals 10 μ m. Timestamp represents min:sec.

Movie 5.5. GFP-Myo19 induced mitochondrial movements are inhibited by latrunculin B treatment, even if microtubules are intact. A549 were transiently transfected with GFP-Myo19 and imaged via time-lapse fluorescence microscopy. Cells expressing full-length GFP-Myo19 were treated with media containing 500nM latrunculin B at 7:21 (min:sec). This perfusion resulted in a cessation of the mitochondrial movements. Prior to LatB treatment, the average velocity of moving mitochondria in this cell was

91±10nm/s (n=6). Following addition of LatB, end-on mitochondrial movements ceased. Images were captured once every 10 seconds. Scale bar equals 10µm. Timestamp represents min:sec.

CHAPTER 6

CONCLUSIONS AND FUTURE DIRECTIONS

MYOSIN-X

Myo10 is a MyTH4-FERM myosin that localizes to and travels within filopodia, is a master regulator of filopodia formation, and can bind to proteins found at the tips of filopodia (reviewed in Chapter 2). Specifically, Myo10 can bind to integrins, but the consequence of this interactions is largely unknown. Here, I provide evidence that suggests that Myo10 co-transport integrins to the tips of filopodia. Moreover, this interaction appears to be important during cell spreading and adhesion, when integrin-rich filopodia are known to mediate initial contacts between the cell and its substrate (Partridge and Marcantonio, 2006). However, the interaction between the FERM domain of Myo10 and β -integrins does not appear to increase integrin activation, unlike the FERM domain of talin. These results begin to describe the function of the Myo10- β -integrin interaction, but unanswered questions still exist.

Although I have shown that integrins can co-transport with Myo10 in filopodia, it remains unknown if Myo10 is required for these movements. Additionally, the details of these movements remain unclear. Does Myo10 bind to integrins regardless of their ligand status, or can Myo10 only bind unliganded/liganded integrins? We can glean some insight into this issue from the co-transport experiments performed here. I

routinely observed stable puncta of integrins localized along the shafts of filopodia (as seen in Figure 4.5). These are likely sites of filopodia shaft adhesions, where integrins are engaged with the ECM, and have been reported by others (Steketee and Tosney, 2002). Importantly, I almost always observed a corresponding, stable puncta of Myo10 overlapping with the stable integrin adhesion. This may represent molecules of Myo10 engaging ECM-bound integrins within a filopodia adhesion to provide traction along the filopodium.

Molecules that are present at the tips of filopodia, such as Myo10 and integrins, are proposed to associate with each other in a filopodial tip complex. In addition to integrins, Myo10 can also bind VASP – another protein that is found at the tips of filopodia and is important for filopodia formation. As more protein interactions are identified between tip-localizing proteins, we must ask, what is the function of the filopodial tip complex? One possibility is that this complex provides the correct components and environment to facilitate actin polymerization at the tip of the filopodium. Indeed, the proteins that are known to localize to the filopodial tip (Table 3.1) possess the necessary abilities – anti-capping, nucleating, elongating, membrane curving, and bundling. In another scenario, the filopodial tip complex may serve as a type of filopodia-specific adhesion, similar to a focal adhesion. It is clear that integrins localize to distinct locations at the tips and along the lengths of filopodia, and Myo10 could provide a link between the filopodial integrins and actin to mediate traction at a filopodial adhesion.

When live-cell imaging Myo10 with other components of the tip complex, such as integrins and VASP, we see these proteins co-localize at the tips of filopodia in large

puncta. Additionally, we often see a fragment of this large puncta break off and travel rearward back towards the cell body. These fragments of the filopodial tip complex can move back and forth within a filopodium for the duration of an imaging experiment, sometimes pausing within their run. What is the function of these mobile tip-complex fragments? Perhaps they on their way back to the cell body to be endocytosed and recycled. Alternatively, they may have they broken off of the tip to become a shaft adhesion? It will be important to explore these and other questions regarding the composition and function of the filopodial tip complex.

Myo10 localizes to the tips of filopodia and is likely to play an important role in the function of the tip complex. However, the forward and rearward movements of Myo10 in filopodia suggest that it has an additional function in filopodia maintenance. The ability of Myo10 to undergo intrafilopodial motility, combined with its capability to bind several tip complex proteins, implies that Myo10 can function to carry cargoes to and from the tips of filopodia (diagrammed in Figure 2.6). As filopodia can reach lengths of tens of microns or greater, intrafilopodial motility provides an ideal mechanism to transport molecules between the cell body and the distal tips of filopodia. This would be important for actin-associating proteins in the tip complex as well as receptors and signaling proteins. Interestingly, Myo10 has been shown to bind to and co-localized with VASP (Tokuo and Ikebe, 2004), integrins (Zhang et al., 2004), the BMP receptor Alk6 (Pi et al., 2007), and the netrin-1 receptor (Zhu et al., 2007). It was previously reported that Myo10 co-transport with VASP and Alk6 and I show here for the first time that Myo10 co-transport with β_1 - and β_3 -integrins. It will be important to determine if Myo10 binds to and co-transport with other filopodial-tip complex

proteins such as fascin and mDia2. Similarly, it will be interesting to find out if Myo10 binds to other receptors that are reported to localize to the tips of filopodia, like EGFR and VEGFR. Furthermore, if Myo10 does co-transport with these receptors, what purpose does this co-transport serve? While it is possible that Myo10 may carry new and unliganded receptors out to the tips of filopodia, it is also possible that Myo10 may carry ligand bound receptors back to the body of the cell where they can be endocytosed. Using GFP-EGFR and quantum dot-tagged EGF, Lidke *et al.* reported that ligand bound EGFR traveled rearward in filopodia, back to the body of the cell, where it was endocytosed at the base of the filopodium. Interestingly, preliminary experiments that I performed using CFP-Myo10, GFP-EGFR, and red quantum dot-tagged EGF revealed that Myo10 can move forward and rearward coordinately with liganded EGFR in A431 cells. It will be important to further test EGFR and other candidate cargoes for Myo10 binding and co-transport.

Filopodia are hypothesized to function as organelles of exploration. They dynamically extend and retract to interact with the cell's surroundings and receive extracellular cues. Myo10 plays several important roles in filopodia formation, maintenance, and function and is undoubtedly a critical component in filopodial biology. Clearly defining the function of Myo10 in the filopodial tip complex and during intrafilopodial motility will surely reveal interesting and important insights.

MYOSIN-XIX

Myo19 was discovered in a study using sequence analysis to predict uncharacterized myosins. It represented the last unidentified myosin in humans and

appears to be vertebrate-specific. Surprisingly, endogenous and exogenous Myo19 localizes to the mitochondria in several cell types. This was an exciting result, as no vertebrate myosin is known to associate with mitochondria. Myo19 appears to associate with mitochondria through its tail domain, which, unexpectedly, has no obvious sequence homology with proteins in the database. Although it appears that the association is not due to insertion of the Myo19 tail into the mitochondrial membrane, it is unknown if the tail associates with the surface of the mitochondria directly, or if it binds to another protein associated with the mitochondria. It will be important to determine how Myo19 recognizes and interacts with mitochondria.

When we over-expressed GFP-Myo19 in several cell types, we observed a striking gain of function phenotype. GFP-Myo19 induced a dramatic increase in mitochondrial motility and dynamics. This movement was independent of the microtubule cytoskeleton, but dependent on the presence of actin. We were excited to observe this result and sought to determine the Myo19 loss of function phenotype. I developed and tested an siRNA-mediated system to knock-down Myo19, but the effects of this knock-down remain unknown. The gain of function phenotype resulted in an increase in mitochondrial movements, so it is likely that knock-down of Myo19 may reveal a decrease in mitochondrial dynamics. Alternatively, Myo19 may function to position or anchor mitochondria in certain areas of the cell, which could be particularly critical in polarized cells where local energy needs are disparate across the cell. Myo19-mediated positioning of mitochondria could also be required during cell division, where organelles such as mitochondria must be partitioned equally into daughter cells. Finally, Myo19 may be important for the regulation of microtubule-mediated

mitochondrial movements. Kinesins and dyneins are known to interact with mitochondria and transport them along microtubules (Nangaku et al., 1994; Tanaka et al., 1998; Martin et al., 1999; Waterman-Storer et al., 1997). It is possible that Myo19 is responsible for creating pauses during the transport of mitochondria on microtubules by interacting with actin as it passes by. It will be essential to explore various cellular scenarios when testing for the function of endogenous Myo19.

In addition to uncovering the loss of function phenotype in Myo19 knock-down cells, it will also be informative to determine how Myo19-mediated mitochondrial motility is regulated. In our gain of function experiments, we over-expressed GFP-Myo19 in cells that contained endogenous Myo19, however, in the absence of over-expression, these cells showed low levels of mitochondrial dynamics. If Myo19 is present in these cells, then what is keeping it “turned off”? Conversely, what induces Myo19 movements? As calcium homeostasis is one of several mitochondrial functions, and many myosins are regulated by the calcium-binding light chain, calmodulin, it is possible that local fluctuations in calcium levels could influence Myo19. Additionally, movements of mitochondria are important for localizing the cell’s powerhouse to areas in need of ATP. Myosins are ATPases and require ATP to translocate along actin. Perhaps Myo19 drives movement of mitochondria until it stops as a result of low local ATP concentration. This would ensure that mitochondria are trafficked to an area of the cell that is in need of ATP production.

Actin dependent movements of mitochondria in mammalian cells have previously been described (Morris and Hollenbeck, 1995), but until now, no myosin was known to associate with mitochondria in mammalian cells. The discovery and

initial characterization of Myo19 provides the first example of a vertebrate-specific myosin that associates with mitochondria and implicates Myo19 in an actin-based form of mitochondrial motility. It will be fascinating to uncover the cell biological functions of this novel mitochondria-associated myosin.

REFERENCES

- Abe, T., M. Kato, H. Miki, T. Takenawa, and T. Endo. 2003. Small GTPase Tc10 and its homologue RhoT induce N-WASP-mediated long process formation and neurite outgrowth. *J.Cell.Sci.* 116:155-168.
- Altmann, K., M. Frank, D. Neumann, S. Jakobs, and B. Westermann. 2008. The class V myosin motor protein, Myo2, plays a major role in mitochondrial motility in *Saccharomyces cerevisiae*. *J.Cell Biol.* 181:119-130.
- Applewhite, D.A., M. Barzik, S. Kojima, T.M. Svitkina, F.B. Gertler, and G.G. Borisy. 2007. Ena/VASP proteins have an anti-capping independent function in filopodia formation. *Mol.Biol.Cell.* 18:2579-2591.
- Aratyn, Y.S., T.E. Schaus, E.W. Taylor, and G.G. Borisy. 2007. Intrinsic dynamic behavior of fascin in filopodia. *Mol.Biol.Cell.* 18:3928-3940.
- Askari, J.A., P.A. Buckley, A.P. Mould, and M.J. Humphries. 2009. Linking integrin conformation to function. *J.Cell.Sci.* 122:165-170.
- Aspenstrom, P., A. Fransson, and J. Saras. 2004. Rho GTPases have diverse effects on the organization of the actin filament system. *Biochem.J.* 377:327-337.
- Atienza, J.M., J. Zhu, X. Wang, X. Xu, and Y. Abassi. 2005. Dynamic monitoring of cell adhesion and spreading on microelectronic sensor arrays. *J.Biomol.Screen.* 10:795-805.
- Balaban, R.S., S. Nemoto, and T. Finkel. 2005. Mitochondria, oxidants, and aging. *Cell.* 120:483-495. doi: 10.1016/j.cell.2005.02.001.
- Banno, A., and M.H. Ginsberg. 2008. Integrin activation. *Biochem.Soc.Trans.* 36:229-234.
- Barreiro, O., and F. Sanchez-Madrid. 2009. Molecular basis of leukocyte-endothelium interactions during the inflammatory response. *Rev.Esp.Cardiol.* 62:552-562.
- Barreiro, O., M. Yanez-Mo, J.M. Serrador, M.C. Montoya, M. Vicente-Manzanares, R. Tejedor, H. Furthmayr, and F. Sanchez-Madrid. 2002. Dynamic interaction of VCAM-1 and ICAM-1 with moesin and ezrin in a novel endothelial docking structure for adherent leukocytes. *J.Cell Biol.* 157:1233-1245.
- Barzik, M., T.I. Kotova, H.N. Higgs, L. Hazelwood, D. Hanein, F.B. Gertler, and D.A. Schafer. 2005. Ena/VASP proteins enhance actin polymerization in the presence of barbed end capping proteins. *J.Biol.Chem.* 280:28653-28662.
- Bear, J.E., and F.B. Gertler. 2009. Ena/VASP: towards resolving a pointed controversy at the barbed end. *J.Cell.Sci.* 122:1947-1953.
- Bear, J.E., T.M. Svitkina, M. Krause, D.A. Schafer, J.J. Loureiro, G.A. Strasser, I.V. Maly, O.Y. Chaga, J.A. Cooper, G.G. Borisy, and F.B. Gertler. 2002. Antagonism between Ena/VASP proteins and actin filament capping regulates fibroblast motility. *Cell.* 109:509-521.

Belyantseva, I.A., E.T. Boger, and T.B. Friedman. 2003. Myosin XVa localizes to the tips of inner ear sensory cell stereocilia and is essential for staircase formation of the hair bundle. *Proc Natl Acad Sci U S A.* 100:13958-13963.

Belyantseva, I.A., E.T. Boger, S. Naz, G.I. Frolenkov, J.R. Sellers, Z.M. Ahmed, A.J. Griffith, and T.B. Friedman. 2005. Myosin-XVa is required for tip localization of whirlin and differential elongation of hair-cell stereocilia. *Nat Cell Biol.* 7:148-156.

Bement, W.M., and M.S. Mooseker. 1995. TEDS rule: a molecular rationale for differential regulation of myosins by phosphorylation of the heavy chain head. *Cell Motil.Cytoskeleton.* 31:87-92.

Bennett, R.D., A.S. Mauer, and E.E. Strehler. 2007. Calmodulin-like protein increases filopodia-dependent cell motility via up-regulation of myosin-10. *J Biol Chem.* 282:3205-3212.

Berg, J.S., and R.E. Cheney. 2002. Myosin-X is an unconventional myosin that undergoes intrafilopodial motility. *Nat Cell Biol.* 4:246-250.

Berg, J.S., B.H. Derfler, C.M. Pennisi, D.P. Corey, and R.E. Cheney. 2000. Myosin-X, a novel myosin with pleckstrin homology domains, associates with regions of dynamic actin. *J Cell Sci.* 113 Pt 19:3439-3451.

Berg, J.S., B.C. Powell, and R.E. Cheney. 2001. A millennial myosin census. *Mol Biol Cell.* 12:780-794.

Blumenthal, A., J. Lauber, R. Hoffmann, M. Ernst, C. Keller, J. Buer, S. Ehlers, and N. Reiling. 2005. Common and unique gene expression signatures of human macrophages in response to four strains of *Mycobacterium avium* that differ in their growth and persistence characteristics. *Infect Immun.* 73:3330-3341.

Bohil, A.B., B.W. Robertson, and R.E. Cheney. 2006. Myosin-X is a molecular motor that functions in filopodia formation. *Proc Natl Acad Sci U S A.* 103:12411-12416.

Boldogh, I.R., H.C. Yang, W.D. Nowakowski, S.L. Karmon, L.G. Hays, J.R. Yates 3rd, and L.A. Pon. 2001. Arp2/3 complex and actin dynamics are required for actin-based mitochondrial motility in yeast. *Proc.Natl.Acad.Sci.U.S.A.* 98:3162-3167.

Borgese, N., S. Colombo, and E. Pedrazzini. 2003. The tale of tail-anchored proteins: coming from the cytosol and looking for a membrane. *J.Cell Biol.* 161:1013-1019.

Brawley, C.M., and R.S. Rock. 2009. Unconventional myosin traffic in cells reveals a selective actin cytoskeleton. *Proc.Natl.Acad.Sci.U.S.A.* 106:9685-9690.

Bretscher, A., K. Edwards, and R.G. Fehon. 2002. ERM proteins and merlin: integrators at the cell cortex. *Nat.Rev.Mol.Cell Biol.* 3:586-599.

Calderwood, D.A. 2004. Talin controls integrin activation. *Biochem.Soc.Trans.* 32:434-437.

- Calderwood, D.A., B. Yan, J.M. de Pereda, B.G. Alvarez, Y. Fujioka, R.C. Liddington, and M.H. Ginsberg. 2002. The phosphotyrosine binding-like domain of talin activates integrins. *J.Biol.Chem.* 277:21749-21758.
- Calderwood, D.A., R. Zent, R. Grant, D.J. Rees, R.O. Hynes, and M.H. Ginsberg. 1999. The Talin head domain binds to integrin beta subunit cytoplasmic tails and regulates integrin activation. *J.Biol.Chem.* 274:28071-28074.
- Cameron, R.S., C. Liu, A.S. Mixon, J.P. Pihkala, R.J. Rahn, and P.L. Cameron. 2007. Myosin16b: The COOH-tail region directs localization to the nucleus and overexpression delays S-phase progression. *Cell Motil.Cytoskeleton.* 64:19-48.
- Campbell, I.D., and M.H. Ginsberg. 2004. The talin-tail interaction places integrin activation on FERM ground. *Trends Biochem Sci.* 29:429-435.
- Cao, T.T., W. Chang, S.E. Masters, and M.S. Mooseker. 2004. Myosin-Va binds to and mechanochemically couples microtubules to actin filaments. *Mol.Biol.Cell.* 15:151-161.
- Carman, C.V., C.D. Jun, A. Salas, and T.A. Springer. 2003. Endothelial cells proactively form microvilli-like membrane projections upon intercellular adhesion molecule 1 engagement of leukocyte LFA-1. *J.Immunol.* 171:6135-6144.
- Carman, C.V., and T.A. Springer. 2004. A transmigratory cup in leukocyte diapedesis both through individual vascular endothelial cells and between them. *J.Cell Biol.* 167:377-388.
- Celsi, F., P. Pizzo, M. Brini, S. Leo, C. Fotino, P. Pinton, and R. Rizzuto. 2009. Mitochondria, calcium and cell death: a deadly triad in neurodegeneration. *Biochim.Biophys.Acta.* 1787:335-344.
- Chan, D.C. 2006a. Mitochondria: dynamic organelles in disease, aging, and development. *Cell.* 125:1241-1252.
- Chan, D.C. 2006b. Mitochondrial fusion and fission in mammals. *Annu.Rev.Cell Dev.Biol.* 22:79-99.
- Chen, H., and D.C. Chan. 2004. Mitochondrial dynamics in mammals. *Curr.Top.Dev.Biol.* 59:119-144.
- Chen, J., A. Salas, and T.A. Springer. 2003. Bistable regulation of integrin adhesiveness by a bipolar metal ion cluster. *Nat.Struct.Biol.* 10:995-1001.
- Chen, L., F. Wang, H. Meng, and J.R. Sellers. 2001. Characterization of Recombinant Myosin X. *Biophys. J. (Annual Meeting Abstracts).* 80:573a.
- Chen, Z.Y., T. Hasson, P.M. Kelley, B.J. Schwender, M.F. Schwartz, M. Ramakrishnan, W.J. Kimberling, M.S. Mooseker, and D.P. Corey. 1996. Molecular cloning and domain structure of human myosin-VIIa, the gene product defective in Usher syndrome 1B. *Genomics.* 36:440-448.

- Cheney, R.E., and M.S. Mooseker. 1992. Unconventional myosins. *Curr.Opin.Cell Biol.* 4:27-35.
- Chishti, A.H., A.C. Kim, S.M. Marfatia, M. Lutchman, M. Hanspal, H. Jindal, S.C. Liu, P.S. Low, G.A. Rouleau, N. Mohandas, J.A. Chasis, J.G. Conboy, P. Gascard, Y. Takakuwa, S.C. Huang, B.E. J. Jr, A. Bretscher, R.G. Fehon, J.F. Gusella, V. Ramesh, F. Solomon, V.T. Marchesi, S. Tsukita, S. Tsukita, and K.B. Hoover. 1998. The FERM domain: a unique module involved in the linkage of cytoplasmic proteins to the membrane. *Trends Biochem Sci.* 23:281-282.
- Cho, S.Y., and R.L. Klemke. 2002. Purification of pseudopodia from polarized cells reveals redistribution and activation of Rac through assembly of a CAS/Crk scaffold. *J.Cell Biol.* 156:725-736.
- Collins, T.J., M.J. Berridge, P. Lipp, and M.D. Bootman. 2002. Mitochondria are morphologically and functionally heterogeneous within cells. *EMBO J.* 21:1616-1627.
- Coluccio, L.M. Myosins: A Superfamily of Molecular Motors. Dordrecht : Springer, c2008.
- Cope, M.J., J. Whisstock, I. Rayment, and J. Kendrick-Jones. 1996. Conservation within the myosin motor domain: implications for structure and function. *Structure.* 4:969-987.
- Cox, D., J.S. Berg, M. Cammer, J.O. Chingwundoh, B.M. Dale, R.E. Cheney, and S. Greenberg. 2002. Myosin X is a downstream effector of PI(3)K during phagocytosis. *Nat Cell Biol.* 4:469-477.
- Cox, D., C.C. Tseng, G. Bjekic, and S. Greenberg. 1999. A requirement for phosphatidylinositol 3-kinase in pseudopod extension. *J Biol Chem.* 274:1240-1247.
- Czuchra, A., X. Wu, H. Meyer, J. van Hengel, T. Schroeder, R. Geffers, K. Rottner, and C. Brakebusch. 2005. Cdc42 is not essential for filopodium formation, directed migration, cell polarization, and mitosis in fibroblastoid cells. *Mol.Biol.Cell.* 16:4473-4484.
- Dai, P.G. 2001. Myosin-VIIb, a novel unconventional myosin, is a constituent of microvilli in transporting epithelia. *Genomics.* 72:285-296.
- Dalby, B., S. Cates, A. Harris, E.C. Ohki, M.L. Tilkins, P.J. Price, and V.C. Ciccarone. 2004. Advanced transfection with Lipofectamine 2000 reagent: primary neurons, siRNA, and high-throughput applications. *Methods.* 33:95-103.
- Davenport, R.W., P. Dou, V. Rehder, and S.B. Kater. 1993. A sensory role for neuronal growth cone filopodia. *Nature.* 361:721-724.
- Davis, D.M., and S. Sowinski. 2008. Membrane nanotubes: dynamic long-distance connections between animal cells. *Nat.Rev.Mol.Cell Biol.* 9:431-436.
- De La Cruz, E.M., and E.M. Ostap. 2004. Relating biochemistry and function in the myosin superfamily. *Curr.Opin.Cell Biol.* 16:61-67.

- De Smet, F., I. Segura, K. De Bock, P.J. Hohensinner, and P. Carmeliet. 2009. Mechanisms of vessel branching: filopodia on endothelial tip cells lead the way. *Arterioscler.Thromb.Vasc.Biol.* 29:639-649.
- Delettre, C., G. Lenaers, L. Pelloquin, P. Belenguer, and C.P. Hamel. 2002. OPA1 (Kjer type) dominant optic atrophy: a novel mitochondrial disease. *Mol.Genet.Metab.* 75:97-107.
- Dent, E.W., A.V. Kwiatkowski, L.M. Mebane, U. Philippar, M. Barzik, D.A. Rubinson, S. Gupton, J.E. Van Veen, C. Furman, J. Zhang, A.S. Alberts, S. Mori, and F.B. Gertler. 2007. Filopodia are required for cortical neurite initiation. *Nat.Cell Biol.* 9:1347-1359.
- DeRosier, D.J., and K.T. Edds. 1980. Evidence for fascin cross-links between the actin filaments in coelomocyte filopodia. *Exp.Cell Res.* 126:490-494.
- Detmer, S.A., and D.C. Chan. 2007. Functions and dysfunctions of mitochondrial dynamics. *Nat.Rev.Mol.Cell Biol.* 8:870-879.
- Disanza, A., S. Mantoani, M. Hertzog, S. Gerboth, E. Frittoli, A. Steffen, K. Berhoerster, H.J. Kreienkamp, F. Milanese, P.P. Di Fiore, A. Ciliberto, T.E. Stradal, and G. Scita. 2006. Regulation of cell shape by Cdc42 is mediated by the synergic actin-bundling activity of the Eps8-IRSp53 complex. *Nat.Cell Biol.* 8:1337-1347.
- Ellis, S., and H. Mellor. 2000. The novel Rho-family GTPase rif regulates coordinated actin-based membrane rearrangements. *Curr.Biol.* 10:1387-1390.
- Fath, K.R., and D.R. Burgess. 1995. Microvillus assembly. Not actin alone. *Curr.Biol.* 5:591-593.
- Galbraith, C.G., K.M. Yamada, and J.A. Galbraith. 2007. Polymerizing actin fibers position integrins primed to probe for adhesion sites. *Science.* 315:992-995.
- Garcia-Alvarez, B., J.M. de Pereda, D.A. Calderwood, T.S. Ulmer, D. Critchley, I.D. Campbell, M.H. Ginsberg, and R.C. Liddington. 2003. Structural determinants of integrin recognition by talin. *Mol.Cell.* 11:49-58.
- Gerdes, H.H., and R.N. Carvalho. 2008. Intercellular transfer mediated by tunneling nanotubes. *Curr.Opin.Cell Biol.* 20:470-475.
- Gerhardt, H., M. Golding, M. Fruttiger, C. Ruhrberg, A. Lundkvist, A. Abramsson, M. Jeltsch, C. Mitchell, K. Alitalo, D. Shima, and C. Betsholtz. 2003. VEGF guides angiogenic sprouting utilizing endothelial tip cell filopodia. *J.Cell Biol.* 161:1163-1177.
- Gibbs, D., J. Kitamoto, and D.S. Williams. 2003. Abnormal phagocytosis by retinal pigmented epithelium that lacks myosin VIIa, the Usher syndrome 1B protein. *Proc Natl Acad Sci U S A.* 100:6481-6486.
- Gogvadze, V., S. Orrenius, and B. Zhivotovsky. 2008. Mitochondria in cancer cells: what is so special about them? *Trends Cell Biol.* 18:165-173.

- Goode, B.L., and M.J. Eck. 2007. Mechanism and function of formins in the control of actin assembly. *Annu.Rev.Biochem.* 76:593-627.
- Grabham, P.W., M. Foley, A. Umeojiako, and D.J. Goldberg. 2000. Nerve growth factor stimulates coupling of beta1 integrin to distinct transport mechanisms in the filopodia of growth cones. *J Cell Sci.* 113:3003-12.
- Grabham, P.W., and D.J. Goldberg. 1997. Nerve growth factor stimulates the accumulation of beta1 integrin at the tips of filopodia in the growth cones of sympathetic neurons. *J.Neurosci.* 17:5455-5465.
- Gupton, S.L., and F.B. Gertler. 2007. Filopodia: the fingers that do the walking. *Sci.STKE.* 2007:re5.
- Hamada, K., T. Shimizu, T. Matsui, S. Tsukita, and T. Hakoshima. 2000. Structural basis of the membrane-targeting and unmasking mechanisms of the radixin FERM domain. *Embo J.* 19:4449-4462.
- Heasman, S.J., and A.J. Ridley. 2008. Mammalian Rho GTPases: new insights into their functions from in vivo studies. *Nat.Rev.Mol.Cell Biol.* 9:690-701.
- Hirokawa, N., and J.E. Heuser. 1981. Quick-freeze, deep-etch visualization of the cytoskeleton beneath surface differentiations of intestinal epithelial cells. *J.Cell Biol.* 91:399-409.
- Hirokawa, N., L.G. Tilney, K. Fujiwara, and J.E. Heuser. 1982. Organization of actin, myosin, and intermediate filaments in the brush border of intestinal epithelial cells. *J.Cell Biol.* 94:425-443.
- Hofmann, W.A., T. Johnson, M. Klapczynski, J.L. Fan, and P. de Lanerolle. 2006. From transcription to transport: emerging roles for nuclear myosin I. *Biochem.Cell Biol.* 84:418-426.
- Hollenbeck, P.J., and W.M. Saxton. 2005. The axonal transport of mitochondria. *J.Cell.Sci.* 118:5411-5419.
- Homma, K., and M. Ikebe. 2005. Myosin X is a high duty ratio motor. *J Biol Chem.* 280:29381-29391.
- Homma, K., J. Saito, R. Ikebe, and M. Ikebe. 2001. Motor function and regulation of myosin X. *J Biol Chem.* 276:34348-34354.
- Horie, C., H. Suzuki, M. Sakaguchi, and K. Mihara. 2002. Characterization of signal that directs C-tail-anchored proteins to mammalian mitochondrial outer membrane. *Mol.Biol.Cell.* 13:1615-1625.
- Horwitz, A., K. Duggan, C. Buck, M.C. Beckerle, and K. Burridge. 1986. Interaction of plasma membrane fibronectin receptor with talin--a transmembrane linkage. *Nature.* 320:531-533.

Hu, Y.F., Z.J. Zhang, and M. Sieber-Blum. 2006. An epidermal neural crest stem cell (EPI-NCSC) molecular signature. *Stem Cells*. 24:2692-2702.

Huang, X., H.J. Cheng, M. Tessier-Lavigne, and Y. Jin. 2002. MAX-1, a novel PH/MyTH4/FERM domain cytoplasmic protein implicated in netrin-mediated axon repulsion. *Neuron*. 34:563-576.

Isakoff, S.J., T. Cardozo, J. Andreev, Z. Li, K.M. Ferguson, R. Abagyan, M.A. Lemmon, A. Aronheim, and E.Y. Skolnik. 1998. Identification and analysis of PH domain-containing targets of phosphatidylinositol 3-kinase using a novel in vivo assay in yeast. *Embo J*. 17:5374-5387.

Jalili, P.R., and C. Dass. 2004. Proteome analysis in the bovine adrenal medulla using liquid chromatography with tandem mass spectrometry. *Rapid Commun Mass Spectrom*. 18:1877-1884.

Katoh, K., K. Hammar, P.J. Smith, and R. Oldenbourg. 1999. Arrangement of radial actin bundles in the growth cone of *Aplysia* bag cell neurons shows the immediate past history of filopodial behavior. *Proc.Natl.Acad.Sci.U.S.A*. 96:7928-7931.

Kerber, M.L., D.T. Jacobs, L. Campagnola, B.D. Dunn, T. Yin, A.D. Sousa, O.A. Quintero, and R.E. Cheney. 2009. A novel form of motility in filopodia revealed by imaging myosin-X at the single-molecule level. *Curr.Biol*. 19:967-973.

Klopfenstein, D.R., M. Tomishige, N. Stuurman, and R.D. Vale. 2002. Role of phosphatidylinositol(4,5)biphosphate organization in membrane transport by the Unc104 kinesin motor. *Cell*. 109:347-358.

Knight, P.J., K. Thirumurugan, Y. Xu, F. Wang, A.P. Kalverda, W.F. Stafford 3rd, J.R. Sellers, and M. Peckham. 2005. The predicted coiled-coil domain of myosin 10 forms a novel elongated domain that lengthens the head. *J Biol Chem*. 280:34702-34708.

Kolesnikova, L., A.B. Bohil, R.E. Cheney, and S. Becker. 2007. Budding of Marburgvirus is associated with filopodia. *Cell.Microbiol*. 9:939-951.

Kovacs, M., F. Wang, and J.R. Sellers. 2005. Mechanism of action of myosin X, a membrane-associated molecular motor. *J Biol Chem*. 280:15071-83.

Krause, M., E.W. Dent, J.E. Bear, J.J. Loureiro, and F.B. Gertler. 2003. Ena/VASP proteins: regulators of the actin cytoskeleton and cell migration. *Annu.Rev.Cell Dev.Biol*. 19:541-564.

Kress, H., E.H. Stelzer, D. Holzer, F. Buss, G. Griffiths, and A. Rohrbach. 2007. Filopodia act as phagocytic tentacles and pull with discrete steps and a load-dependent velocity. *Proc.Natl.Acad.Sci.U.S.A*. 104:11633-11638.

Krugmann, S., I. Jordens, K. Gevaert, M. Driessens, J. Vandekerckhove, and A. Hall. 2001. Cdc42 induces filopodia by promoting the formation of an IRSp53:Mena complex. *Curr.Biol*. 11:1645-1655.

- Kuwana, T., and D.D. Newmeyer. 2003. Bcl-2-family proteins and the role of mitochondria in apoptosis. *Curr.Opin.Cell Biol.* 15:691-699.
- Lan, Y., and G.A. Papoian. 2008. The stochastic dynamics of filopodial growth. *Biophys.J.* 94:3839-3852.
- Larkin, M.A., G. Blackshields, N.P. Brown, R. Chenna, P.A. McGettigan, H. McWilliam, F. Valentin, I.M. Wallace, A. Wilm, R. Lopez, J.D. Thompson, T.J. Gibson, and D.G. Higgins. 2007. Clustal W and Clustal X version 2.0. *Bioinformatics.* 23:2947-2948.
- Lebrand, C., E.W. Dent, G.A. Strasser, L.M. Lanier, M. Krause, T.M. Svitkina, G.G. Borisy, and F.B. Gertler. 2004. Critical role of Ena/VASP proteins for filopodia formation in neurons and in function downstream of netrin-1. *Neuron.* 42:37-49.
- Letourneau, P.C., and T.A. Shattuck. 1989. Distribution and possible interactions of actin-associated proteins and cell adhesion molecules of nerve growth cones. *Development.* 105:505-519.
- Lewis, A.K., and P.C. Bridgman. 1992. Nerve growth cone lamellipodia contain two populations of actin filaments that differ in organization and polarity. *J.Cell Biol.* 119:1219-1243.
- Lidke, D.S., K.A. Lidke, B. Rieger, T.M. Jovin, and D.J. Arndt-Jovin. 2005. Reaching out for signals: filopodia sense EGF and respond by directed retrograde transport of activated receptors. *J.Cell Biol.* 170:619-626.
- Liesa, M., M. Palacin, and A. Zorzano. 2009. Mitochondrial dynamics in mammalian health and disease. *Physiol.Rev.* 89:799-845.
- Lim, K.B., W. Bu, W.I. Goh, E. Koh, S.H. Ong, T. Pawson, T. Sudhakaran, and S. Ahmed. 2008. The Cdc42 effector IRSp53 generates filopodia by coupling membrane protrusion with actin dynamics. *J.Biol.Chem.* 283:20454-20472.
- Lin, C.H., E.M. Espreafico, M.S. Mooseker, and P. Forscher. 1996. Myosin drives retrograde F-actin flow in neuronal growth cones. *Neuron.* 16:769-782.
- Liu, R., S. Woolner, J.E. Johndrow, D. Metzger, A. Flores, and S.M. Parkhurst. 2008. Sisyphus, the Drosophila myosin XV homolog, traffics within filopodia transporting key sensory and adhesion cargos. *Development.* 135:53-63.
- Lowell, B.B., and G.I. Shulman. 2005. Mitochondrial dysfunction and type 2 diabetes. *Science.* 307:384-387.
- Lowery, L.A., and D. Van Vactor. 2009. The trip of the tip: understanding the growth cone machinery. *Nat.Rev.Mol.Cell Biol.* 10:332-343.
- Lupas, A., M. Van Dyke, and J. Stock. 1991. Predicting coiled coils from protein sequences. *Science.* 252:1162-1164.

- Machesky, L.M., and R.H. Insall. 1998. Scar1 and the related Wiskott-Aldrich syndrome protein, WASP, regulate the actin cytoskeleton through the Arp2/3 complex. *Curr.Biol.* 8:1347-1356.
- Macias, M.J., A. Musacchio, H. Ponstingl, M. Nilges, M. Saraste, and H. Oschkinat. 1994. Structure of the pleckstrin homology domain from beta-spectrin. *Nature.* 369:675-677.
- Mallavarapu, A., and T. Mitchison. 1999. Regulated actin cytoskeleton assembly at filopodium tips controls their extension and retraction. *J Cell Biol.* 146:1097-1106.
- Manor, U., and B. Kachar. 2008. Dynamic length regulation of sensory stereocilia. *Semin.Cell Dev.Biol.* 19:502-510.
- Marshall, J.G., J.W. Booth, V. Stambolic, T. Mak, T. Balla, A.D. Schreiber, T. Meyer, and S. Grinstein. 2001. Restricted accumulation of phosphatidylinositol 3-kinase products in a plasmalemmal subdomain during Fc gamma receptor-mediated phagocytosis. *J Cell Biol.* 153:1369-1380.
- Martin, M., S.J. Iyadurai, A. Gassman, J.G. Gindhart Jr, T.S. Hays, and W.M. Saxton. 1999. Cytoplasmic dynein, the dynactin complex, and kinesin are interdependent and essential for fast axonal transport. *Mol.Biol.Cell.* 10:3717-3728.
- Mashanov, G.I., D. Tacon, M. Peckham, and J.E. Molloy. 2004. The spatial and temporal dynamics of pleckstrin homology domain binding at the plasma membrane measured by imaging single molecules in live mouse myoblasts. *J Biol Chem.* 279:15274-15280.
- Mattila, P.K., A. Pykalainen, J. Saarikangas, V.O. Paavilainen, H. Vihinen, E. Jokitalo, and P. Lappalainen. 2007. Missing-in-metastasis and IRSp53 deform PI(4,5)P2-rich membranes by an inverse BAR domain-like mechanism. *J.Cell Biol.* 176:953-964.
- McBride, H.M., M. Neuspiel, and S. Wasiak. 2006. Mitochondria: more than just a powerhouse. *Curr.Biol.* 16:R551-60.
- Medalia, O., M. Beck, M. Ecke, I. Weber, R. Neujahr, W. Baumeister, and G. Gerisch. 2007. Organization of actin networks in intact filopodia. *Curr.Biol.* 17:79-84.
- Mellor, H. 2009. The role of formins in filopodia formation. *Biochim.Biophys.Acta.* doi: 10.1016/j.bbamcr.2008.12.018.
- Mercer, J., and A. Helenius. 2008. Vaccinia virus uses macropinocytosis and apoptotic mimicry to enter host cells. *Science.* 320:531-535.
- Millard, T.H., and P. Martin. 2008. Dynamic analysis of filopodial interactions during the zipper phase of *Drosophila* dorsal closure. *Development.* 135:621-626.
- Minin, A.A., A.V. Kulik, F.K. Gyoeva, Y. Li, G. Goshima, and V.I. Gelfand. 2006. Regulation of mitochondria distribution by RhoA and formins. *J.Cell.Sci.* 119:659-670.
- Mogilner, A., and B. Rubinstein. 2005. The physics of filopodial protrusion. *Biophys.J.* 89:782-795.

- Mooseker, M.S., and L.G. Tilney. 1975. Organization of an actin filament-membrane complex. Filament polarity and membrane attachment in the microvilli of intestinal epithelial cells. *J Cell Biol.* 67:725-43.
- Morris, R.L., and P.J. Hollenbeck. 1995. Axonal transport of mitochondria along microtubules and F-actin in living vertebrate neurons. *J.Cell Biol.* 131:1315-1326.
- Moser, M., K.R. Legate, R. Zent, and R. Fassler. 2009. The tail of integrins, talin, and kindlins. *Science.* 324:895-899.
- Murphy, G.A., P.A. Solski, S.A. Jillian, P. Perez de la Ossa, P. D'Eustachio, C.J. Der, and M.G. Rush. 1999. Cellular functions of TC10, a Rho family GTPase: regulation of morphology, signal transduction and cell growth. *Oncogene.* 18:3831-3845.
- Musacchio, A., T. Gibson, P. Rice, J. Thompson, and M. Saraste. 1993. The PH domain: a common piece in the structural patchwork of signalling proteins. *Trends Biochem Sci.* 18:343-348.
- Nagy, S., B.L. Ricca, M.F. Norstrom, D.S. Courson, C.M. Brawley, P.A. Smithback, and R.S. Rock. 2008. A myosin motor that selects bundled actin for motility. *Proc.Natl.Acad.Sci.U.S.A.* 105:9616-9620.
- Nakagawa, H., H. Miki, M. Nozumi, T. Takenawa, S. Miyamoto, J. Wehland, and J.V. Small. 2003. IRSp53 is colocalised with WAVE2 at the tips of protruding lamellipodia and filopodia independently of Mena. *J.Cell.Sci.* 116:2577-2583.
- Nangaku, M., R. Sato-Yoshitake, Y. Okada, Y. Noda, R. Takemura, H. Yamazaki, and N. Hirokawa. 1994. KIF1B, a novel microtubule plus end-directed monomeric motor protein for transport of mitochondria. *Cell.* 79:1209-1220.
- Narasimhulu, S.B., and A.S. Reddy. 1998. Characterization of microtubule binding domains in the Arabidopsis kinesin-like calmodulin binding protein. *Plant Cell.* 10:957-965.
- Nayak, G.D., H.S. Ratnayaka, R.J. Goodyear, and G.P. Richardson. 2007. Development of the hair bundle and mechanotransduction. *Int.J.Dev.Biol.* 51:597-608.
- Nekrasova, O., A. Kulik, and A. Minin. June 2007. Protein kinase C regulates mitochondrial motility. *Biochemistry (Moscow) Supplement Series A: Membrane and Cell Biology.* 1:108-113(6).
- Nobes, C.D., and A. Hall. 1995. Rho, rac, and cdc42 GTPases regulate the assembly of multimolecular focal complexes associated with actin stress fibers, lamellipodia, and filopodia. *Cell.* 81:53-62.
- Odronitz, F., and M. Kollmar. 2007. Drawing the tree of eukaryotic life based on the analysis of 2,269 manually annotated myosins from 328 species. *Genome Biol.* 8:R196. .

Okabe, S., and N. Hirokawa. 1991. Actin dynamics in growth cones. *J.Neurosci.* 11:1918-1929.

Otto, J.J., R.E. Kane, and J. Bryan. 1979. Formation of filopodia in coelomocytes: localization of fascin, a 58,000 dalton actin cross-linking protein. *Cell.* 17:285-293.

Park, H., B. Ramamurthy, M. Travaglia, D. Safer, L.Q. Chen, C. Franzini-Armstrong, P.R. Selvin, and H.L. Sweeney. 2006. Full-length myosin VI dimerizes and moves processively along actin filaments upon monomer clustering. *Mol Cell.* 21:331-336.

Partridge, M.A., and E.E. Marcantonio. 2006. Initiation of attachment and generation of mature focal adhesions by integrin-containing filopodia in cell spreading. *Mol.Biol.Cell.* 17:4237-4248.

Paul, A.S., and T.D. Pollard. 2009. Review of the mechanism of processive actin filament elongation by formins. *Cell Motil.Cytoskeleton.* 66:606-617.

Pearson, M.A., D. Reczek, A. Bretscher, and P.A. Karplus. 2000. Structure of the ERM protein moesin reveals the FERM domain fold masked by an extended actin binding tail domain. *Cell.* 101:259-270.

Pellegrin, S., and H. Mellor. 2005. The Rho family GTPase Rif induces filopodia through mDia2. *Curr.Biol.* 15:129-133.

Peng, J., B.J. Wallar, A. Flanders, P.J. Swiatek, and A.S. Alberts. 2003. Disruption of the Diaphanous-Related Formin Drf1 Gene Encoding mDia1 Reveals a Role for Drf3 as an Effector for Cdc42. *Current Biology.* 13:534-545.

Pi, X., R. Ren, R. Kelley, C. Zhang, M. Moser, A.B. Bohil, M. Divito, R.E. Cheney, and C. Patterson. 2007. Sequential roles for myosin-X in BMP6-dependent filopodial extension, migration, and activation of BMP receptors. *J Cell Biol.* 179:1569-1582.

Pollard, T.D., and G.G. Borisy. 2003. Cellular motility driven by assembly and disassembly of actin filaments. *Cell.* 112:453-465.

Post, P.L., G.M. Bokoch, and M.S. Mooseker. 1998. Human myosin-IXb is a mechanochemically active motor and a GAP for rho. *J.Cell.Sci.* 111:941-950.

Price, L.S., J. Leng, M.A. Schwartz, and G.M. Bokoch. 1998. Activation of Rac and Cdc42 by integrins mediates cell spreading. *Mol.Biol.Cell.* 9:1863-1871.

Priddle, H., L. Hemmings, S. Monkley, A. Woods, B. Patel, D. Sutton, G.A. Dunn, D. Zicha, and D.R. Critchley. 1998. Disruption of the talin gene compromises focal adhesion assembly in undifferentiated but not differentiated embryonic stem cells. *J.Cell Biol.* 142:1121-1133.

Qi, Y., J.K. Wang, M. McMillian, and D.M. Chikaraishi. 1997. Characterization of a CNS cell line, CAD, in which morphological differentiation is initiated by serum deprivation. *J.Neurosci.* 17:1217-1225.

Quintero, O.A., T.M. Svitkina, O.Y. Chago, A. Bhaskar, G.G. Borisy, and R.E. Cheney. 2003. Dynamics of myosin-X (Myo10) and VASP at the filopodial tip. *Mol Biol Cell*. 14s.

Rabinovitz, I., and A.M. Mercurio. 1997. The integrin alpha6beta4 functions in carcinoma cell migration on laminin-1 by mediating the formation and stabilization of actin-containing motility structures. *J.Cell Biol.* 139:1873-1884.

Raich, W.B., C. Agbunag, and J. Hardin. 1999. Rapid epithelial-sheet sealing in the *Caenorhabditis elegans* embryo requires cadherin-dependent filopodial priming. *Curr.Biol.* 9:1139-1146.

Rajnicek, A.M., L.E. Foubister, and C.D. McCaig. 2006. Growth cone steering by a physiological electric field requires dynamic microtubules, microfilaments and Rac-mediated filopodial asymmetry. *J.Cell.Sci.* 119:1736-1745.

Ramirez-Weber, F.A., and T.B. Kornberg. 1999. Cytonemes: cellular processes that project to the principal signaling center in *Drosophila* imaginal discs. *Cell.* 97:599-607.

Rao, M.V., L.J. Engle, P.S. Mohan, A. Yuan, D. Qiu, A. Cataldo, L. Hassinger, S. Jacobsen, V.M. Lee, A. Andreadis, J.P. Julien, P.C. Bridgman, and R.A. Nixon. 2002. Myosin Va binding to neurofilaments is essential for correct myosin Va distribution and transport and neurofilament density. *J.Cell Biol.* 159:279-290.

Ratnikov, B.I., A.W. Partridge, and M.H. Ginsberg. 2005. Integrin activation by talin. *J Thromb Haemost.* 3:1783-1790.

Rechsteiner, M., and S.W. Rogers. 1996. PEST sequences and regulation by proteolysis. *Trends Biochem Sci.* 21:267-271.

Reddy, A.S., F. Safadi, S.B. Narasimhulu, M. Golovkin, and X. Hu. 1996. A novel plant calmodulin-binding protein with a kinesin heavy chain motor domain. *J Biol Chem.* 271:7052-7060.

Ridley, A.J. 2006. Rho GTPases and actin dynamics in membrane protrusions and vesicle trafficking. *Trends Cell Biol.* 16:522-529.

Ritzenthaler, S., and A. Chiba. 2003. Myopodia (postsynaptic filopodia) participate in synaptic target recognition. *J.Neurobiol.* 55:31-40.

Rodriguez, O.C., A.W. Schaefer, C.A. Mandato, P. Forscher, W.M. Bement, and C.M. Waterman-Storer. 2003. Conserved microtubule-actin interactions in cell movement and morphogenesis. *Nat Cell Biol.* 5:599-609.

Rogers, M.S., and E.E. Strehler. 2001. The tumor-sensitive calmodulin-like protein is a specific light chain of human unconventional myosin X. *J Biol Chem.* 276:12182-12189.

Rohatgi, R., L. Ma, H. Miki, M. Lopez, T. Kirchhausen, T. Takenawa, and M.W. Kirschner. 1999. The interaction between N-WASP and the Arp2/3 complex links Cdc42-dependent signals to actin assembly. *Cell.* 97:221-231.

Ross, M.E., X. Zhou, G. Song, S.A. Shurtleff, K. Girtman, W.K. Williams, H.C. Liu, R. Mahfouz, S.C. Raimondi, N. Lenny, A. Patel, and J.R. Downing. 2003. Classification of pediatric acute lymphoblastic leukemia by gene expression profiling. *Blood*. 102:2951-2959.

Rube, D.A., and A.M. van der Blik. 2004. Mitochondrial morphology is dynamic and varied. *Mol.Cell.Biochem*. 256-257:331-339.

Rubinson, D.A., C.P. Dillon, A.V. Kwiatkowski, C. Sievers, L. Yang, J. Kopinja, D.L. Rooney, M. Zhang, M.M. Ihrig, M.T. McManus, F.B. Gertler, M.L. Scott, and L. Van Parijs. 2003. A lentivirus-based system to functionally silence genes in primary mammalian cells, stem cells and transgenic mice by RNA interference. *Nat.Genet*. 33:401-406.

Rustom, A., R. Saffrich, I. Markovic, P. Walther, and H.H. Gerdes. 2004. Nanotubular highways for intercellular organelle transport. *Science*. 303:1007-1010.

Ruusala, A., and P. Aspenstrom. 2008. The atypical Rho GTPase Wrch1 collaborates with the nonreceptor tyrosine kinases Pyk2 and Src in regulating cytoskeletal dynamics. *Mol.Cell.Biol*. 28:1802-1814.

Rzadzinska, A.K., E.M. Nevalainen, H.M. Prosser, P. Lappalainen, and K.P. Steel. 2009. MyosinVIIa interacts with Twinfilin-2 at the tips of mechanosensory stereocilia in the inner ear. *PLoS One*. 4:e7097.

Rzadzinska, A.K., M.E. Schneider, C. Davies, G.P. Riordan, and B. Kachar. 2004. An actin molecular treadmill and myosins maintain stereocilia functional architecture and self-renewal. *J Cell Biol*. 164:887-897.

Saarikangas, J., H. Zhao, A. Pykalainen, P. Laurinmaki, P.K. Mattila, P.K. Kinnunen, S.J. Butcher, and P. Lappalainen. 2009. Molecular mechanisms of membrane deformation by I-BAR domain proteins. *Curr.Biol*. 19:95-107.

Salles, F.T., R.C. Merritt Jr, U. Manor, G.W. Dougherty, A.D. Sousa, J.E. Moore, C.M. Yengo, A.C. Dose, and B. Kachar. 2009. Myosin IIIa boosts elongation of stereocilia by transporting espin 1 to the plus ends of actin filaments. *Nat.Cell Biol*. 11:443-450.

Saotome, M., D. Safiulina, G. Szabadkai, S. Das, A. Fransson, P. Aspenstrom, R. Rizzuto, and G. Hajnoczky. 2008. Bidirectional Ca²⁺-dependent control of mitochondrial dynamics by the Miro GTPase. *Proc.Natl.Acad.Sci.U.S.A*. 105:20728-20733.

Schafer, C., B. Borm, S. Born, C. Mohl, E.M. Eibl, and B. Hoffmann. 2009. One step ahead: role of filopodia in adhesion formation during cell migration of keratinocytes. *Exp.Cell Res*. 315:1212-1224.

Schaller, M.D., C.A. Otey, J.D. Hildebrand, and J.T. Parsons. 1995. Focal adhesion kinase and paxillin bind to peptides mimicking beta integrin cytoplasmic domains. *J.Cell Biol*. 130:1181-1187.

Schirenbeck, A., R. Arasada, T. Bretschneider, M. Schleicher, and J. Faix. 2005. Formins and VASPs may co-operate in the formation of filopodia. *Biochem.Soc.Trans.* 33:1256-1259.

Schirenbeck, A., R. Arasada, T. Bretschneider, T.E. Stradal, M. Schleicher, and J. Faix. 2006. The bundling activity of vasodilator-stimulated phosphoprotein is required for filopodium formation. *Proc.Natl.Acad.Sci.U.S.A.* 103:7694-7699.

Schirenbeck, A., T. Bretschneider, R. Arasada, M. Schleicher, and J. Faix. 2005. The Diaphanous-related formin dDia2 is required for the formation and maintenance of filopodia. *Nat.Cell Biol.* 7:619-625.

Schneider, M.E., A.C. Dose, F.T. Salles, W. Chang, F.L. Erickson, B. Burnside, and B. Kachar. 2006. A new compartment at stereocilia tips defined by spatial and temporal patterns of myosin IIIa expression. *J Neurosci.* 26:10243-10252.

Scholey, J.M. 2008. Intraflagellar transport motors in cilia: moving along the cell's antenna. *J.Cell Biol.* 180:23-29.

Scita, G., S. Confalonieri, P. Lappalainen, and S. Suetsugu. 2008. IRSp53: crossing the road of membrane and actin dynamics in the formation of membrane protrusions. *Trends Cell Biol.* 18:52-60.

Shekarabi, M., and T.E. Kennedy. 2002. The netrin-1 receptor DCC promotes filopodia formation and cell spreading by activating Cdc42 and Rac1. *Mol.Cell.Neurosci.* 19:1-17.

Sherer, N.M., M.J. Lehmann, L.F. Jimenez-Soto, C. Horensavitz, M. Pypaert, and W. Mothes. 2007. Retroviruses can establish filopodial bridges for efficient cell-to-cell transmission. *Nat.Cell Biol.* 9:310-315.

Shi, X., Y.Q. Ma, Y. Tu, K. Chen, S. Wu, K. Fukuda, J. Qin, E.F. Plow, and C. Wu. 2007. The MIG-2/integrin interaction strengthens cell-matrix adhesion and modulates cell motility. *J.Biol.Chem.* 282:20455-20466.

Shulman, Z., V. Shinder, E. Klein, V. Grabovsky, O. Yeger, E. Geron, A. Montresor, M. Bolomini-Vittori, S.W. Feigelson, T. Kirchhausen, C. Laudanna, G. Shakhar, and R. Alon. 2009. Lymphocyte crawling and transendothelial migration require chemokine triggering of high-affinity LFA-1 integrin. *Immunity.* 30:384-396.

Silverman, M.A., and M.R. Leroux. 2009. Intraflagellar transport and the generation of dynamic, structurally and functionally diverse cilia. *Trends Cell Biol.* 19:306-316.

Small, J.V., T. Stradal, E. Vignal, and K. Rottner. 2002. The lamellipodium: where motility begins. *Trends Cell Biol.* 12:112-120.

Smith, C.L. 1994. Cytoskeletal movements and substrate interactions during initiation of neurite outgrowth by sympathetic neurons in vitro. *J.Neurosci.* 14:384-398.

- Snapper, S.B., F. Takeshima, I. Anton, C.H. Liu, S.M. Thomas, D. Nguyen, D. Dudley, H. Fraser, D. Purich, M. Lopez-Illasaca, C. Klein, L. Davidson, R. Bronson, R.C. Mulligan, F. Southwick, R. Geha, M.B. Goldberg, F.S. Rosen, J.H. Hartwig, and F.W. Alt. 2001. N-WASP deficiency reveals distinct pathways for cell surface projections and microbial actin-based motility. *Nat.Cell Biol.* 3:897-904.
- Solc, C.K., B.H. Derfler, G.M. Duyk, and D.P. Corey. 1994. Molecular cloning of myosins from the bullfrog saccular macula: a candidate for the hair cell adaptation motor. *Aud Neurosci.* 1:63-75.
- Sousa, A.D., J.S. Berg, B.W. Robertson, R.B. Meeker, and R.E. Cheney. 2006. Myo10 in brain: developmental regulation, identification of a headless isoform and dynamics in neurons. *J Cell Sci.* 119:184-194.
- Spat, A., G. Szanda, G. Csordas, and G. Hajnoczky. 2008. High- and low-calcium-dependent mechanisms of mitochondrial calcium signalling. *Cell Calcium.* 44:51-63.
- Steketee, M.B., and K.W. Tosney. 2002. Three functionally distinct adhesions in filopodia: shaft adhesions control lamellar extension. *J.Neurosci.* 22:8071-8083.
- Suetsugu, S., K. Murayama, A. Sakamoto, K. Hanawa-Suetsugu, A. Seto, T. Oikawa, C. Mishima, M. Shirouzu, T. Takenawa, and S. Yokoyama. 2006. The RAC binding domain/IRSp53-MIM homology domain of IRSp53 induces RAC-dependent membrane deformation. *J.Biol.Chem.* 281:35347-35358.
- Svitkina, T.M., E.A. Bulanova, O.Y. Chaga, D.M. Vignjevic, S. Kojima, J.M. Vasiliev, and G.G. Borisy. 2003. Mechanism of filopodia initiation by reorganization of a dendritic network. *J.Cell Biol.* 160:409-421.
- Sweeney, H.L., and A. Houdusse. 2007. What can myosin VI do in cells? *Curr.Opin.Cell Biol.* 19:57-66.
- Tacon, D., P.J. Knight, and M. Peckham. 2004. Imaging myosin 10 in cells. *Biochem Soc Trans.* 32:689-693.
- Tadokoro, S., S.J. Shattil, K. Eto, V. Tai, R.C. Liddington, J.M. de Pereda, M.H. Ginsberg, and D.A. Calderwood. 2003. Talin binding to integrin beta tails: a final common step in integrin activation. *Science.* 302:103-106.
- Tanabe, K., I. Bonilla, J.A. Winkles, and S.M. Strittmatter. 2003. Fibroblast growth factor-inducible-14 is induced in axotomized neurons and promotes neurite outgrowth. *J Neurosci.* 23:9675-9686.
- Tanaka, Y., Y. Kanai, Y. Okada, S. Nonaka, S. Takeda, A. Harada, and N. Hirokawa. 1998. Targeted disruption of mouse conventional kinesin heavy chain, kif5B, results in abnormal perinuclear clustering of mitochondria. *Cell.* 93:1147-1158.
- Tang, P., C. Cao, M. Xu, and L. Zhang. 2007. Cytoskeletal protein radixin activates integrin alpha(M)beta(2) by binding to its cytoplasmic tail. *FEBS Lett.* 581:1103-1108.

- Tatusova, T.A., and T.L. Madden. 1999. BLAST 2 Sequences, a new tool for comparing protein and nucleotide sequences. *FEMS Microbiol.Lett.* 174:247-250.
- Titus, M.A. 1999. A class VII unconventional myosin is required for phagocytosis. *Curr Biol.* 9:1297-1303.
- Tokuo, H., and M. Ikebe. 2004. Myosin X transports Mena/VASP to the tip of filopodia. *Biochem Biophys Res Commun.* 319:214-220.
- Tokuo, H., K. Mabuchi, and M. Ikebe. 2007. The motor activity of myosin-X promotes actin fiber convergence at the cell periphery to initiate filopodia formation. *J.Cell Biol.* 179:229-238.
- Tomishige, M., D.R. Klopfenstein, and R.D. Vale. 2002. Conversion of Unc104/KIF1A kinesin into a processive motor after dimerization. *Science.* 297:2263-2267.
- Toyoshima, F., and E. Nishida. 2007. Integrin-mediated adhesion orients the spindle parallel to the substratum in an EB1- and myosin X-dependent manner. *Embo J.* 26:1487-1498.
- Tuxworth, R.I., I. Weber, D. Wessels, G.C. Addicks, D.R. Soll, G. Gerisch, and M.A. Titus. 2001. A role for myosin VII in dynamic cell adhesion. *Curr Biol.* 11:318-29.
- Tyska, M.J., A.T. Mackey, J.D. Huang, N.G. Copeland, N.A. Jenkins, and M.S. Mooseker. 2005. Myosin-1a is critical for normal brush border structure and composition. *Mol.Biol.Cell.* 16:2443-2457.
- Tyska, M.J., and M.S. Mooseker. 2002. MYO1A (brush border myosin I) dynamics in the brush border of LLC-PK1-CL4 cells. *Biophys.J.* 82:1869-1883.
- Ulmer, T.S., D.A. Calderwood, M.H. Ginsberg, and I.D. Campbell. 2003. Domain-specific interactions of talin with the membrane-proximal region of the integrin beta3 subunit. *Biochemistry.* 42:8307-8312.
- Van Blerkom, J. 2009. Mitochondria in early mammalian development. *Semin.Cell Dev.Biol.* 20:354-364.
- van den Boom, F., H. Dussmann, K. Uhlenbrock, M. Abouhamed, and M. Bahler. 2007. The Myosin IXb motor activity targets the myosin IXb RhoGAP domain as cargo to sites of actin polymerization. *Mol.Biol.Cell.* 18:1507-1518.
- Vasioukhin, V., C. Bauer, M. Yin, and E. Fuchs. 2000. Directed actin polymerization is the driving force for epithelial cell-cell adhesion. *Cell.* 100:209-219.
- Vicente-Manzanares, M., X. Ma, R.S. Adelstein, and A.R. Horwitz. 2009. Non-muscle myosin II takes centre stage in cell adhesion and migration. *Nat.Rev.Mol.Cell Biol.* 10:778-790.
- Vignjevic, D., S. Kojima, Y. Aratyn, O. Danciu, T. Svitkina, and G.G. Borisy. 2006. Role of fascin in filopodial protrusion. *J.Cell Biol.* 174:863-875.

- Vinogradova, O., A. Velyvis, A. Velyviene, B. Hu, T. Haas, E. Plow, and J. Qin. 2002. A structural mechanism of integrin alpha(IIb)beta(3) "inside-out" activation as regulated by its cytoplasmic face. *Cell*. 110:587-597.
- von Andrian, U.H., S.R. Hasslen, R.D. Nelson, S.L. Erlandsen, and E.C. Butcher. 1995. A central role for microvillous receptor presentation in leukocyte adhesion under flow. *Cell*. 82:989-999.
- Vonna, L., A. Wiedemann, M. Aepfelbacher, and E. Sackmann. 2007. Micromechanics of filopodia mediated capture of pathogens by macrophages. *Eur.Biophys.J.* 36:145-151.
- Vreugde, S., C. Ferrai, A. Miluzio, E. Hauben, P.C. Marchisio, M.P. Crippa, M. Bussi, and S. Biffo. 2006. Nuclear myosin VI enhances RNA polymerase II-dependent transcription. *Mol.Cell*. 23:749-755.
- Wallace, D.C., and W. Fan. 2009. The pathophysiology of mitochondrial disease as modeled in the mouse. *Genes Dev*. 23:1714-1736.
- Wang, A., Y. Liang, R.A. Fridell, F.J. Probst, E.R. Wilcox, J.W. Touchman, C.C. Morton, R.J. Morell, K. Noben-Trauth, S.A. Camper, and T.B. Friedman. 1998. Association of unconventional myosin MYO15 mutations with human nonsyndromic deafness DFNB3. *Science*. 280:1447-51.
- Wang, X., and T.L. Schwarz. 2009. The mechanism of Ca²⁺ -dependent regulation of kinesin-mediated mitochondrial motility. *Cell*. 136:163-174.
- Waterman-Storer, C.M., S.B. Karki, S.A. Kuznetsov, J.S. Tabb, D.G. Weiss, G.M. Langford, and E.L. Holzbaur. 1997. The interaction between cytoplasmic dynein and dynactin is required for fast axonal transport. *Proc.Natl.Acad.Sci.U.S.A.* 94:12180-12185.
- Weber, K.L., A.M. Sokac, J.S. Berg, R.E. Cheney, and W.M. Bement. 2004. A microtubule-binding myosin required for nuclear anchoring and spindle assembly. *Nature*. 431:325-9.
- Wegener, K.L., A.W. Partridge, J. Han, A.R. Pickford, R.C. Liddington, M.H. Ginsberg, and I.D. Campbell. 2007. Structural basis of integrin activation by talin. *Cell*. 128:171-182.
- Wehrle-Haller, B., and B.A. Imhof. 2003. Actin, microtubules and focal adhesion dynamics during cell migration. *Int.J.Biochem.Cell Biol.* 35:39-50.
- Wolfrum, U., X. Liu, A. Schmitt, I.P. Udovichenko, and D.S. Williams. 1998. Myosin VIIa as a common component of cilia and microvilli. *Cell Motil.Cytoskeleton*. 40:261-271.
- Wood, W., A. Jacinto, R. Grose, S. Woolner, J. Gale, C. Wilson, and P. Martin. 2002. Wound healing recapitulates morphogenesis in Drosophila embryos. *Nat.Cell Biol.* 4:907-912.
- Wu, D.Y., L.C. Wang, C.A. Mason, and D.J. Goldberg. 1996. Association of beta 1 integrin with phosphotyrosine in growth cone filopodia. *J.Neurosci.* 16:1470-1478.

- Yang, C., L. Czech, S. Gerboth, S. Kojima, G. Scita, and T. Svitkina. 2007. Novel roles of formin mDia2 in lamellipodia and filopodia formation in motile cells. *PLoS Biol.* 5:e317.
- Yonezawa, S., A. Kimura, S. Koshihara, S. Masaki, T. Ono, A. Hanai, S. Sonta, T. Kageyama, T. Takahashi, and A. Moriyama. 2000. Mouse myosin X: molecular architecture and tissue expression as revealed by northern blot and in situ hybridization analyses. *Biochem Biophys Res Commun.* 271:526-33.
- Yonezawa, S., N. Yoshizaki, M. Sano, A. Hanai, S. Masaki, T. Takizawa, T. Kageyama, and A. Moriyama. 2003. Possible involvement of myosin-X in intercellular adhesion: importance of serial pleckstrin homology regions for intracellular localization. *Dev Growth Differ.* 45:175-85.
- Yoshihara, Y., M. De Roo, and D. Muller. 2009. Dendritic spine formation and stabilization. *Curr.Opin.Neurobiol.* 19:146-153.
- Zamudio-Meza, H., A.M. Castillo, C. Gonzalez-Bonilla, and I. Meza. 2009. Rac1 and Cdc42 GTPases cross-talk regulates formation of filopodia required for Dengue virus type-2 entry into HMEC-1 cells. *J.Gen.Virol.* 90:2902-11.
- Zhang, H., J.S. Berg, Z. Li, Y. Wang, P. Lang, A.D. Sousa, A. Bhaskar, R.E. Cheney, and S. Stromblad. 2004. Myosin-X provides a motor-based link between integrins and the cytoskeleton. *Nat Cell Biol.* 6:523-31.
- Zheng, J.Q., J.J. Wan, and M.M. Poo. 1996. Essential role of filopodia in chemotropic turning of nerve growth cone induced by a glutamate gradient. *J.Neurosci.* 16:1140-1149.
- Zhu, X.J., C.Z. Wang, P.G. Dai, Y. Xie, N.N. Song, Y. Liu, Q.S. Du, L. Mei, Y.Q. Ding, and W.C. Xiong. 2007. Myosin X regulates netrin receptors and functions in axonal path-finding. *Nat Cell Biol.* 9:184-92.
- Zhuravlev, P.I., and G.A. Papoian. 2009. Molecular noise of capping protein binding induces macroscopic instability in filopodial dynamics. *Proc.Natl.Acad.Sci.U.S.A.* 106:11570-11575.
- Zuchner, S., I.V. Mersyanova, M. Muglia, N. Bissar-Tadmouri, J. Rochelle, E.L. Dadali, M. Zappia, E. Nelis, A. Patitucci, J. Senderek, Y. Parman, O. Evgrafov, P.D. Jonghe, Y. Takahashi, S. Tsuji, M.A. Pericak-Vance, A. Quattrone, E. Battaloglu, A.V. Polyakov, V. Timmerman, J.M. Schroder, and J.M. Vance. 2004. Mutations in the mitochondrial GTPase mitofusin 2 cause Charcot-Marie-Tooth neuropathy type 2A. *Nat.Genet.* 36:449-451.